CN TOWER LIGHTNING FLASH CHARACTERISTICS BASED ON HIGH-SPEED IMAGING

by

Ishmeen Sra

M. Eng., McMaster University, Hamilton, ON, Canada, 2016

B. Tech., Guru Nanak Dev Engineering College, Punjab, India, 2014

A thesis

presented to Ryerson University

in partial fulfilment of the

requirements for the degree of

Master of Applied Science

in the program of

Electrical and Computer Engineering

Toronto, Ontario, Canada, 2018

AUTHOR'S DECLARATION

I hereby declare that I am the sole author of this thesis. This is a true copy of the thesis, including any required final revisions, as accepted by my examiners.

I authorize Ryerson University to lend this thesis to other institutions or individuals for the sole purpose of scholarly research.

I further authorize Ryerson University to reproduce this thesis by photocopying or by other means, in total or in part, at the request of other institutions or individuals for the sole purpose of scholarly research.

I understand that my thesis may be made electronically available to the public.

ABSTRACT

CN Tower Lightning Flash Characteristics Based on High-Speed Imaging

Ishmeen Sra

Master of Applied Science

Department of Electrical and Computer Engineering

Ryerson University, Toronto

2018

The thesis emphasizes the analysis of fifty-eight flashes that struck the CN Tower during the last five years (2013-2017), based on video records of Phantom v5.0 digital high-speed imaging system, operating at 1 ms resolution. (A Sony HDR PJ790VB digital camera, operating at 16.67 ms resolution, provided a continuous recording of each CN Tower lightning storm.) It was observed that every recorded flash contained initial-stage current, confirming that all analyzed flashes were upward initiated. It was also observed that only 27 flashes out of the 58 contained return strokes. The number of strokes per flash varied between 1 and 9, with an average multiplicity of 2.16. The time variation of the channel luminosity of each flash was precisely analyzed for the characterization of flash components. A yearly statistical comparison regarding CN Tower lightning macroscopic (number of flashes, inter-flash times and flash durations) and microscopic (initial-stage current durations, number of the return strokes per flash, M-components and inter-stroke times) characteristics was conducted. The analysis of these extensive data (2013-2017) clearly showed that the 50% cumulative probability distribution (CPD) of flash duration in 2017 was found to be the largest in comparison with other data (2013-2016). Whereas, the 50% CPD of inter-flash time duration in 2015 was the shortest. Furthermore, the 2014 data showed the longest 50% CPD of the initial-stage current duration as well as the inter-stroke time duration. In

2016, one flash was found to contain the highest number of return strokes. 2015 was distinguished by having the longest 50% CPD of the continuing current duration. It was also noted that two significantly major storms were captured during the nights of September 5, 2014 and September 4, 2017. During the storm of September 5, 2014, the CN Tower imaging systems recorded 13 flashes. The storm lasted for 111.4 minutes, resulting on average a flash to the tower every 9.28 minutes. Whereas, the September 4, 2017 storm continued for 49.35 minutes, producing 11 flashes for the tower every 4.9 minutes. The characterisation of CN Tower lightning is pivotal to the protection of tall structures against lightning hazards. It's worth mentioning that flashes with longer flash duration, containing high number of return strokes and have shorter inter-stroke time durations pose severe threats to tall structures, electrical and communication systems.

ACKNOWLEDGMENTS

I would like to express my sincere appreciation to my supervisor Professor Dr. Ali Hussein for his continuous guidance and support during my research work. I would like to thank you for your encouragement and your financial support. Also, the numerous discussions we had during these years proved invaluable.

I would like to express my gratitude to Mr. Petros Liatos for his help in operating the high-speed imaging system and the continually recording Sony camera during 2013-2017.

I would like to thank Natural Sciences and Engineering Research Council (NSERC) and Ryerson University for the financial support during my research work.

A special thank you goes to the graduate program administrator, Ms. Dawn Wright, for her help and encouragement during my MASc program.

I would surely like to thank the Department of Electrical and Computer Engineering and Yeates School of Graduate Studies for giving me the opportunity to pursue my fruitful research work.

TABLE OF CONTENT

Abstract ..... **iii**

List of Tables ..... **viii**

List of Figures ..... **ix**

1. **Introduction** **1**

2. Lightning Phenomenon **4**

2.1 Physics of Lightning 4
2.2 Downward Negative Lightning 8
2.3 Downward Positive Lightning 10
2.4 Upward Initiated Lightning 11

3. CN Tower Lightning Measurement Systems **13**

3.1 Overview of the Measurement Systems 13
3.2 Old Rogowski Coil 15
3.3 New Rogowski Coil 17
3.4 Real-Time Digitizers 18
3.5 Flash Trajectory Imaging Systems 19

4. CN Tower Lightning Imaging Systems **20**

4.1 High-Speed Digital Camera 20
4.2 September 5, 2014 Storm Captured by HSC 27
4.3 Continuously Recording Digital Camera 31

5. Lightning Storm Observed at CN Tower on September 4, 2017 ..... **36**

6. Flash Characteristics **44**

6.1 Flash Duration (2013-2017) 45
6.2 Inter-flash Time Duration (2013-2017) 50
6.3 Initial-Stage Current Duration (2013-2017) 53
6.4 Flash Multiplicity (2013-2017) 59
6.5 Inter-Stroke Time Duration (2013-2017) 64

6.6 Continuing Current Duration (2013-2017) 67
6.7 Comparison of CN Tower Major Storms 72
6.7.1 Flash Duration 73
6.7.2 Inter-Flash Time Duration 76
6.7.3 Initial-Stage Current Duration 80
6.7.4 Flash Multiplicity 82
6.7.5 Inter-Stroke Time Duration 85
6.7.6 Continuing Current Duration 88

7. Conclusions and Future recommendations 92

7.1 Conclusions 92
7.2 Future Research and Recommendations 94

References 96

Glossary 99

List of Tables

Table 6.1 Flash durations and inter-flash time durations of all 58 flashes based on video records (2013-2017) 45

Table 6.2 Statistics of flash durations based on video records (2013-2017) 50

Table 6.3 Statistics of inter-flash time duration based on the video records (2013-2017) 53

Table 6.4 Initial-stage current durations based on video records (2013-2017) 54

Table 6.5 Statistics of initial-stage current durations based on video records (2013-2017) 58

Table 6.6 Flash multiplicity and inter-stroke time duration based on video records (2013-2017) 59

Table 6.7 Statistics of flash multiplicity for 27 flashes based on video records (2013-2017) 64

Table 6.8 Statistics of inter-stroke time durations based on video records (2013-2017) 67

Table 6.9 Continuing current time durations based on video records (2013-2017) 68

Table 6.10 Statistics of continuing current time durations based on video records (2013-2017) 72

Table 6.11 Statistical summary of flash durations of flashes recorded during major storms (Sept. 5, 2014 and Sept. 4, 2017) 76

Table 6.12 Statistical summary of inter-flash time durations of flashes recorded during major storms (Sept. 5, 2014 and Sept. 4, 2017) 79

Table 6.13 Statistical summary of initial-stage current durations of flashes recorded during major storms (Sept. 5, 2014 and Sept. 4, 2017) 82

Table 6.14 Statistical summary of a flash multiplicity of flashes recorded during major storms (Sept. 5, 2014 and Sept. 4, 2017) 85

Table 6.15 Statistical summary of inter-stroke time durations of flashes recorded during major storms (Sept. 5, 2014 and Sept. 4, 2017) 88

Table 6.16 Statistical summary of continuing current durations of flashes recorded during major storms (Sept. 5, 2014 and Sept. 4, 2017) 91

List of Figures

Figure 2.1 The thundercloud 5

Figure 2.2 A thundercloud, with a fundamental demonstration of electric charge distribution inside the thundercloud. 6

Figure 2.3 Major Types of Lightning 7

Figure 2.4 Different types of cloud-to-ground lightning 7

Figure 2.5 The sequence of processes involved in a negative downward lightning flash 10

Figure 2.6 The sequence of processes involved in upward negative lightning. 12

Figure 3.1 The CN Tower and Location of Instruments 14

Figure 3.2 The Old Rogowski Coil location and connection 16

Figure 3.3 The new Rogowski Coil location and connection 17

Figure 4.1 Phantom v5.0 digital high-speed camera 21

Figure 4.2 Location of Phantom v5.0 HSC and Sony HDR PJ790VB LSC. 22

Figure 4.3 Flow chart describing the methodology of analysis of video records. 23

Figure 4.4 Channel trajectory image of the second flash recorded on July 8, 2013. 24

Figure 4.5 Maximum and average channel luminosity time variations along the horizontal pixel line Y = 322 25

Figure 4.6 Channel trajectory image of the fourth flash recorded on July 14, 2016. 26

Figure 4.7 Maximum and average channel luminosity time variations along the horizontal pixel line Y = 326. 26

Figure 4.8 Flash multiplicity of flashes September 5, 2014 storm 27

Figure 4.9 Channel trajectory image of the third flash recorded on September 5, 2014. 28

Figure 4.10 Maximum and average channel luminosity time variations along the horizontal pixel line Y = 299 29

Figure 4.11 Channel trajectory image of the twelfth flash recorded on September 5, 2014. 30

Figure 4.12 Maximum and average channel luminosity time variations along the horizontal pixel line Y = 270. 30

Figure 4.13 Sony HDR PJ790VB digital low-speed camera 31

Figure 4.14 Channel trajectory image of the second flash recorded on September 7, 2016 32

Figure 4.15 Maximum and average channel luminosity time variations along the horizontal pixel line Y = 320 33

Figure 4.16 Channel trajectory image of the third flash recorded on July 8, 2013 34

Figure 4.17 Maximum and average channel luminosity time variations along the horizontal pixel line Y = 360 35

Figure 5.1 Channel luminosity variation with time for the Sept. 4, 2017 based on LSC and HSC records 37

Figure 5.2 Channel trajectory images of flash 1 of HSC (left) and its matched LSC flash 7 (right) 38

Figure 5.3 Channel luminosity variation with time based on flash 1 (HSC) and flash 7 (LSC) 38

Figure 5.4 Channel trajectory images of flash 2 of HSC (left) and its matched LSC flash 8 (right) 39

Figure 5.5 Channel luminosity variation with time based on flash 2 (HSC) and flash 8 (LSC) 40

Figure 5.6 Channel trajectory images of flash 3 of HSC (left) and its matched LSC flash 9 (right) 41

Figure 5.7 Channel luminosity variation with time based on flash 3 (HSC) and flash 9 (LSC) 41

Figure 5.8 Channel trajectory images of flash 4 of HSC (left) and its matched LSC flash 11 (right) 42

Figure 5.9 Channel luminosity variation with time based on flash 4 (HSC) and flash 11 (LSC) 43

Figure 6.1 Frequency distribution of flash durations (2013-2017) 48

Figure 6.2 Cumulative probability distribution of flash durations (2013-2017) 49

Figure 6.3 Frequency distribution of inter-flash time duration (2013-2017) 51

Figure 6.4 Cumulative probability distribution of inter-flash time durations (2013-2017) 52

Figure 6.5 Frequency distribution of initial-stage current durations (2013-2017) 56

Figure 6.6 Cumulative probability distribution of initial-stage current duration (2013-2017) 57

Figure 6.7 Frequency distribution of flash multiplicity (2013-2017) 62

Figure 6.8 Cumulative probability distribution of flash multiplicity (2013-2017) 63

Figure 6.9 Frequency distribution of inter-stroke time duration (2013-2017) 65

Figure 6.10 Cumulative probability distribution of inter-stroke time (2013-2017) 66

Figure 6.11 Frequency distribution of continuing current time duration (2013-2017) 70

Figure 6.12 Cumulative probability distribution of continuing current time duration (2013-2017) 71

Figure 6.13 Frequency distribution of flash time duration of flashes recorded during major storms (Sept. 5, 2014 and Sept. 4, 2017) 74

Figure 6.14 Cumulative probability distribution of flash duration of flashes recorded during major storms (Sept. 5, 2014 and Sept. 4, 2017) 75

Figure 6.15 Frequency distribution of inter-flash time duration of flashes recorded during major storms (Sept. 5, 2014 and Sept. 4, 2017) 77

Figure 6.16 Cumulative probability distribution of inter-flash time of flashes recorded during major storms (Sept. 5, 2014 and Sept. 4, 2017) 78

Figure 6.17 Frequency distribution of initial-stage current duration of flashes recorded during major storms (Sept. 5, 2014 and Sept. 4, 2017) 80

Figure 6.18 Cumulative probability distribution of initial-stage current duration of flashes recorded during major storms (Sept. 5, 2014 and Sept. 4, 2017) 81

Figure 6.19 Frequency distribution of flash multiplicity of flashes recorded during major storms (Sept. 5, 2014 and Sept. 4, 2017) 83

Figure 6.20 Cumulative probability distribution of flash multiplicity of flashes recorded during major storms (Sept. 5, 2014 and Sept. 4, 2017) 84

Figure 6.21 Frequency distribution of inter-stroke time duration of flashes recorded during major storms (Sept. 5, 2014 and Sept. 4, 2017) 86

Figure 6.22 Cumulative probability distribution of inter-stroke time duration of flashes recorded during major storms (Sept. 5, 2014 and Sept. 4, 2017) 87

Figure 6.23 Frequency distribution of continuing current of flashes recorded during major storms (Sept. 5, 2014 and Sept. 4, 2017) 89

Figure 6.24 Cumulative probability distribution of continuing current duration of flashes recorded during major storms (Sept. 5, 2014 and Sept. 4, 2017) 90

Chapter 1

Introduction

Lightning is a natural phenomenon; it has likely been present before the emergence of life. Evidence of 250,000-year-old lightning has been found in ancient fulgurites (glassy tubes that lightning forms in sand). Lightning plays a vital role in maintaining the global electric circuit (the fair-weather electric field being about 100 V/m pointing downwards, due to negatively charged earth surface and positively charged air aloft). It also produces chemicals in and around its discharge channel including fixed nitrogen, which plants use in the food-making process [1].

Lightning can be defined as a transient high current electric discharge whose path length is generally measured in kilometres, which discharges regions of excess electrical charge developed in thunderclouds [1], [2]. The lightning discharge, in its entirety, whether it strikes the ground or not, is usually termed as a lightning flash [3]. A lightning flash may contain several components referred to as strokes. Every ground flash contains a downward leader and an upward return stroke and may immediately be succeeded by a relatively slow "continuing current." The transient processes prevailing in the lightning channel during the flow of the continuing current are referred to as M-components. The first stroke is initiated by a "stepped leader," while subsequent strokes are initiated by "dart" or "dart-stepped leaders."

A lightning discharge that involves an object on the ground is termed as a lightning strike [3]. Lightning flashes can kill or injure humans and animals by direct strikes. Lightning can trigger electrical shocks in its vicinity. Lightning strikes can also damage aircrafts,

wind turbines and trees. Lightning strikes are accountable for numerous forest fires [2]. It's observed that lightning flashes that include continuing currents have the ability to set forest fires [2].

Benjamin Franklin showed that a grounded metallic rod placed on the top of a tall structure may protect it from lightning damage. In 1876, James Clerk Maxwell proposed that if lightning were to strike a metal-enclosed building, the current would concentrate on the exterior of the metal enclosure and it would not even be necessary to ground such enclosure.

Since the past few decades, with the escalation of the socio-economic development across the world, a number of tall structures are constructed worldwide. The erection of such tall structures resulted in the obstruction of broadcasting signals. In order to diminish the hindrance to the broadcasting signals, many tall free-standing structures got constructed worldwide to broadcast signals without interruption or the interference caused by ordinary structures in their surrounding vicinities. Important broadcasting tall structures are briefly referred to here. Tokyo Skytree (Japan), the world's tallest tower with a height of 634 m; Canton Tower, located in Guangzhou, China, is 600-m tall; Canadian National (CN) Tower, located at Toronto, with an altitude of 553.3 m. Several broadcasting towers of moderate heights are located on mountain tops. Their effective elevations are higher than their physical heights [3]. Some of these towers are constructed in Europe, namely, Gaisberg Tower (100-m tall), located in Austria, placed on the top of a 1287-m mountain; Peissenberg Tower (150-m tall) in Germany, located on a 988-m; and the 55-m tall tower Mount San Salvatore in Switzerland erected at the top of 640-m mountain.

The probability of a structure being struck by lightning increases with its height and the flash density it its vicinity. Most lightning flashes to a very tall structure are initiated by the structure itself [3]. Therefore, tall broadcasting towers are often struck by lightning. Hence, it's vital to protect these tall broadcasting structures against the destructive effects of lightning strikes. The prescribed tall structures are well equipped with lightning measurement systems to facilitate lightning studies, which can further assist in the formation of more advanced lightning protection systems. It also helps in understanding the risk posed to electronic and communication systems located in the vicinity of tall structures due to electromagnetic interference (EMI), resulting from the lightning-generated electromagnetic pulse (LEMP).

The lightning phenomenon is discussed in **Chapter 2**, which is followed by a discussion about cloud electrification and different types of lightning.

Chapter 3 contributes to a discussion about CN Tower lightning measurement systems since 1991.

Chapter 4 discusses the presently operational imaging systems (Phantom v5.0 high-speed digital camera and the continuously-recording Sony HDR VJ790VB digital camera) used to record CN Tower lightning flashes. Followed by demonstrating luminosity versus time based on video records obtained from the two imaging systems, to further characterize flash components.

Chapter 5 emphasizes the analysis of a major storm that took place during the night of September 4, 2017, based on the records of high-speed and low-speed digital imaging systems. In this chapter, the comparison between the data sets recorded by the two cameras is conducted. Furthermore, this chapter provides insight on storm's macroscopic characteristics, including the number of flashes, inter-flash time and flash duration.

Chapter 6 focuses on the primary objective of this work, namely the statistical analysis of CN Tower lightning flash components based on the video data, recorded during the past five years (2013-2017). A yearly statistical comparison regarding CN Tower lightning macroscopic (number of flashes, inter-flash times and flash durations) and microscopic (initial-stage current durations, number return strokes and M-components and inter-stroke times) characteristics is conducted. In addition, a vital comparison between two major storms, which took place September 5, 2014 and on September 4, 2017, is performed based on various flash components.

Chapter 7 presents the conclusions that are based on the results of previous chapters. It also includes suggestions for future research based on the contributions of this thesis.

Chapter 2

Lightning Phenomenon

2.1 Physics of Lightning

Lightning is an electrostatic discharge of an excess electric charge developed in a thunderstorm cloud. The primary source of lightning is a cloud type termed cumulonimbus, commonly referred to as thundercloud [3]. Thunderclouds are formed in an atmosphere containing cold dense air aloft and warm moist air at low levels [4]. The parcels of warm moist air at low levels rise in strong updrafts to form clouds. When a parcel rises above the temperature colder than 0 ℃, some water particles starts to freeze, but others remain in a liquid state (they are termed supercooled water droplets) [3]. At temperatures colder than - 40 ℃, all water droplets are frozen. In the temperature range of 0 ℃ to - 40 ℃ supercooled water droplets and ice crystals coexist, forming a mixed phase region where most electrifications occur [3], as shown in Figure 2.1.

The precipitation model of the thundercloud suggests that gravity pulls heavy raindrops, hail, and graupel particles; the small water droplets and ice crystals remains suspended [6]. The microphysics of charge transfer explains that the collisions between falling graupel particles and suspended ice crystals, provided that the temperature is below a critical value called a charge reversal temperature T_R, the falling graupel particles acquire negative charges and the ice crystals attain positive charges. At a temperature above T_R, graupel particles attain positive charges and ice crystals acquire negative charges. T_R is thought to be about -15 ℃ [6].

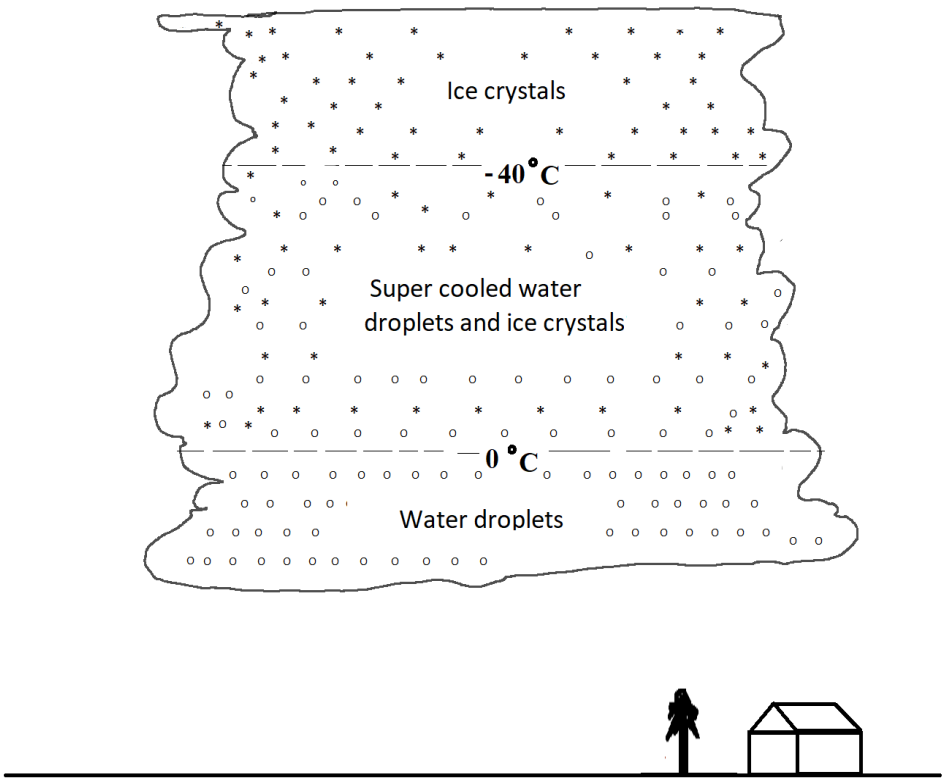

Figure 2.1 – The thundercloud.

It has been observed that a thundercloud comprises a tripolar structure [2], as illustrated in Figure 2.2; with an upper positive charge region (the presence of suspended ice crystals forms the top region), central layer of negative charge (created due to graupel particles that pick negative charges below T_R), and a lower positive charge (created due to graupel particles that pick up positive charges when falling below temperatures higher than T_R). The primary negative charge layer at the center of the thundercloud is always found to be at temperatures between -10 ℃ to -30 ℃ [5]. The top two charge regions (P and N), are usually called main charges, which are often specified to be equal in magnitude. At the bottom of the cloud the small pocket of positive charge exists (p). The two main charge regions (P and N) form a positive dipole. Screening layers are found at the top and sides of the cloud; its origin may be due to cosmic rays, which ionize air molecules [5].

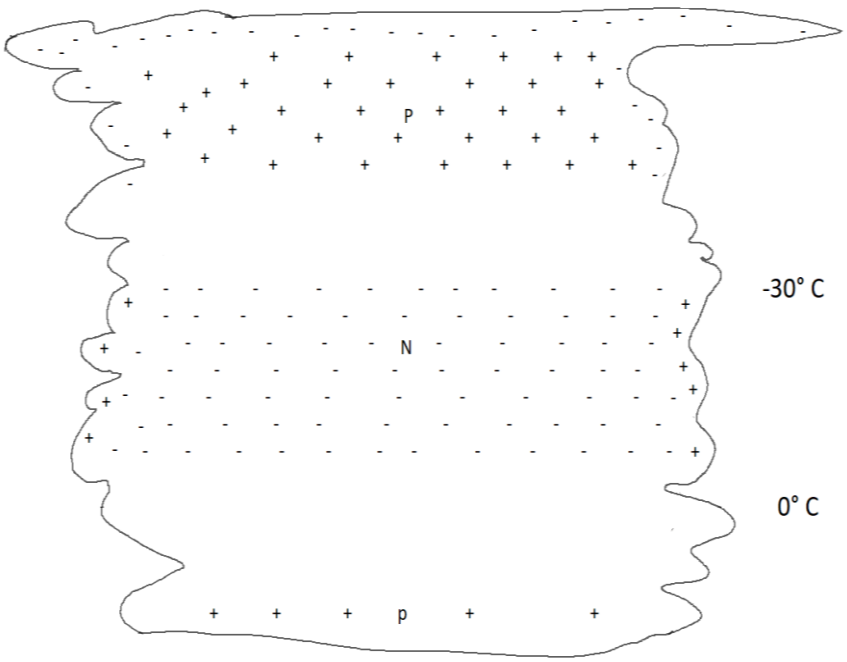

Figure 2.2 – A thundercloud with a fundamental demonstration of electric charge distribution inside the thundercloud.

The electric field intensity at the ground level, under a thunderstorm is typically 1000 V/m (100 to 300 V/m during fair weather conditions). Enhancements of the electric field at the sharp objects on the ground lead to corona discharge and spray positive charge into the air near ground. The ground under the main part of the thunderstorm is also positively charged (which is negative during fair weather conditions) [5].

Lightning can occur between two different charged regions within a single cloud (intracloud), between adjacent clouds (intercloud), between cloud and the air above (cloud-to-air) or between cloud and ground (cloud-to-ground), as illustrated in Figure 2.4 [4]. The cloud-to-ground lightning has been of great interest than other forms of lightning, as it causes numerous injuries to humans and animals, forest fires and disturbance in power transmission and distribution systems [1]. Lightning discharges between a cloud and the ground can be categorized in accordance with the polarity of charge lowered to a ground and the direction of motion of initial leader [3], as illustrated in Figure 2.4.

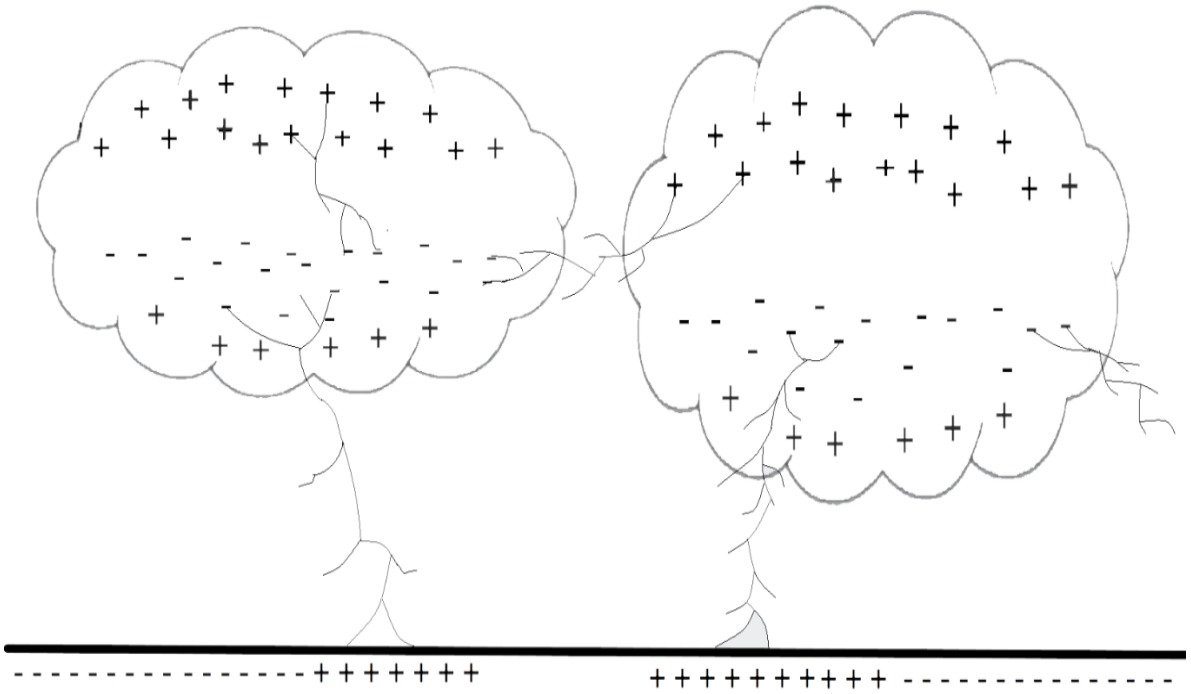

Figure 2.3 – Major Types of Lightning.

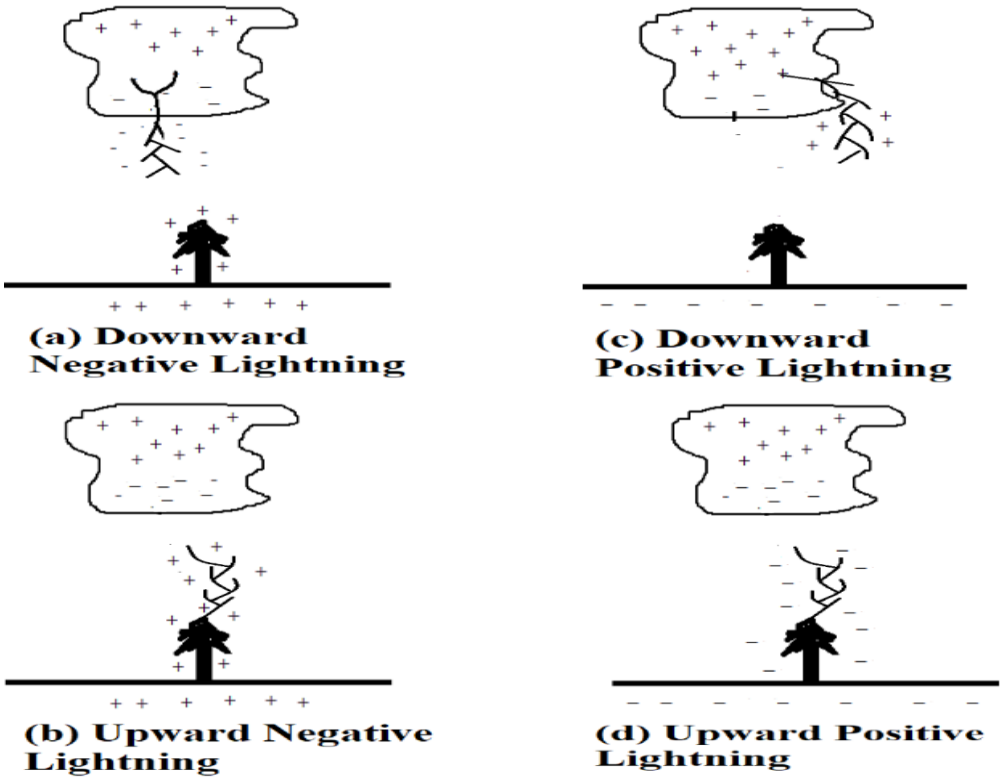

Figure 2.4 – Different types of cloud-to-ground lightning.

It has been observed that about 90% of cloud-to-ground (CG) discharges are negative and about 10% or less are downward positive. The upward negative and positive discharges initiated from tall structures higher than 100-m or objects of reasonable height situated on top of the mountains [3].

2.2 Downward Negative Lightning

Downward negative lightning discharges are initiated in the cloud and propagates in a downward direction, transporting negative charge to ground. The overall cloud-to-ground discharge is referred to as a flash. Each cloud-to-ground flash is composed of a number of strokes. The minimum number of strokes is one [1].

Figure 2.5 illustrates the sequence of processes comprising a negative downward lightning flash. Downward negative lightning discharges are initiated as a result of in-cloud preliminary discharge involving the main negative charge center and the lower positive charge center [3]. The *stepped leader* (SL) is initiated by preliminary breakdown. In negative downward lightning, the stepped leader is a negatively charged plasma channel propagating towards the ground in a series of discrete steps, each is about 50-m in length. As the stepped leader approaches the ground the electric field intensity at the grounded objects is enhanced, and when a specific critical value is exceeded, the upward connecting leader from grounded objects are initiated. This indicates the beginning of the *attachment process* [3]. This process is completed when the upward and downward leaders attain contact, probably some tens of meters above ground. The completion of the attachment process is succeeded by the flow of a *return stroke* (RS) from the ground object to the cloud, which neutralizes the leader charge and effectively lowers several coulombs of the charge deposited on the stepped leader channel, to the ground. The return stroke can often be followed by a continuing current phase, of some hundreds of amperes, lasting for some milliseconds. The perturbations often occur during the steady flow of the continuing current with an associated channel luminosity; such surges are called *M-components* [3]. The M-component mode of charge transfer to the ground requires the existence of a grounded channel carrying a continuing current that acts as a waveguiding structure. It's possible that, as the conductivity of the path to ground decreases, the downward M-component wave can transform into a dart leader.

When the first return stroke and an in-cloud charge activity terminate, the flash may end, and such case is referred to as a single-stroke flash. However, often the residual of the first stroke channel is transversed by a continuous leader known as dart leader [3].

During the time interval between the return strokes and the initiation of the subsequent leader, *J and K processes* occur in the cloud. The J-process amounts to a redistribution of charge in the cloud, in response to the preceding return stroke. The K-processes can be viewed as transients occurring during the slow J-processes. The J-process is often regarded as a relatively slow positive leader extending from the top of the previous channel into the higher areas of the negative charge region, the K-process than being a relatively fast recoil streamer that begins at the tip of the positive leader and propagates to the flash origin. Both the J and K processes, in cloud-to-ground lightning discharges serve to transport additional negative charge into the existing channel, although not all the way to the ground [3]. From a photographic point of view, the K-processes are accompanied by detectable luminosity and are observed to be attempted leaders towards the ground [2], [3]. When this additional charge is available, a continuous leader, known as the *dart leader* (DL), moves through the defunct return stroke channel and deposits a negative charge along the channel length. Some dart leaders exhibit stepping upon approaching the ground, which are referred to as dart-stepped leaders. The apparent difference between the two types of leaders is related to the fact that the stepped leader develops in the virgin air while the dart leader follows the pre-conditioned path of preceding strokes [3]. When dart or dart-stepped leaders approach the ground, the attachment process takes place, after the downward dart leader makes contact with the upward leader initiated from the ground. Once the attachment process is accomplished, the subsequent return stroke wave is initiated and moves upward to neutralizes the leader charge [1], [3].

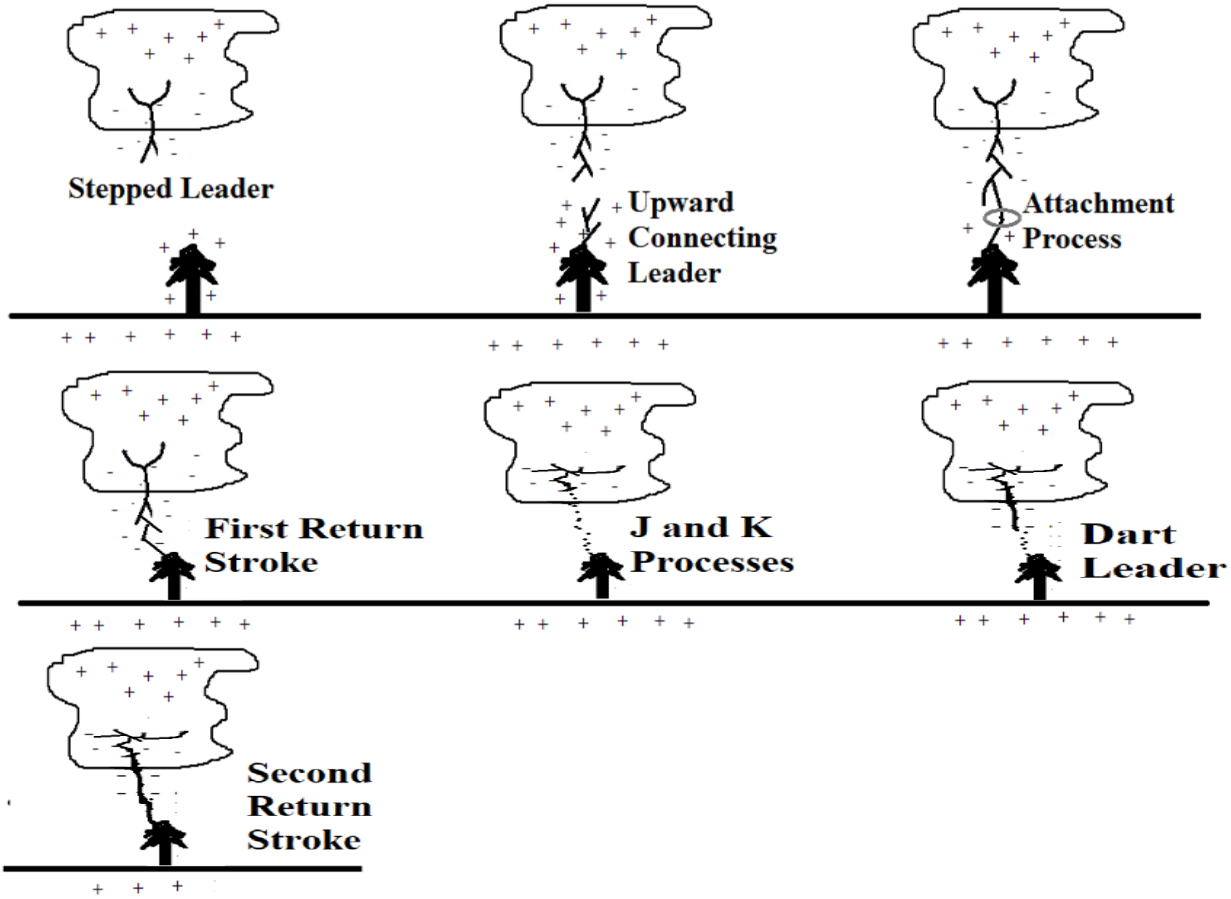

Figure 2.5 – The sequence of processes involved in negative downward lightning flash.

2.3 Downward Positive Lightning

The downward positive lightning transports positive charge from cloud to ground (CG). The positive lightning is of significant practical interest because of its higher current peak and a more substantial amount of charge transferred to the ground as compared to downward negative lightning flash. Positive flashes are generally composed of a single return stroke succeeded by a phase of a continuing current, preceded by significant in-cloud activity. Photographic observations show that positive lightning discharges usually exhibit up to tens of kilometers of horizontal channels. The positive cloud-to-ground lightning is relatively frequent during the dissipating stage of a thunderstorm or winter thunderstorms [1], [3].

2.4 Upward Initiated Lightning

The discovery of upward-initiated-lightning is generally attributed to McEachron (1939) who made photographic and current measurements at the Empire State Building (a steel frame building 443.2-m in height) in New York. Upward lightning discharges are usually initiated by leaders that originate from grounded objects, generally tall towers or moderate height structures located on the top of a mountain and propagate upwards towards the charged clouds aloft. Structures with elevation less than 100-m usually experience downward lightning, objects within the altitude of 100-500 m experience both upward and downward lightning flashes, and structures with height above 500-m experience upward-inititated lightning. Upward negative discharges are initiated by upward positive leader initiated from tall grounded objects, Figure 2.4(b), and upward positive discharges are initiated by upward negative leaders initiated from ground objects, Figure 2.4(d). It has been observed that upward-initiated lightning usually lowers negative charge to ground than positive charge [3].

Upward leaders are initiated from the tops of the tall grounded structure when the electric field intensity due to in-cloud discharge occurring in the charged cloud built overhead of tall structure, exceeds the breakdown value over some critical distance from the tip of the tall object. As the upward leader from the top of a tall structure links the gap between the tall grounded structure and the thundercloud aloft, the initial continuous current flows from the cloud toward the tall grounded object. The lightning flash may terminate after the flow of the initial continuous current or can be followed, after a phase of a no current interval, by a sequence of the subsequent downward leader and upward return stroke [3], as illustrated in Figure 2.6.

Upward lightning can also be initiated artificially by launching a rocket that extends a thin wire into the gap between the charged cloud and the ground that later gets replaced by the plasma channel of an upward leader. Like tall object-initiated lightning discharges, rocket-triggered flashes are composed of initial stage current (ISC) followed by downward-leader-upward-return-stroke sequences [3]. The initial stage current in tall object-initiated lightning is similar to the initial stage current in rocket-triggered lightning, except for ISC pulses, which in object-initiated lightning exhibit larger peaks, shorter risetimes and shorter half-peak widths than those for ISC pulses in rocket-triggered lightning. The observed differences are assumed to be a result of the

more profound branching of tower-initiated lightning discharges in comparison with rocket-triggered lightning [7], [8].

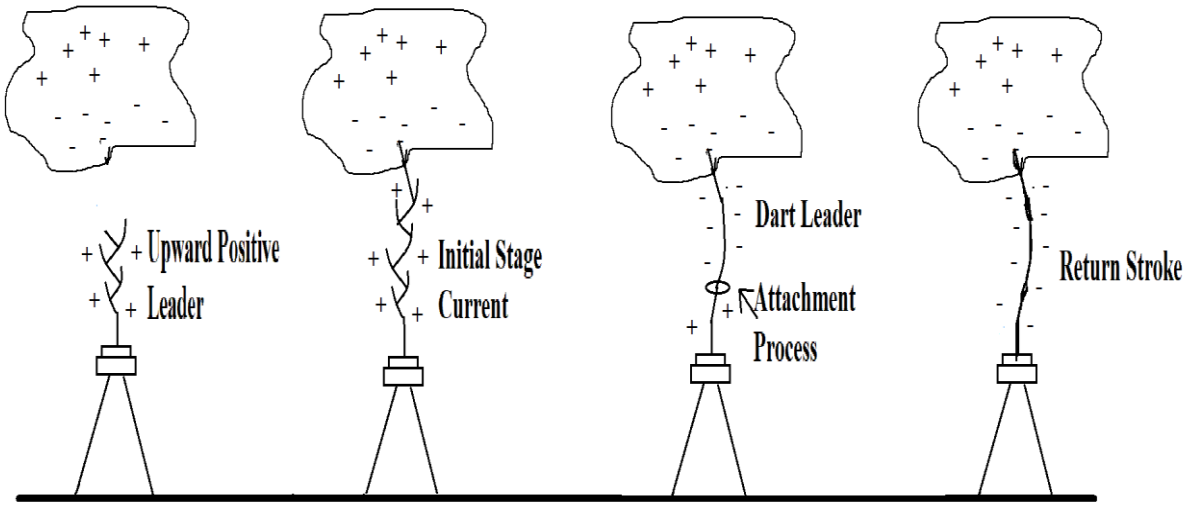

Figure 2.6 – The sequence of processes involved in an upward negative lightning.

Chapter 3

CN Tower Lightning Measurement Systems

3.1 Overview of the Measurement Systems

The Canadian National (CN) Tower is 553-m high, one of the tallest free-standing structure in the world located at 43.64°N and 79.38°W, in downtown Toronto, Ontario, Canada. CN Tower usually receives several dozens of lightning flashes yearly [9], due to its high altitude. Although, the lightning ground flash density is about two [10]. Therefore, CN Tower presents one of the best sites in the world to observe lightning to study the physics of lightning phenomenon and to collect the characteristics of optical parameters [11], [12]. The lightning strikes to the CN Tower were first observed in 1978. Since 1991, five measurement systems commenced to operate to simultaneously capture the return stroke current derivative (using Rogowski coil and Tektronix RTD 710A digitizer), the vertical component of electric field; the azimuthal and radial component of magnetic field (using broadband active sensors and Tektronix RTD 710A digitizers), the 2-D images of flash trajectories (using the VHS cameras) and the return stroke velocity (using photodiode system). Since 1996, the proliferation of measurement systems has been occurring. In 1996, a high-speed camera with a frame rate of 1000 frames/second (vision research phantom v2.0). In 1997, an optical fiber link and a new Rogowski coil with a noise protected current sensing system was installed.

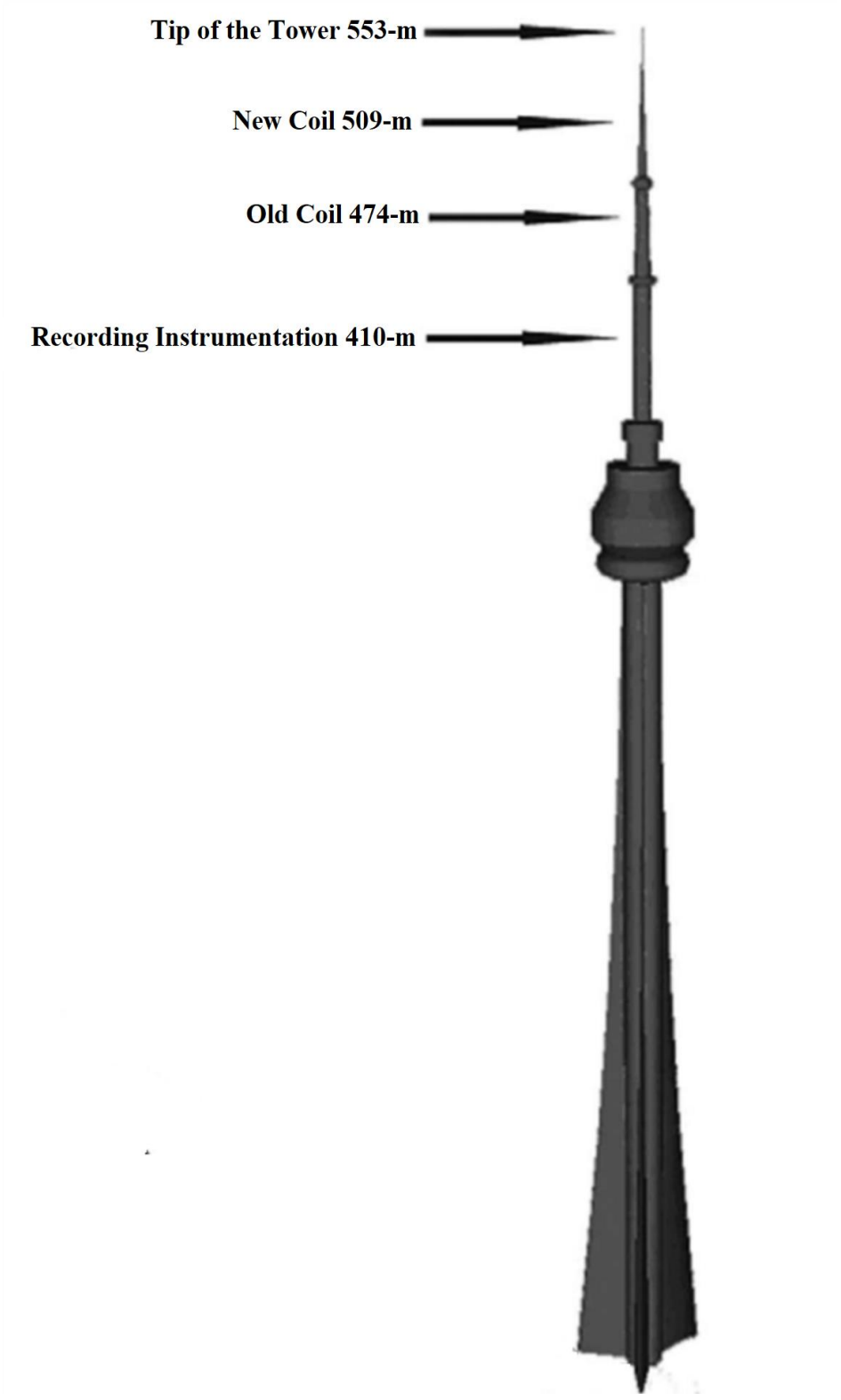

Figure 3.1 – The CN Tower and Location of Instruments.

In 2001, two double-channel digitizers (LeCroy LT362), with 2 ns time resolution were acquired to record the current derivative and its radiated electromagnetic fields for lightning return strokes. The four units of a Global Positioning System (GPS) were also acquired for time synchronization of CN Tower lightning recording instruments [13]. In order to avoid the contamination of the initially-injected lightning current by reflections from the tower's structural discontinuities, the Rogowski coils were placed as far as possible from main structural discontinuities, namely the tip of the tower, the top and bottom of the Space Deck, the top and bottom of the Sky Pod, and ground [14]. The locations of the CN Tower lightning measurement systems are illustrated in Figure 3.1 [15].

3.2 Old Rogowski Coil

In order to measure the lightning current derivative a 40 MHz bandwidth, a Rogowski coil was installed in 1990 at the 474-m above ground level (AGL). The coil has a sensitivity of 0.359 V/(A/ns) and it encircles one-fifth of the CN Tower's pentagonal structure, as illustrated in Figure 3.2 [16]. Due to the cross-sectional symmetry of the structure, the measured signal corresponds to 20% of the total lightning current. The 3-m long coil consists of two 1.5 m pieces, which are connected to a matching impedance at one end and resistors at another end, to absorb any reflections and damp oscillations in the coil. The impedance box is connected via 165 m, 50 Ω triaxial cable (Belden RG-8/U) to one channel of LeCroy LT342L digitizer.

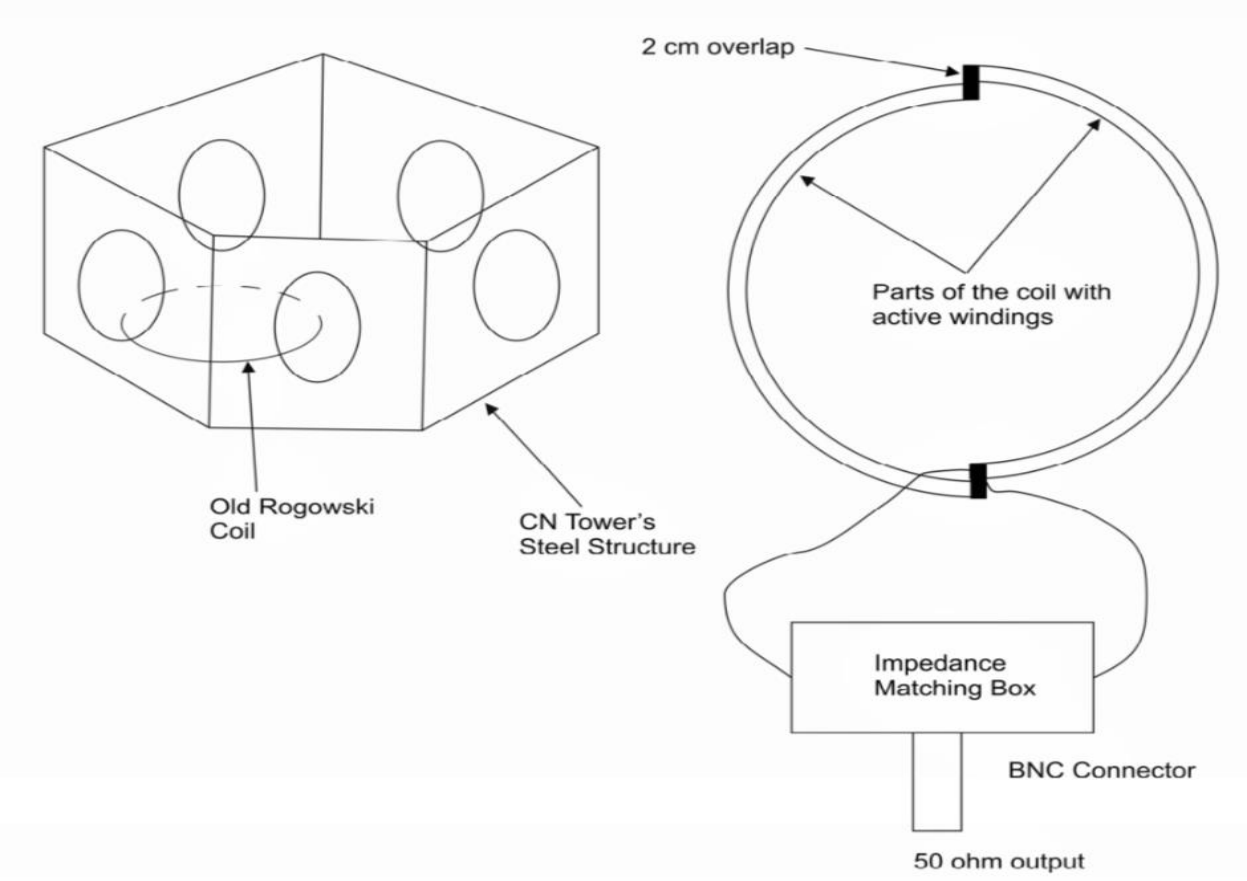

Figure 3.2 – The Old Rogowski Coil location and connection.

The lightning current measured by the old Rogowski coil, contains a significant amount of noise and the apparent reasons for that are:

- The coil encircling one-fifth of the CN Tower's pentagonal steel structure, and thus leading to the measurement of only 20% of the total amount of current.
- The use of 50 Ω, 165-m triaxial cable, to connect the old Rogowski coil to the digitizer.
- The old Rogowski coil is susceptible to noise from communication antennas as well as the LORAN-C signals used for radio navigation by the ships [24].

3.3 New Rogowski Coil

In 1997, a new Rogowski coil with 20-MHz bandwidth was installed at 509 m AGL. Its first measurement current derivative signal was recorded in 1999. The new 6-m long Rogowski coil comprises four 1.5 m long segments, and it encircles the whole CN Tower's steel structure. Hence it measures the total lightning current derivative signal. The sensitivity of the new coil is 1.264 V/(A/ns). The coil is connected to the recording station placed at 403 m AGL, via an optical fiber link, as illustrated in Figure 3.3 [16]. The two segments of the coil are connected to a matching box 1, and another two sections are connected to matching box 3. Matching boxes 1 and 3 are then connected to matching box 2 so that a 50 Ω impedance is obtained at the output of matching box 2. Furthermore, a 30-dB attenuator was used between matching box 2 and an optical transmitter, to avoid the saturation of the optical fiber link.

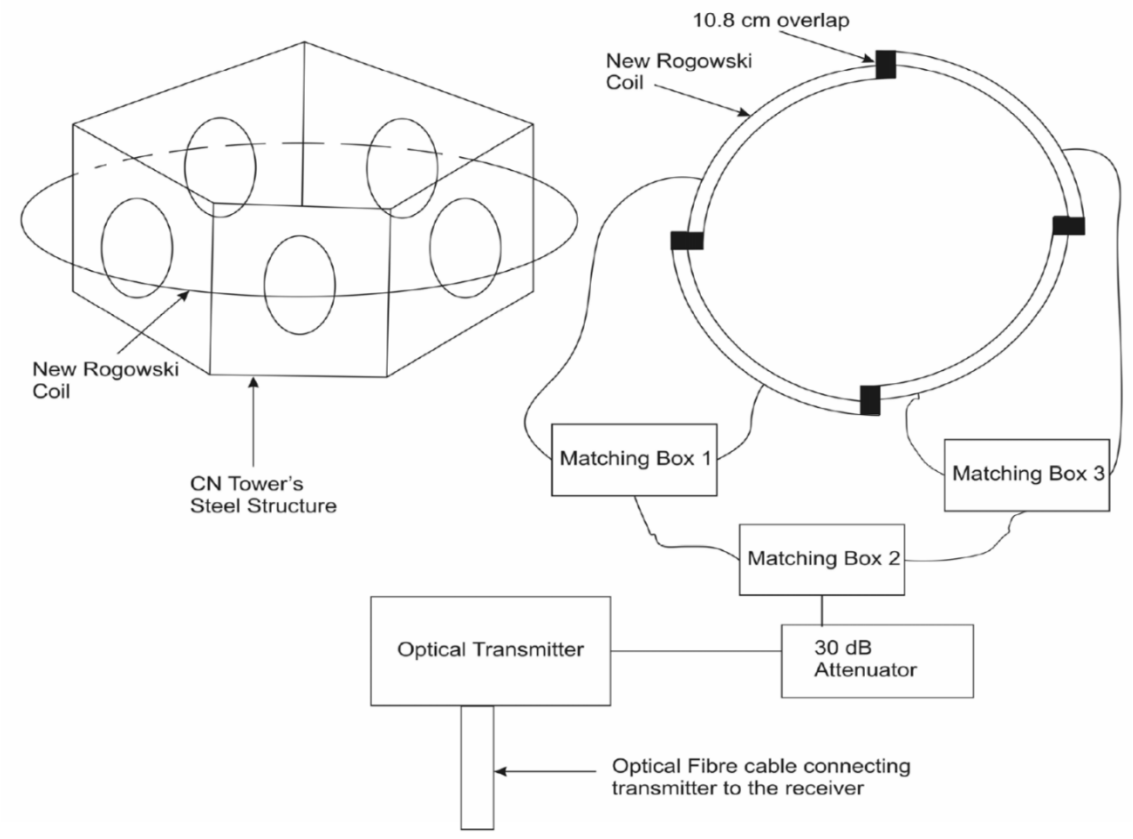

Figure 3.3 – The new Rogowski Coil location and connection.

The current derivative signals recorded by the new Rogowski coil has better signal-to-noise ratio in comparison with the current derivative signal recorded by the old Rogowski coil due to the following facts:

- The new Rogowski coil measures 100% of the total lightning current derivative signal.
- The coil is connected to the recording station via an optical fiber link.
- The advanced design of the new Rogowski coil makes it less susceptible to noise.

3.4 Real-Time Digitizers

The real-time digitizers are used to obtain the lightning current derivative signals. Since 2011, two independent measurement systems have been recording CN Tower lightning current derivative signals and each system had its digitizer. The old Rogowski coil is connected via a triaxial cable to a new double-channel 8-bit National Instrument (NI) PCI 5114 digitizer. The new Rogowski coil is connected via NanoFast optical fiber link to the LeCroy LT342L digitizer. In 2014, a more advanced NI PXIe 5160 digitizer was acquired. The NI PXIe 5160 digitizer along with a timing module and the embedded controller is placed in NI PXIe-1082 chassis [17].

Technical Specifications of NI PCI 5114 digitizer

- Number of channels: 2
- Memory per channel: 64 MB
- Bandwidth: 12 Hz to 125 MHz
- Resolution: 8 bits
- Sampling: up to 250 MS/s

Technical Specifications of LeCroy LT342L

- Number of channels: 2
- Memory per channel: 2 MB
- Bandwidth: 25 Hz to 500 MHz
- Resolution: 8 bits
- Sampling: up to 500 MS/s

Technical Specifications of NI PXIe 5160

- Number of channels: 2
- Memory per channel: 2 MB
- Bandwidth: 500 MHz
- Resolution: 10 bits
- Sampling: up to 50 GS/s

3.5 Flash Trajectory Imaging Systems

Although the lightning current derivative has been measured at the tower since 1991, the characterization of CN Tower lightning flash components has been a significant challenge because the current derivative measurement systems have been configured to trigger on the high rate of rise of the current [18], [19]. It was impossible to record currents with low rates of rise, such as the initial-stage current (ISC), the M-components and the continuing current (CC), with such measurement configuration of the current derivative measurement systems. The acquisition of the digital imaging systems provides the detailed information of flash components including the ISC, M-components, return strokes, continuing current duration and flash duration. The video records also provide the details regarding flash direction (upwards or downwards).

Chapter 4

CN Tower Lightning Imaging Systems

CN Tower lightning trajectories are recorded by a continuously recording Sony HDR PJ790VB digital camera (CRC), operating at 60 fps and a Vision Research Phantom v5.0 digital high-speed camera (HSC), operating at 1000 fps.

The analysis of CN Tower lightning flashes captured by the two cameras is carried out by studying the maximum and average lightning channel luminosity variation along successive frames, across a certain pixel level, within each flash [13], [25]. The luminosity variation with time is analyzed with the help of RGB values recorded for the pixels, in successive frames of a video, captured by the two digital cameras. The records of both HSC and LSC are used to characterize the various CN Tower lightning flash components, within each flash.

It's important to mention that, in many cases, when the low-speed camera records were perfectly time matched with the lightning currents measured at the tower, a linear correlation between channel luminosity peak and the current peak has been established [13].

4.1 High-Speed Digital Camera

In 2006, a phantom v5.0 HSC (Fig. 4.1) operating at 1 ms resolution (capturing 1000 frames per second), representing each frame is captured in 1 ms was acquired and it is placed at 4.31 km, 36.54° north-north-east (NNE) of the tower at Broadview Ave., as illustrated in Figure 4.2. The pixel resolution of HSC is 1024x1024. However, it has been set to operate at 512x512 pixel

resolution, to provide a longer recording time of 1300 ms, out of which 300 ms is used as a pre-triggering time to ensure the recording of the initial stage current. The remaining time (1000 ms) is set to record the return strokes, continuing currents (CC) and M-components. Phantom v5.0 HSC has internal image storage memory of 1024 images per second, at 1000 fps [21], [25].

The exposure time of HSC is 10 μs, and it's triggered by external Miops Nero trigger. The Phantom v5.0 has SR-CMOS anti-blooming sensors, which allows continuously variable shutter speeds down to 10 μs. [20], [21].

Figure 4.1 – Phantom v5.0 digital high-speed camera.

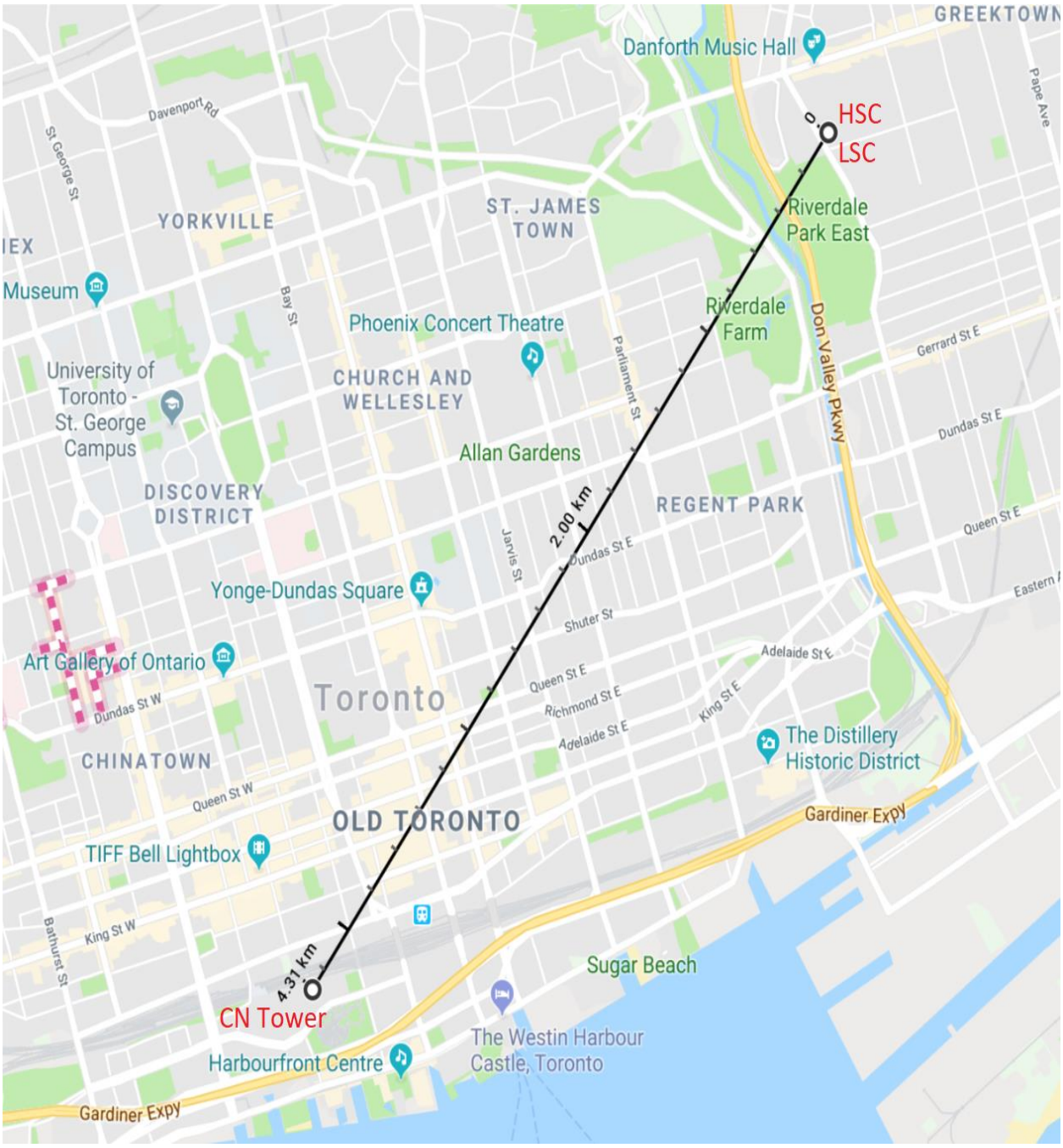

Figure 4.2 – Location of Phantom v5.0 HSC and Sony HDR PJ790VB LSC.

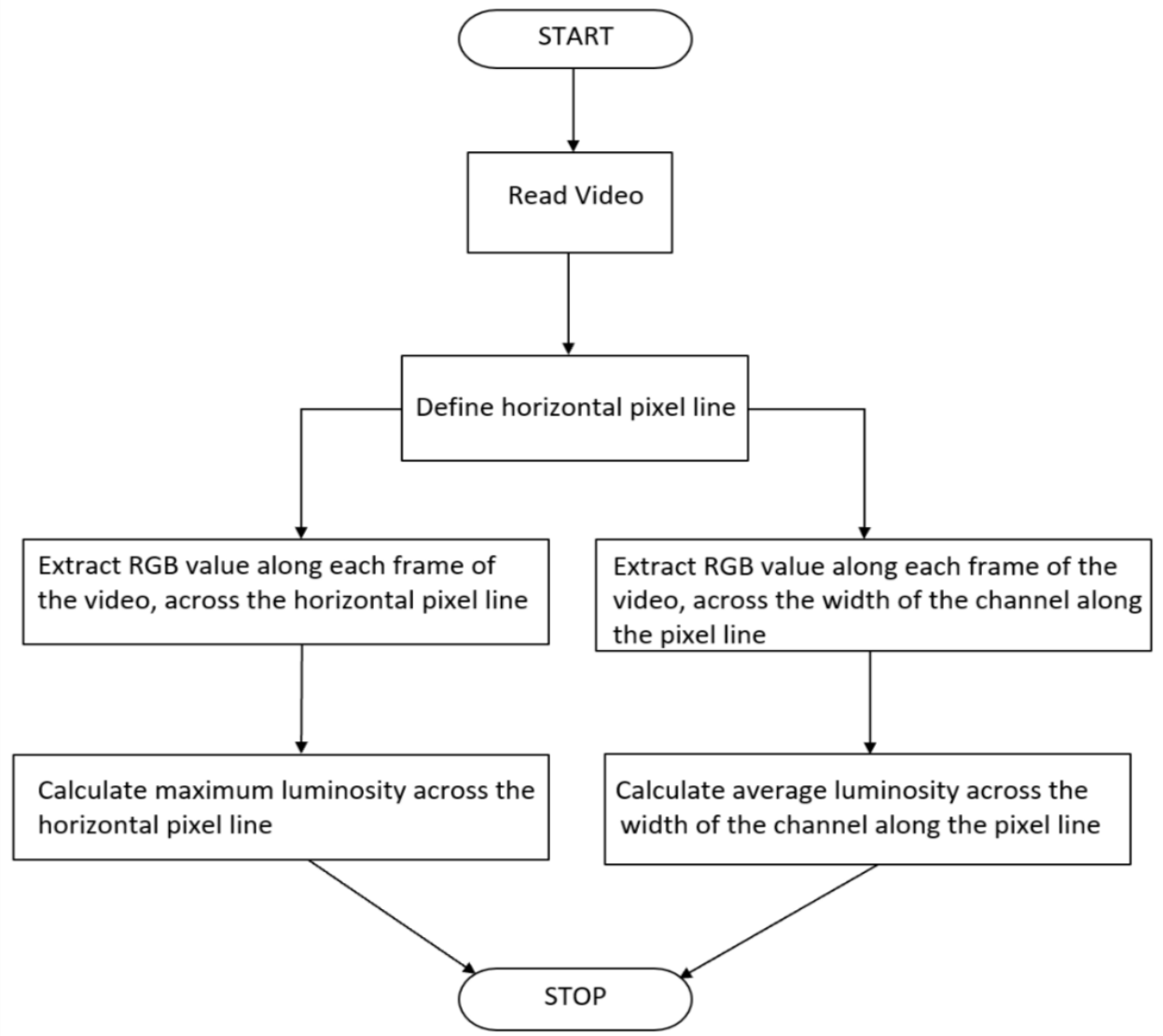

Figure 4.3 – Flow chart describing the methodology of analysis of video records.

The HSC comprises 24 bits-per-pixel (bpp), which indicates that the red, green and blue subpixels, for each pixel, use 8 bits each, which have integer value from 0 to 255. Due to the saturation level at 255, the luminosity variation beyond that level is not recorded. To resolve this problem, the average luminosity variation with time across the width of the channel is determined.

The images recorded for each flash captured by Phantom v5.0 are saved in separate files with extension *.cine*. The raw .cine files can be converted to the desired format using Phantom Camera Control (PCC) software, which can be further processed in MATLAB to obtain luminosity variation with time, for each flash recorded [25]. The analysis of luminosity time variation is

performed along the successive frames of the video records, along the horizontal pixel line carrying the brightest pixels. The maximum and average luminosity variation with time for various flashes, captured by Phantom v5.0 HSC are presented in the following figures. Flash trajectory images presented in this thesis represents the brightest frames of flashes and are used to represent the horizontal pixel line level, across which the luminosity time variations for each flash is calculated. The horizontal level of the pixel line is different for every flash because every flash have different lightning channel trajectory with different brightest levels that shows the appropriate luminosity variations that could help to determine various flash components

Figure 4.4 illustrates the channel trajectory image of the second flash recorded on July 8, 2013. The figure demonstrates that the flash struck the tower 17 m below its tip. At the horizontal pixel line Y = 322, the maximum luminosity variation with time across the whole pixel line is evaluated over 1300 frames and presented in Figure 4.5 (blue). The average luminosity variation across the 10-pixel wide channel is also demonstrated in Figure 4.5 (red).

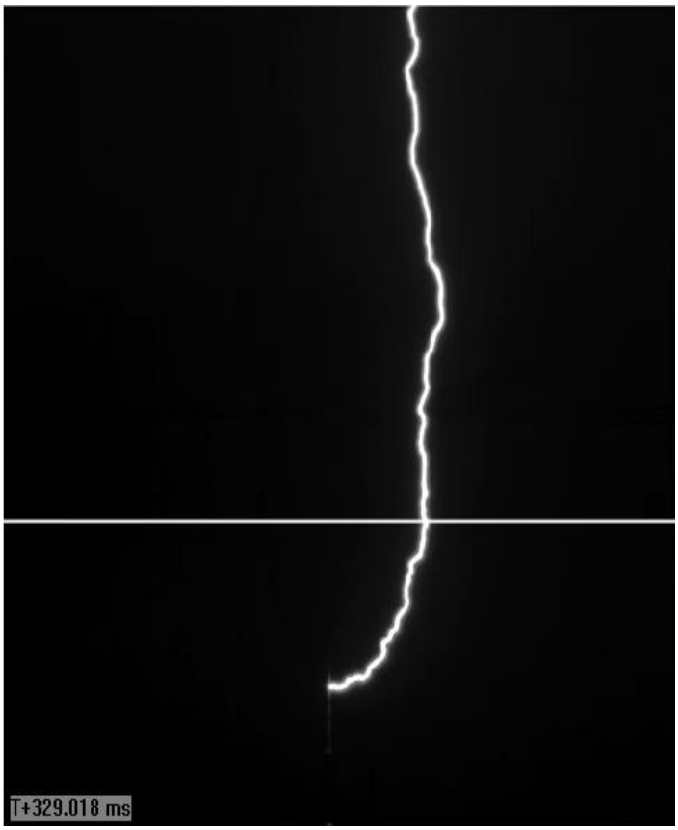

Figure 4.4 – Channel trajectory image of the second flash recorded on July 8, 2013.

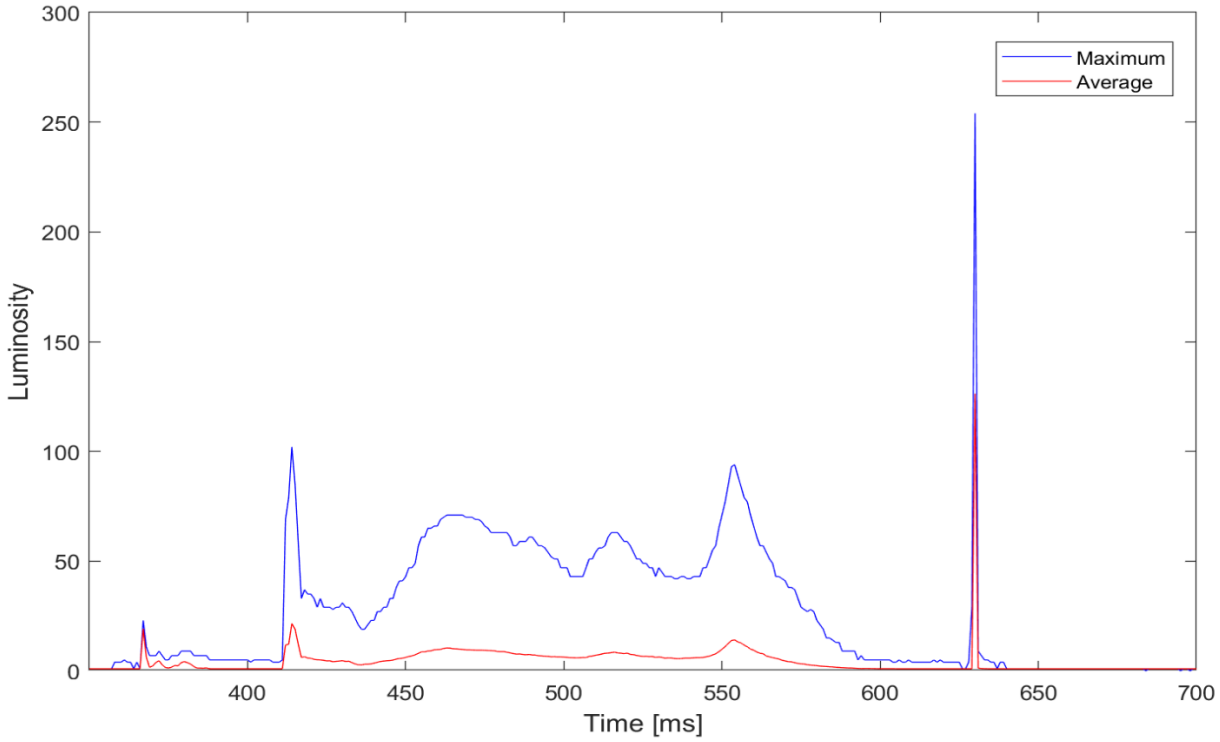

Figure 4.5 – Maximum and average channel luminosity time variations along the horizontal pixel line Y=322.

The channel luminosity variation with time, as illustrated in Figure 4.5 presents the existence of an initial stage current (ISC) that lasted for 267 ms, followed by a single return stroke.

Figure 4.6 presents the channel trajectory image of the fourth flash recorded on July 14, 2016. At the horizontal pixel line of 326, the maximum luminosity variation with time is evaluated across the whole pixel line (blue) and the average luminosity variation with time is calculated across a 12-pixel wide channel (red), is illustrated in Figure 4.7.

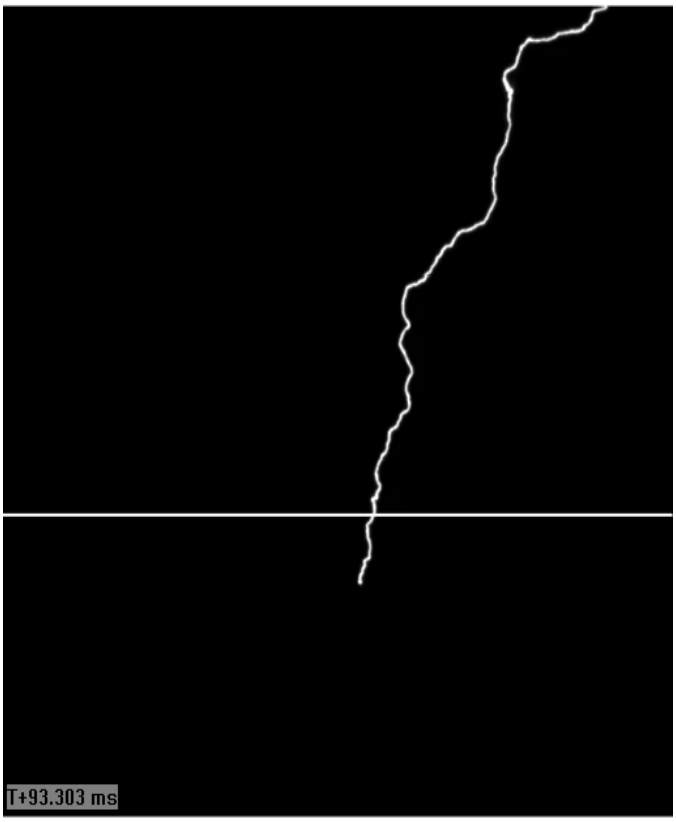

Figure 4.6 – Channel trajectory image of the fourth flash recorded on July 14, 2016.

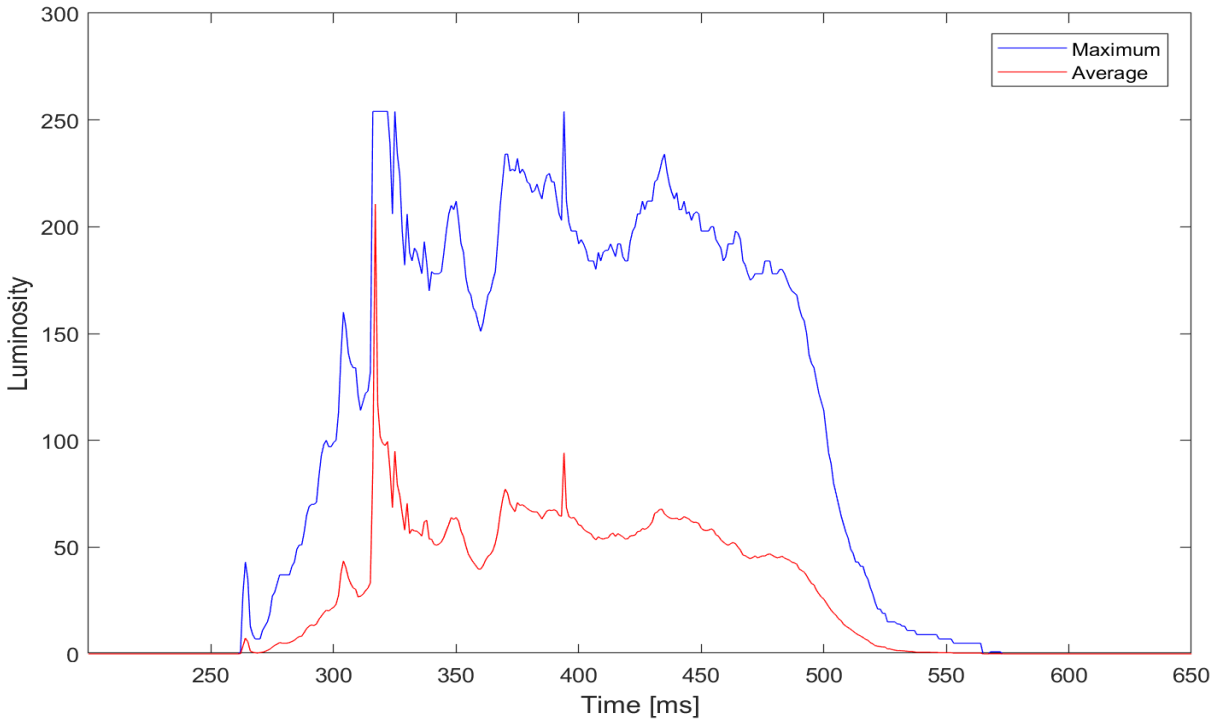

Figure 4.7 – Maximum and average channel luminosity time variations along the horizontal pixel line Y=326.

The luminosity variation with time as demonstrated in Figure 4.7, reveals the existence of an ISC of duration 310 ms, containing several M-components.

4.2 September 5, 2014 Storm Captured by HSC

It was observed that on September 05, 2014, the HSC recorded a total of thirteen CN Tower flashes. The storm lasted for 111.4 mins, resulting in, on an average, a flash to the tower every nine mins. The storm led to 13 flashes containing a total of 10 return strokes and the flash multiplicity varied between 1 to 3. Figure 4.8 presents the flash multiplicity of flashes with respect to time of occurrence. The figure demonstrates the flash multiplicity of the six flashes (blue lines) and the red squares represents the flashes that contained only the initial-stage current (ISC).

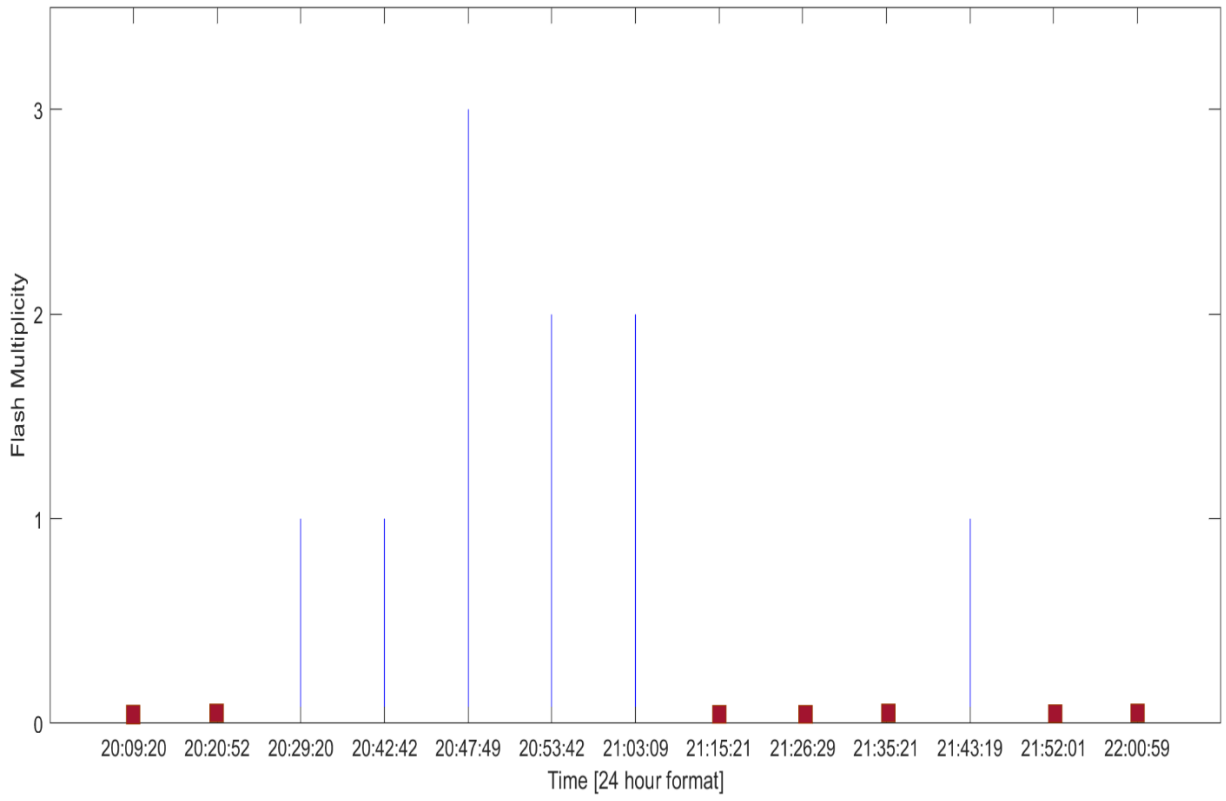

Figure 4.8 – Flash multiplicity of September 5, 2014 storm.

The following figures present the maximum and average luminosity variation with time for the two flashes that struck the tower during 2014 storm.

Figure 4.9 illustrates the channel trajectory image of the third flash that struck the tower during the storm. At the horizontal pixel line Y = 299, the maximum and average luminosity variation across the whole pixel line and across the 15-pixel wide channel is evaluated respectively, as shown in Figure 4.10.

Figure 4.9 – Channel trajectory image of the third flash recorded on September 5, 2014.

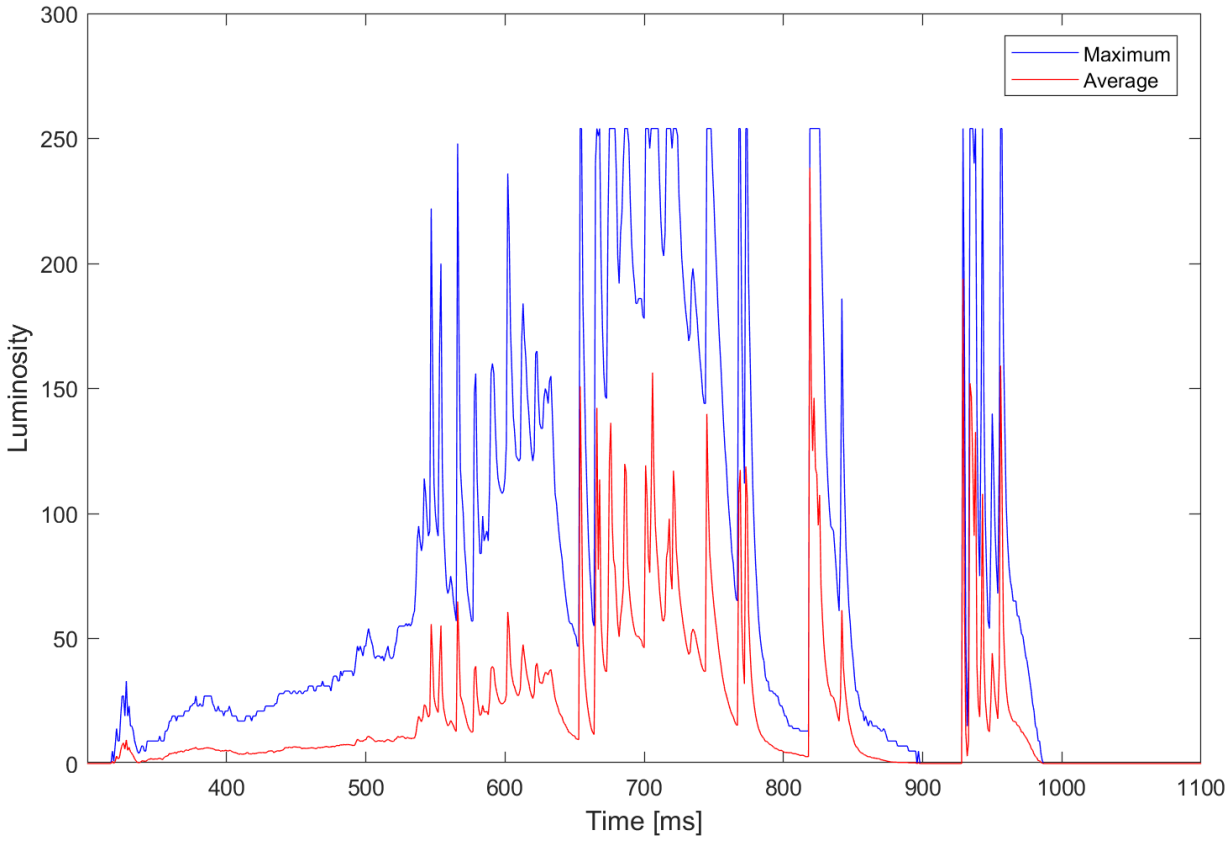

Figure 4.10 – Maximum and average channel luminosity time variations along the horizontal pixel line Y=299.

The luminosity variation with time as illustrated in Figure 4.10 reveals the existence of ISC of duration 591 ms, containing several M-components, followed by one return stroke and a continuing current, containing several M-components.

Figure 4.11 presents the channel trajectory image of the twelfth flash that CN Tower received. At the horizontal pixel line Y = 270, the maximum and average luminosity variation across the whole pixel line and across the 10-pixel wide channel is evaluated respectively, as presented in Figure 4.12.

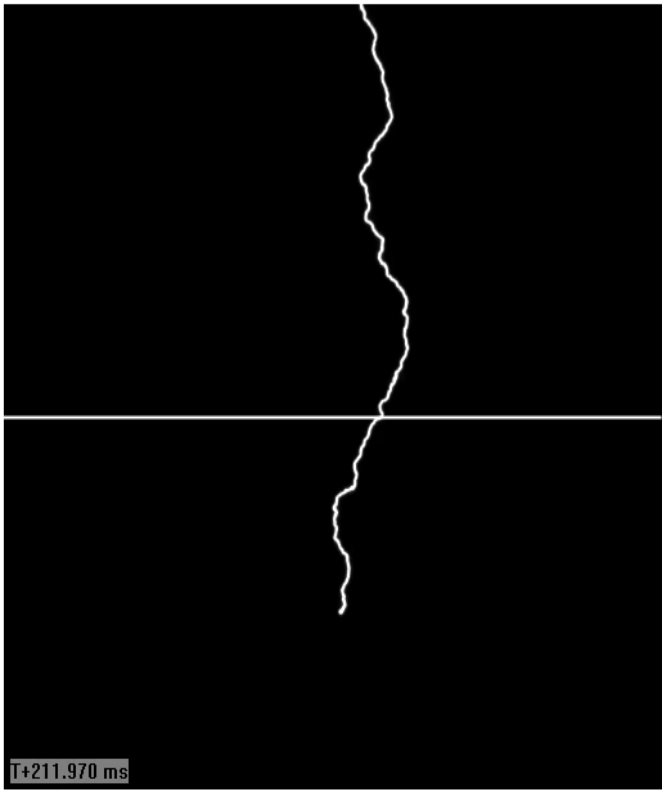

Figure 4.11 – Channel trajectory image of the twelfth flash recorded on September 5, 2014.

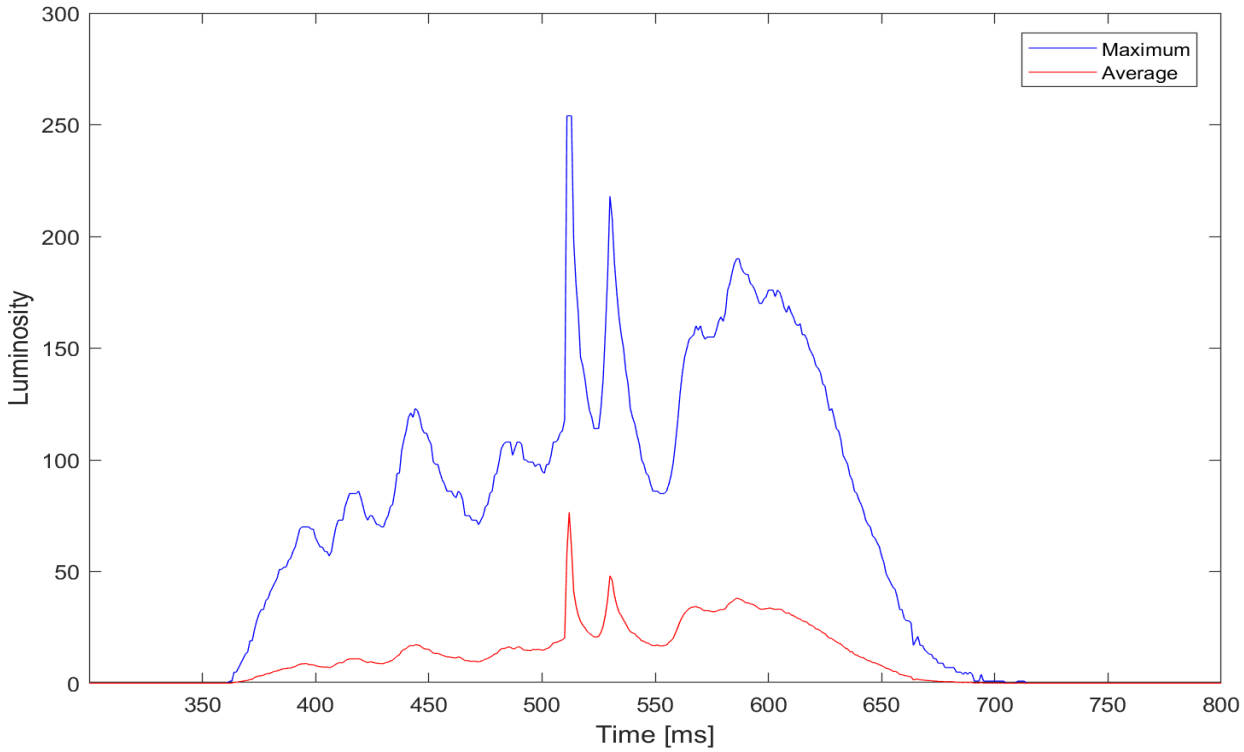

Figure 4.12 – Maximum and average channel luminosity time variations along the horizontal pixel line Y=270.

The luminosity variation with time as demonstrated in figure 4.12, reveals the existence of only ISC of duration 360 ms, containing several M-components.

4.3 Continuously Recording Digital Camera

The Sony HDR PJ790VB digital low-speed camera (LSC) is placed beside the HSC (Figure 4.13). It operates at 60 frames/sec (time resolution of 16.67 ms), representing that every single frame of video is captured in 16.67 ms and it has 1090x1080 pixel resolution. It has an embedded flash memory of 96 GB, which allows the continuous recording up to 37 hours and 50 mins. It has back-illuminated Exmor CMOS sensor which performs on-chip analog to digital signal conversion and noise reduction. It comprises 24 bits per pixel, which indicates that the red, green and blue subpixels, for each pixel uses 8 bits each. The Sony HDR PJ790VB store the recorded files in *.m2ts* format. The raw .m2ts format can be converted to the desired format using Sony PlayMemories software, that can be further processed in MATLAB to obtain luminosity time variation plots for the recorded flashes. The following figures demonstrate the maximum and average luminosity time variation of several flashes captured by LSC.

Figure 4.13 – Sony HDR PJ790VB digital low-speed camera.

Figure 4.14 illustrates the channel trajectory image of the second flash recorded by LSC on September 7, 2016. At a horizontal pixel level of Y = 320, the maximum and average luminosity variation with time is evaluated, across the whole pixel line and the 12-pixel wide channel respectively, as shown in Figure 4.15.

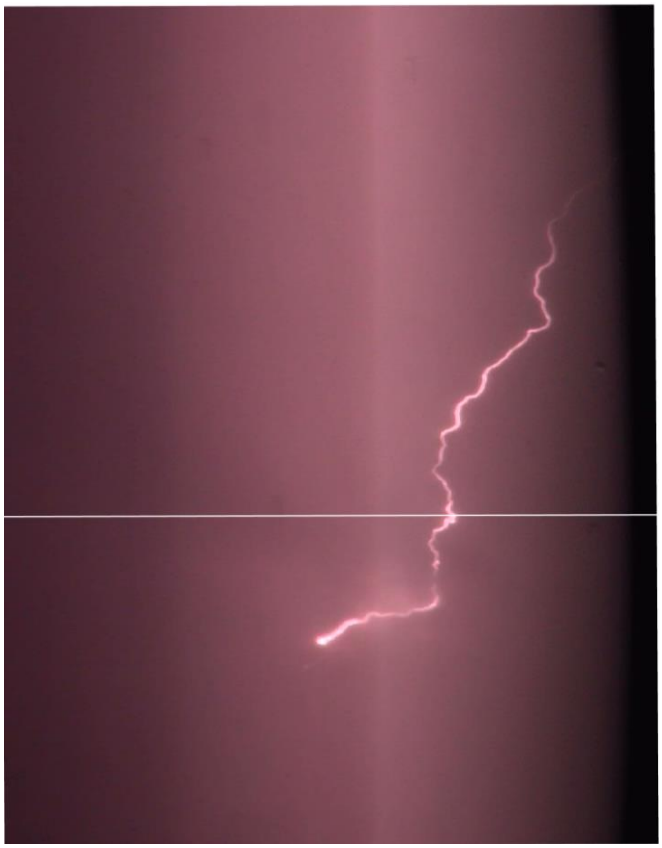

Figure 4.14 – Channel trajectory image of the second flash recorded on September 7, 2016.

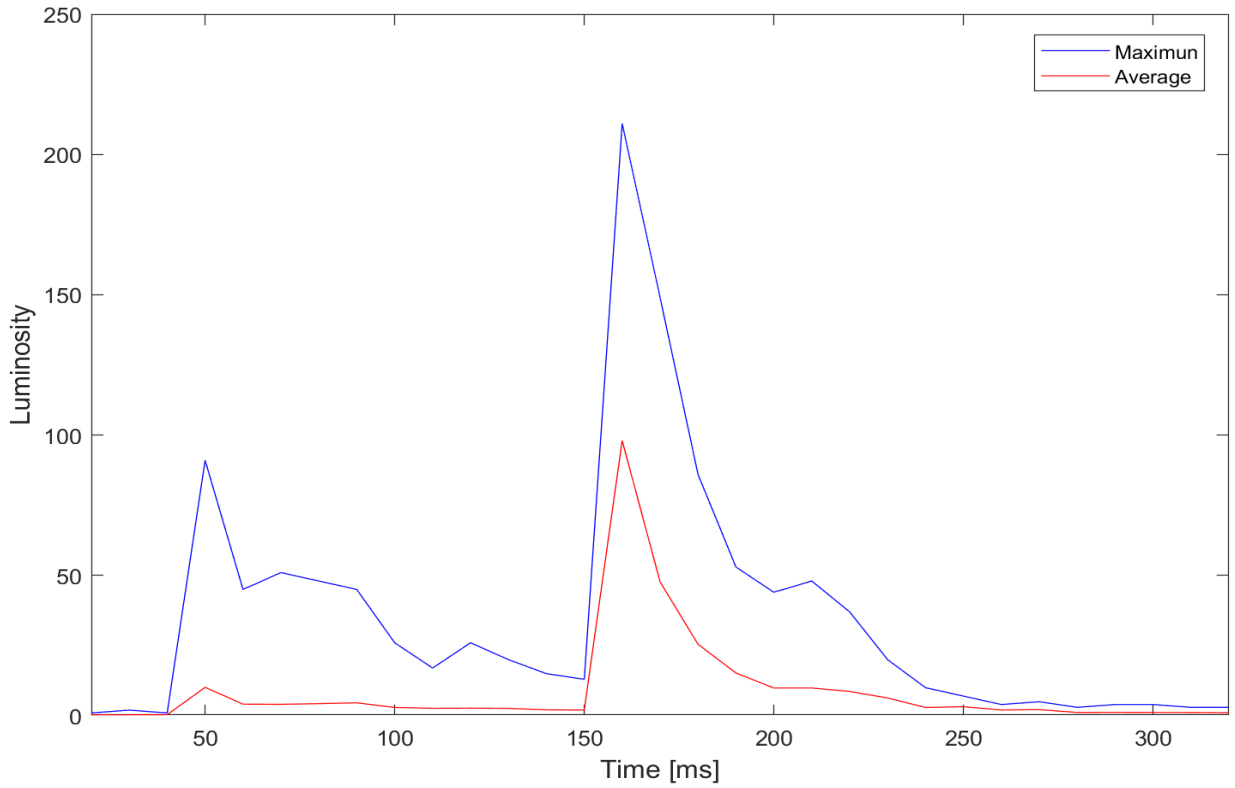

Figure 4.15 – Maximum and average channel luminosity time variations along the horizontal pixel line Y=320.

The luminosity variation with time as presented in Figure 4.15 reveals the existence of only ISC, with a duration of 198 ms, containing several M-components.

Figure 4.16 demonstrates the channel trajectory image of the third flash recorded on July 8, 2013. The maximum and average luminosity variation with time is evaluated at a horizontal pixel line level of Y = 360, across a whole pixel line and a 15-pixel wide channel respectively, as shown in Figure 4.17.

Figure 4.16 – Channel trajectory image of the third flash recorded on July 8, 2013.

The luminosity variation with time as illustrated in Figure 4.17, reveals the existence of an ISC, with a duration of 158 ms, containing several M-components.

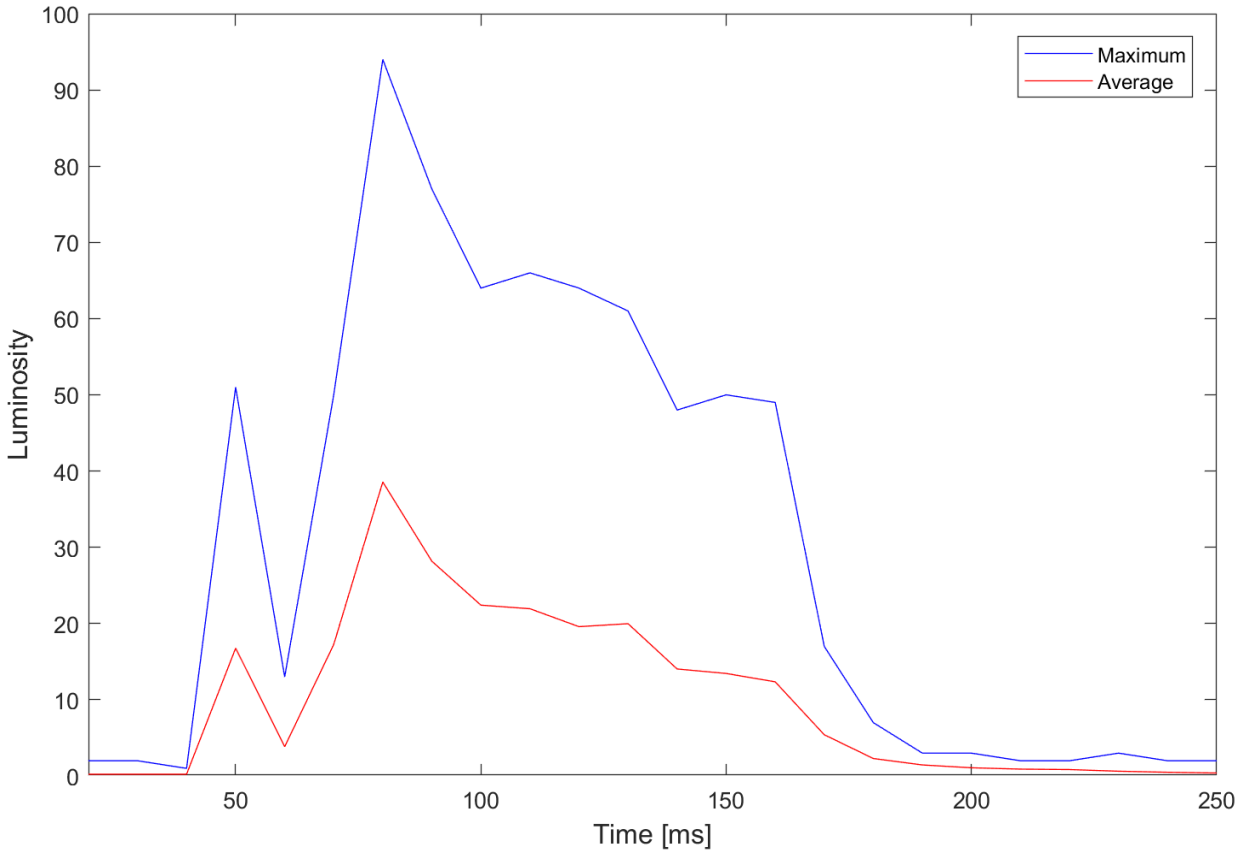

Figure 4.17 – Maximum and average channel luminosity time variations along the horizontal pixel line Y=360.

Chapter 5

Lightning Storm Observed at CN Tower on September 4, 2017

The Sony HDRPJ790VB digital low-speed camera (LSC) proved to be pivotal for continuously recording all lighting events at the tower, and its records are later analyzed to confirm the operation and failure of other CN Tower lightning measurement systems. The September 4, 2017 storm, which lasted for 2961 s (49.35 minutes), produced eleven flashes to the tower with an average inter-flash time of 291.9 s. Figure 5.1 presents the channel luminosity variation with time for the entire storm based on LSC trajectory records. The figure indicates the existence of eleven flashes during the storm [22].

Although it was observed that LSC recorded eleven CN Tower flashes, the HSC records were found to only contain four flashes. It's worth mentioning that the absence of GPS timing in LSC records required extensive analysis of the inter-flash timing of the two data sets to match the four HSC records, with the corresponding LSC flashes. This comprehensive analysis produced exact matching. It was found out that the four HSC flashes matched the LSC flashes HSC1, HSC2, HSC3, and HSC4, as illustrated in Figure 5.1. The inter-flash times for the two data sets were found to be 282s, 192s, 695s respectively [22].

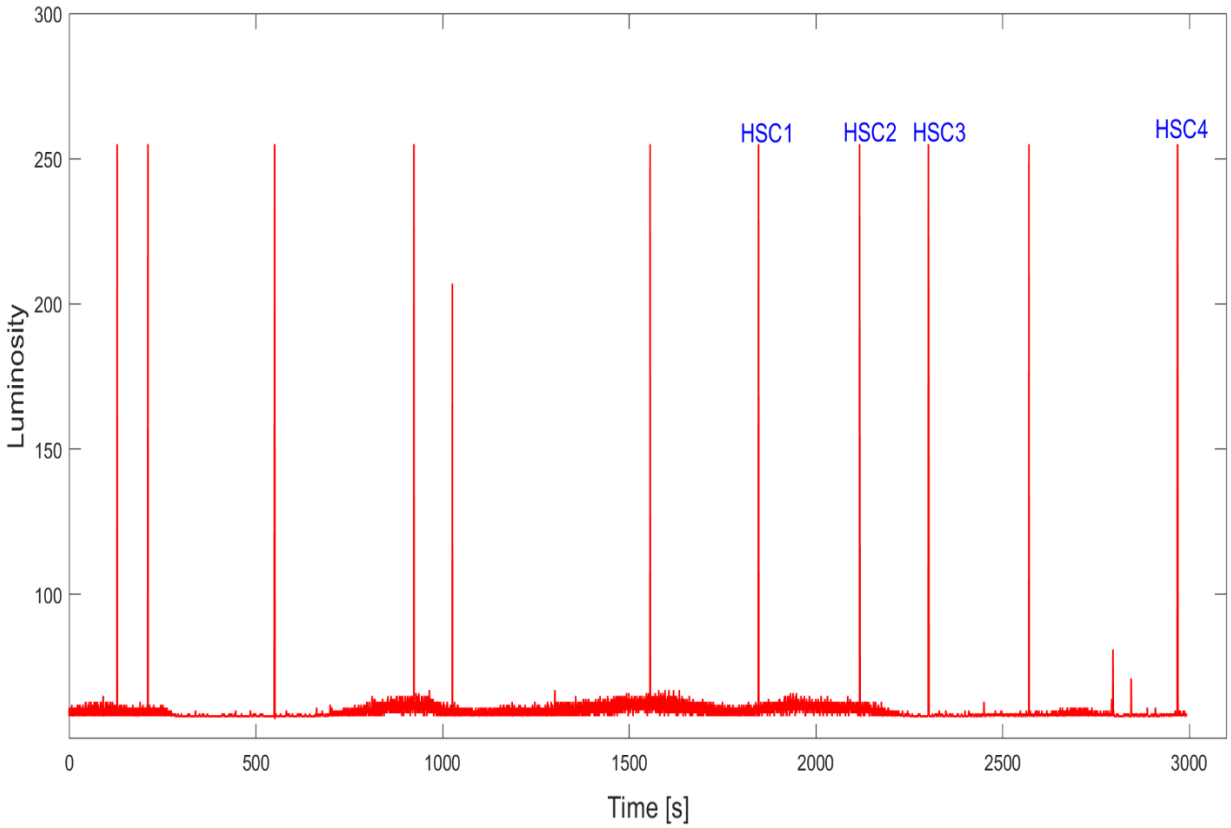

Figure 5.1 – Channel luminosity variation with time for the Sept. 4, 2017, based on LSC and HSC records.

The comparison between the lightning data recorded by HSC and LSC illustrated that the economical LSC turns out to be an extremely valuable imaging system. As the significantly valuable continuously recording imaging system (LSC) confirmed the operation or the failure of the HSC. However, LSC does not have an adequate frame rate (60 fps) to capture every subtle detail of a flash, including the M-components. Figure 5.2 presents the channel trajectories of the first flash recorded by HSC (left) and its matched seventh flash recorded by LSC (right). The variation of the maximum luminosity, as a function of time, is evaluated along horizontal pixel line of Y = 288 over 1300 frames (HSC) and another one Y = 350 over 60 frames (LSC) and is plotted in Figure 5.3 [22].

Figure 5.2 – Channel trajectory images of flash 1 of HSC (left) and its matched LSC flash 7 (right).

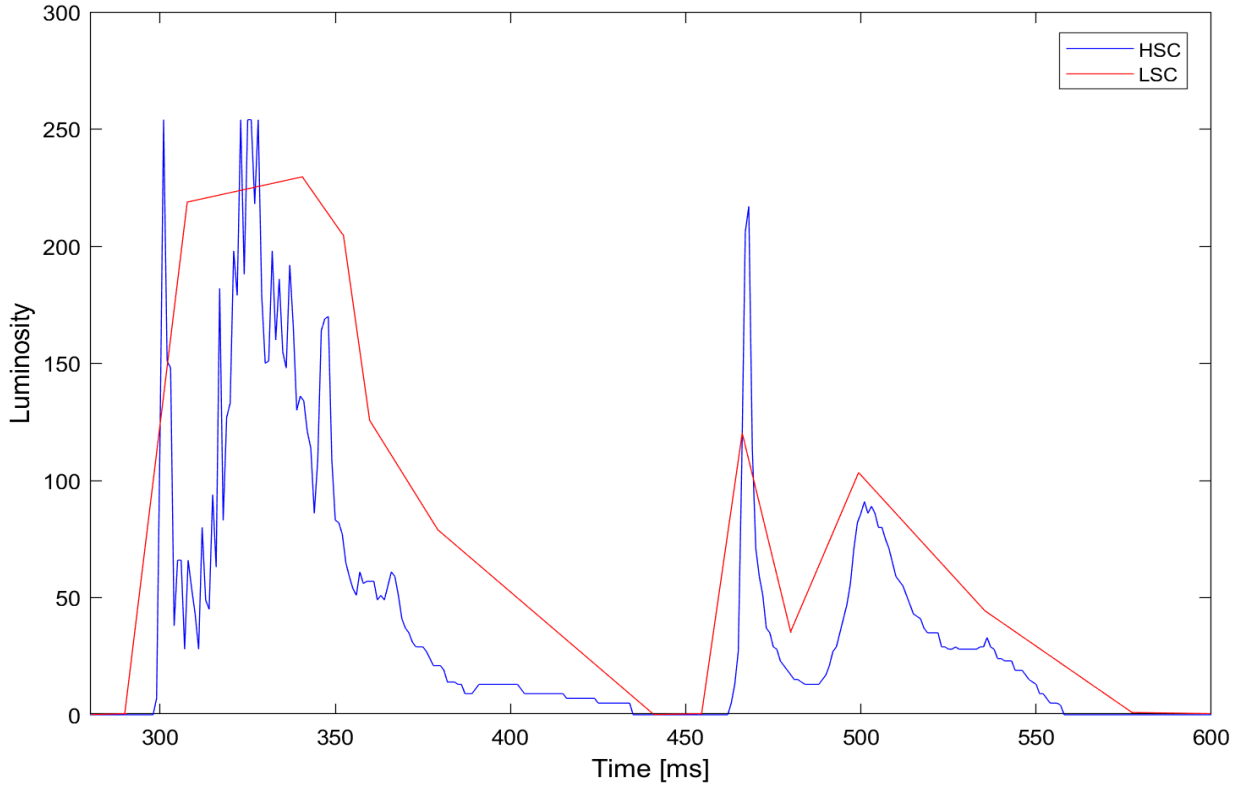

Figure 5.3 – Channel luminosity variations with time based on flash 1 (HSC) and flash 7 (LSC).

Figure 5.3 displays a flash that begins with an initial stage current (ISC), with a duration of 167 ms and includes several M-components, which is followed by a single return stroke. The return stroke is followed by a continuing current, with at least one M-component superimposed on it. Based on Figure 5.3, it's evident that the detailed characteristics of flash components require at least 1 ms resolution imaging system. The imaging systems with a higher frame rate than 1000 fps would be of much interest to use [22].

Figure 5.4 illustrates the channel trajectories of the second flash recorded by HSC (left) and its matched eighth flash recorded by LSC (right). The time variation of the maximum channel luminosities is analyzed along the horizontal pixel lines Y = 261, and Y = 322 for HSC and LSC, respectively, and are demonstrated in Figure 5.5.

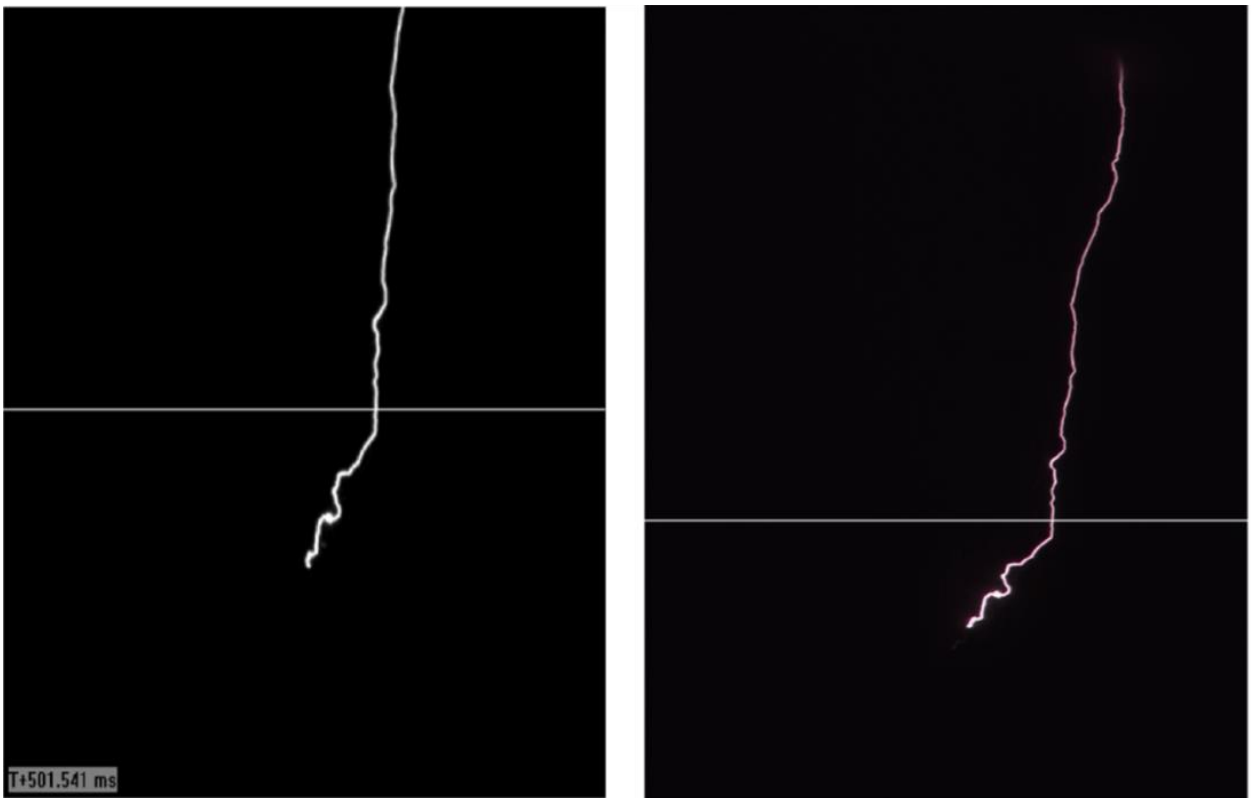

Figure 5.4 – Channel trajectory images of flash 2 of HSC (left) and its matched LSC flash 8 (right).

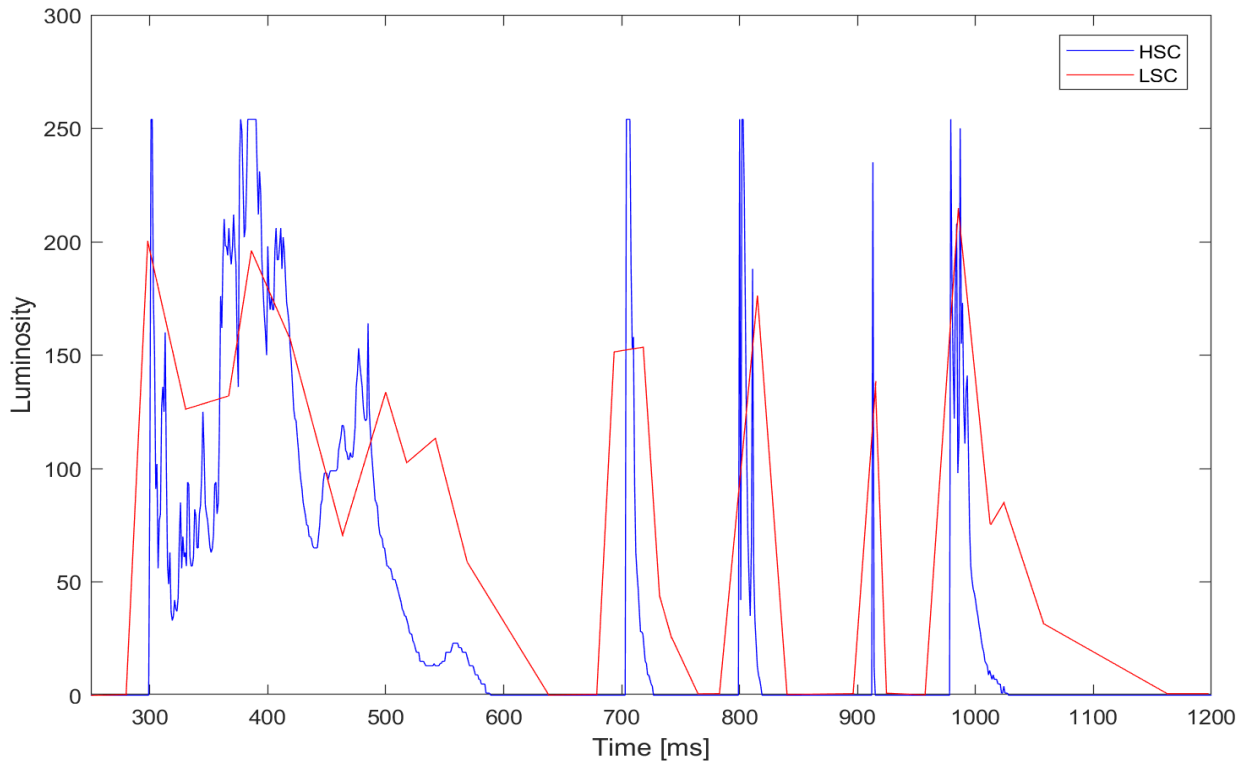

Figure 5.5 – Channel luminosity variations with time based on flash 2 (HSC) and flash 8 (LSC).

The luminosity variation with time, along with successive frames, as illustrated in Figure 5.5, displays a flash starting with ISC of 293 ms duration, containing several M-components, and followed by four return strokes. The second and fourth return strokes are followed by containing current, with several M-components superimposed on it.

Figure 5.6 presents the channel trajectory of the third flash, recorded by the HSC (left), and its matched ninth flash recorded by LSC (right). The time variation of the maximum channel luminosity is analyzed along the horizontal pixel lines Y = 283 and Y = 345 for HSC and LSC, respectively, and are demonstrated in Figure 5.7.

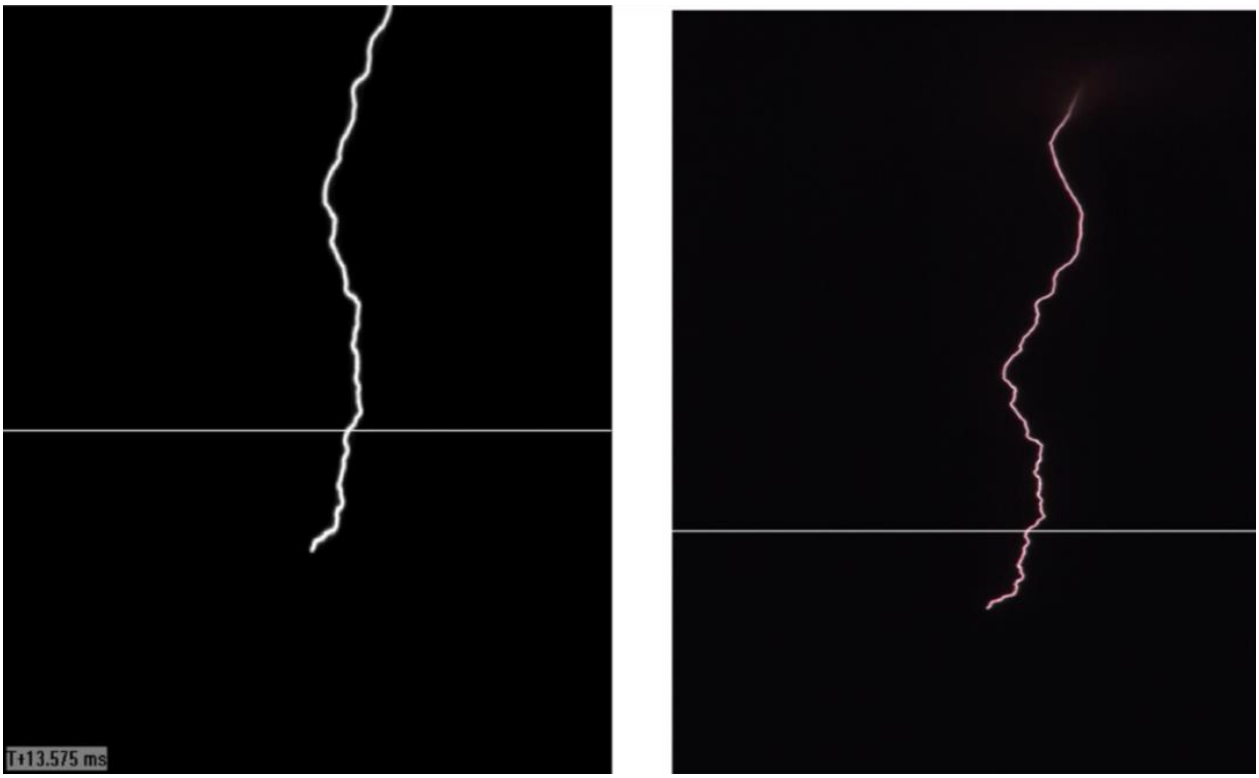

Figure 5.6 – Channel trajectory images of flash 3 of HSC (left) and its matched LSC flash 9 (right).

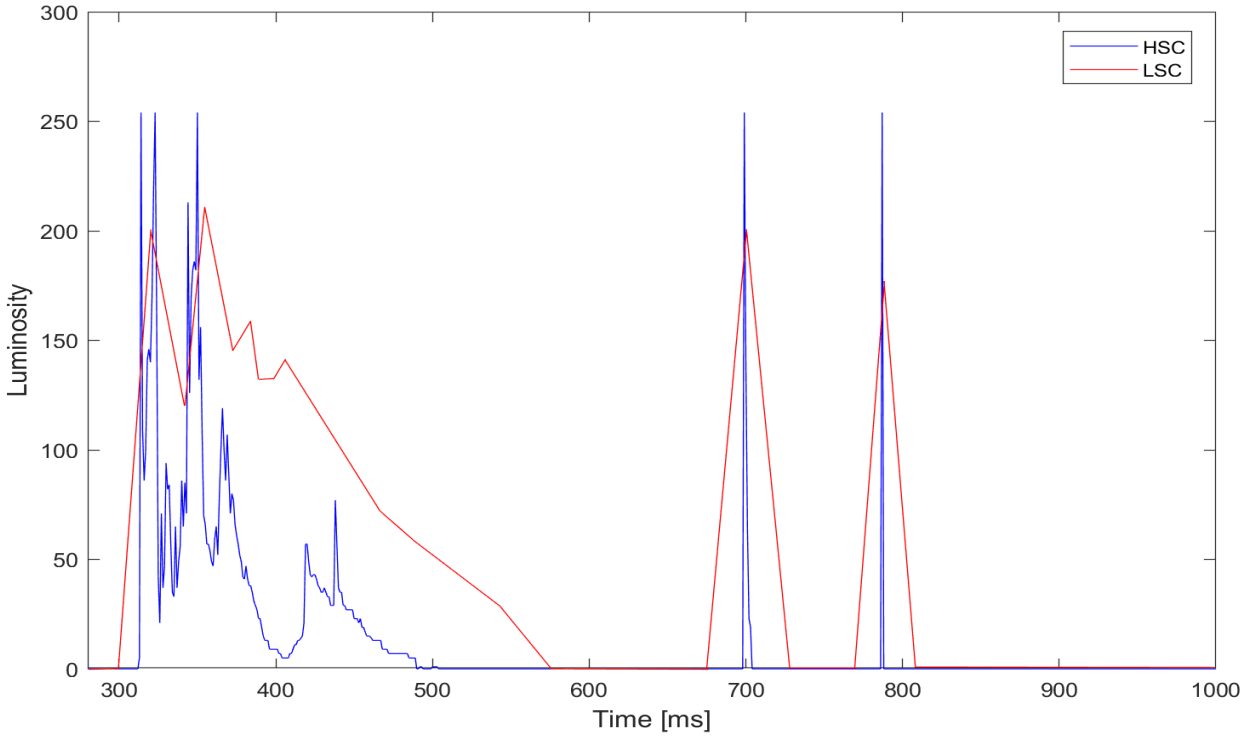

Figure 5.7 – Channel luminosity variations with time based on flash 3 (HSC) and flash 9 (LSC).

Figure 5.7 presents a flash that begins with ISC of 170 ms duration, containing several M-components, and followed by two return strokes.

Figure 5.8 illustrates the channel trajectory image of the fourth flash, recorded by HSC (left), and its matched eleventh flash, recorded by LSC (right). The time variation of maximum channel luminosity is analyzed along horizontal pixel lines Y = 292 for HSC and Y = 354 for LSC, respectively, are demonstrated in Figure 5.9.

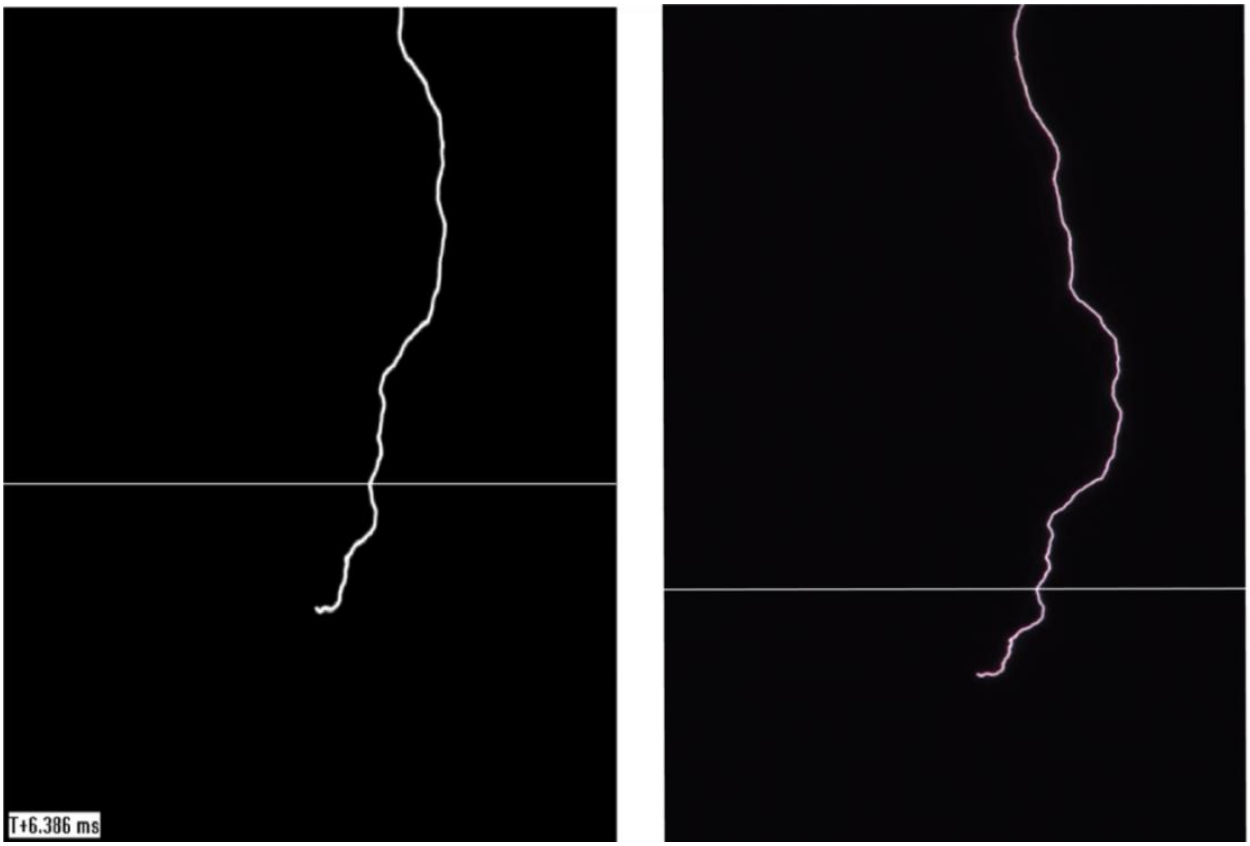

Figure 5.8 – Channel trajectory images of flash 4 of HSC (left) and its matched LSC flash 11 (right).

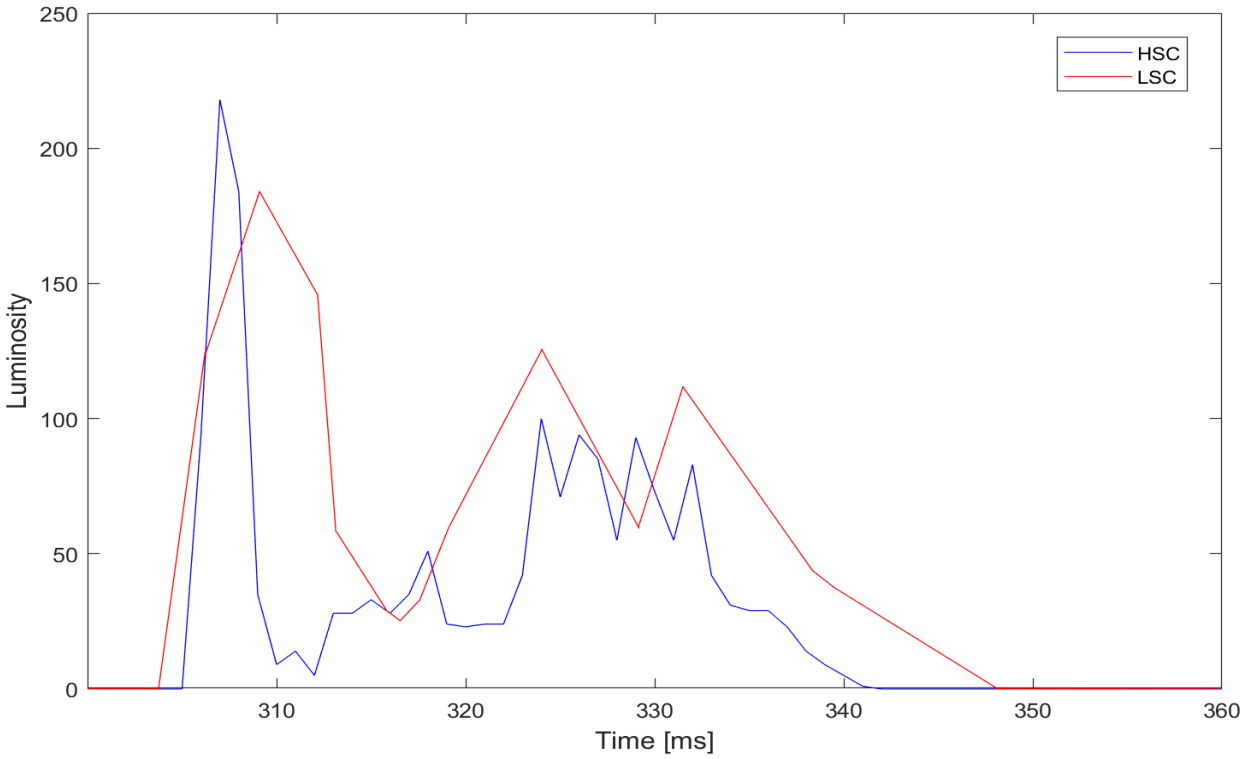

Figure 5.9 – Channel luminosity variations with time based on flash 4 (HSC) and flash 11 (LSC).

Figure 5.9 illustrates a flash containing only ISC with time duration of 37 ms, comprising several M-components.

The comparison between the lightning data recorded by HSC and LSC illustrated that the economical continuously recording LSC turns out to be an extremely valuable imaging system, without which the storm would not have materialized. Also, such continuously recording imaging system (LSC) would confirm the operation or the failure of other CN Tower lightning measurement systems, including the current recording system at the tower [22].

Chapter 6

Flash Characteristics

The acquisition of the data from Sony HDRPJ790VB low-speed camera (LSC) and Phantom v5.0 high-speed camera (HSC) provides necessary details, by analysing luminosity variation with time, regarding different flash components namely initial-stage current (ISC) duration, flash multiplicity, inter-stroke time (IST), flash duration, inter-flash time and continuing current time duration.

This section focuses on analyzing fifty-eight CN Tower lightning flashes captured by LSC and HSC, in the period of last five years (2013-2017), which can be classified as 2013 received seven flashes, 2014 received eighteen flashes, 2015 received eight flashes, 2016 received fourteen flashes and 2017 received eleven flashes. Also, the comparison has been conducted between the two storms received on September 5, 2014, and September 4, 2017, which contained thirteen and eleven flashes respectively.

The statistical results presented in this thesis will further help in the establishment of a more advanced approach in designing the protective measures against the lightning hazards to the tall structures.

6.1 Flash Duration (2013-2017)

The flash duration is defined total discharge time. The flash duration of each CN Tower flash (usually upward initiated), begins with an initial-stage current (ISC), which contains several M-components superimposed on it. In many cases the ISC is followed by downward-leader-upward-return-stroke sequences. Flashes with long flash durations represents severe threat to electrical power installations and tall structures [23]. Table 6.1 demonstrates the flash duration and the inter-flash time duration of all 58 flashes, based on HSC and LSC video records.

Table 6.1 Flash durations and inter-flash time durations of all 58 flashes based on video records (2013-2017).

Flash Duration and Inter-Flash Time [2013-2017]				
Year	Flash number	Date	Flash Duration [ms]	Inter-Flash Time [s]
2013	1	July 8	85	
				462
	2	July 8	287	
				267
	3	July 8	158	
	4	July 19	262	
				382
	5	July 19	476	
	6	September 11	240	
				101
	7	September 11	267	
2014	8	July 7	240	
				347
	9	July 7	219	
				168
	10	July 7	111	
	11	September 1	161	
				343
	12	September 1	125	
	13	September 5	240	

				692
	14	September 5	191	
				508
	15	September 5	767	
				792
	16	September 5	370	
				307
	17	September 5	702	
				353
	18	September 5	510	
				567
	19	September 5	708	
				722
	20	September 5	390	
				668
	21	September 5	210	
				532
	22	September 5	293	
				478
	23	September 5	364	
				522
	24	September 5	360	
				538
	25	September 5	99	
2015	26	July 17	167	
				228
	27	July 17	225	
				327
	28	July 17	382	
	29	September 8	132	
				192
	30	September 8	185	
	31	September 12	576	
				187
	32	September 12	32	
				292
	33	September 12	264	
2016	34	July 14	397	
				231
	35	July 14	350	
				324
	36	July 14	602	
				248
	37	July 14	310	

	38	July 25	307	
				432
	39	July 25	482	
				264
	40	July 25	472	
	41	September 7	220	
				242
	42	September 7	198	
				344
	43	September 7	142	
	44	September 9	282	
				149
	45	September 9	392	
				167
	46	September 9	46	
				372
	47	September 9	432	
2017	48	September 4	175	
				80
	49	September 4	160	
				340
	50	September 4	150	
				370
	51	September 4	210	
				120
	52	September 4	148	
				540
	53	September 4	660	
				300
	54	September 4	290	
				282
	55	September 4	720	
				192
	56	September 4	480	
				180
	57	September 4	510	
				515
	58	September 4	37	

Figure 6.1 illustrates the frequency distribution of the flash duration of all 58 flashes recorded over the last five years (Table 6.1). The figure shows that 76% of flashes have flash

durations within 400 ms and 24% of flashes have flash durations within the range 400 ms - 800 ms. It's worth mentioning that the flash durations within 400 ms were found to be 85% in 2013, 77.8% in 2014, 87.5% in 2015, 71% in 2016, and 63.6% in 2017. The longest flash duration of 767 ms, was received in 2014. However, the flashes with flash duration beyond 400 ms were 14.2% in 2013, 22% in 2014, 12.5% in 2015, 28.5% in 2016, and 36.4% in 2017.

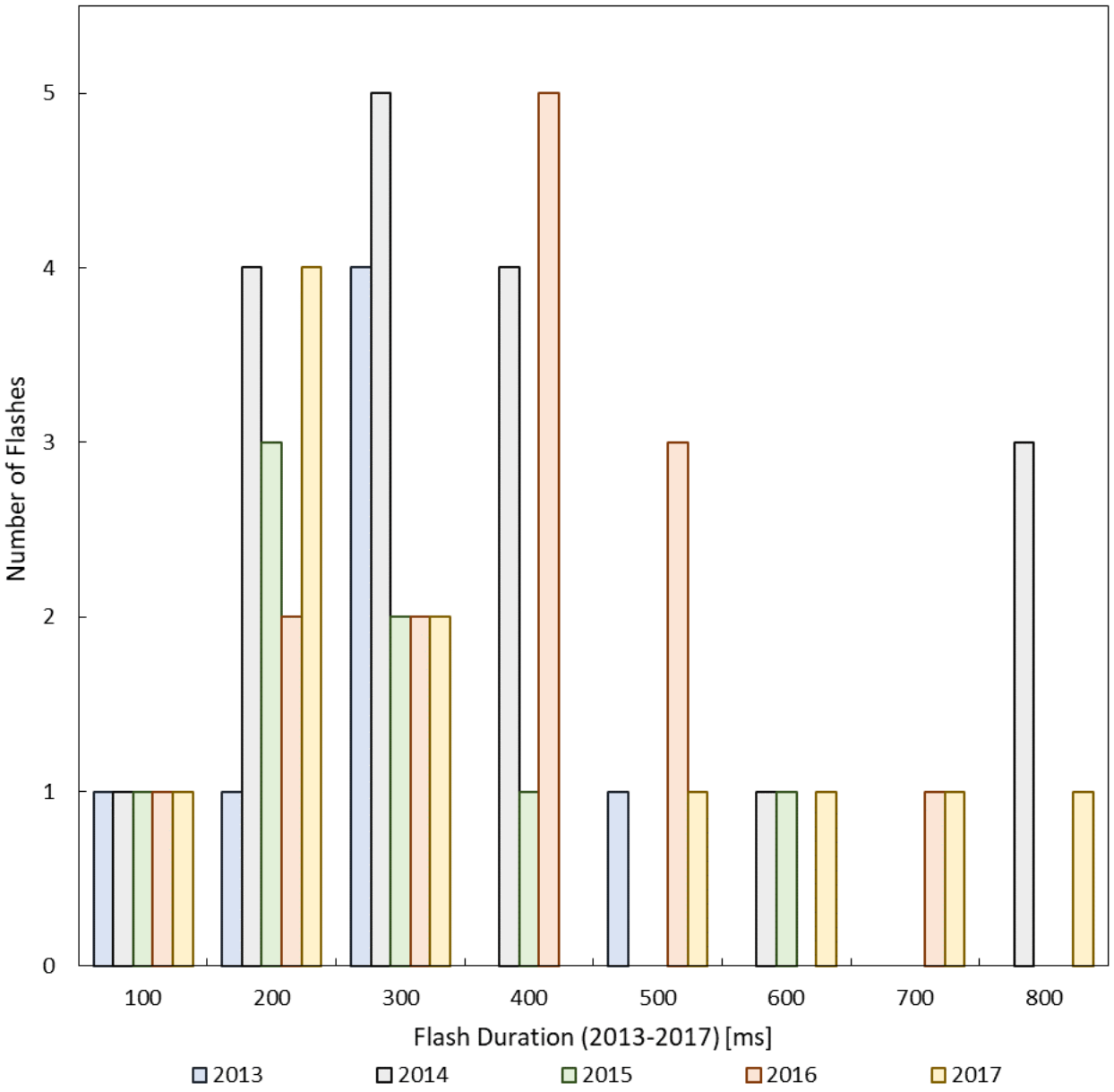

Figure 6.1 – Frequency distribution of flash durations (2013- 2017).

Figure 6.2 presents the cumulative probability of flash duration comprised by CN Tower flashes in each year, for comparison purpose. The cumulative probability distribution (CPD) of any flash parameter indicates the percentage of flashes having the parameter value equal to or higher than the specified value.

The longest flash duration of 767 ms, was received in 2014, followed by 2017, which received the longest flash duration of 720 ms, 6.1% smaller flash duration as compared to 2014. Whereas, Figure 6.2 and Table 6.2 demonstrates that 50% CPD of flashes received in 2017 had 28% longer flash duration as compared to 2014. Though, the average flash duration of 2014 is the largest out of all years, due to the highest number of flashes received.

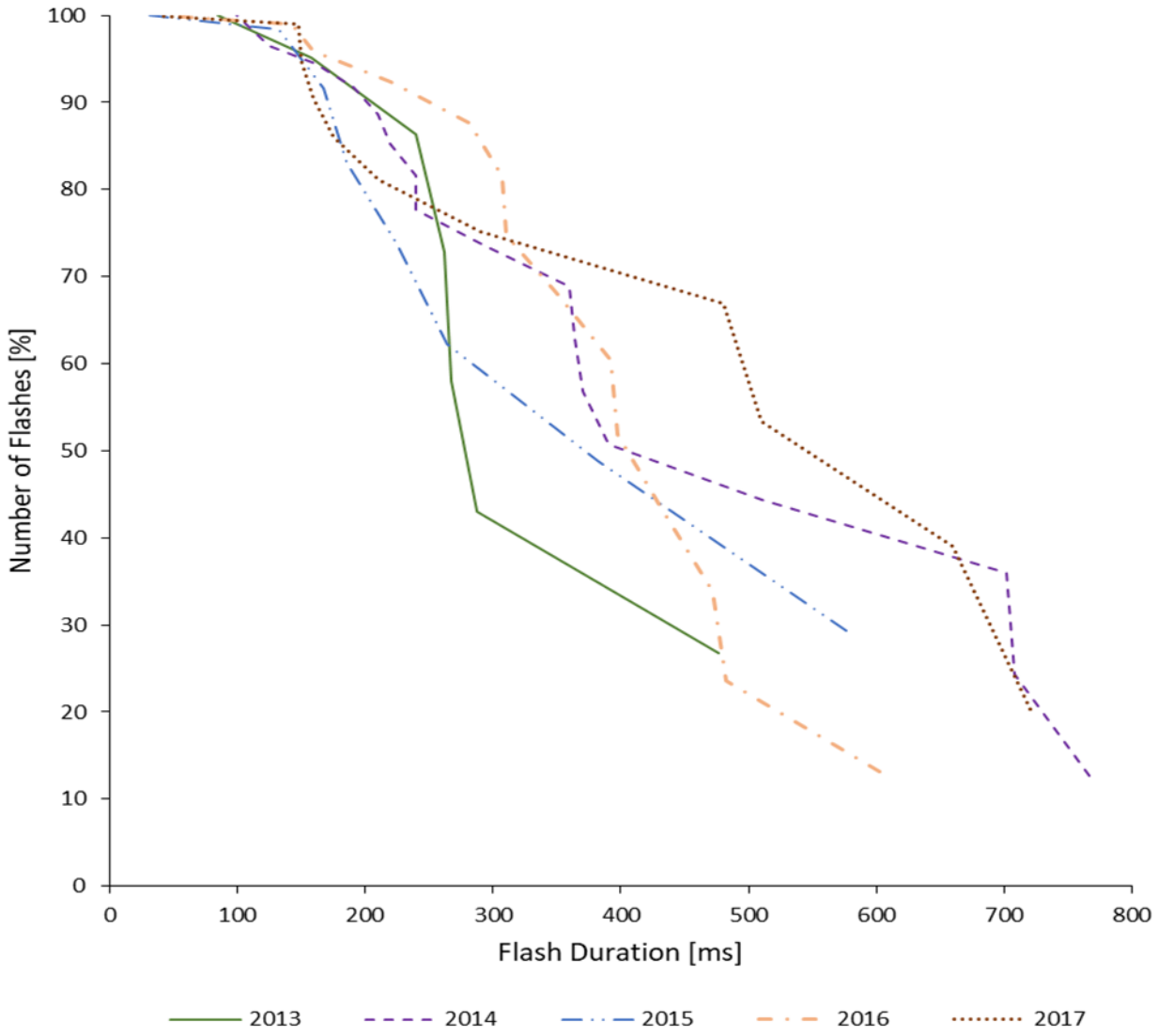

Figure 6.2 – Cumulative probability distribution of flash durations (2013-2017).

Table 6.2 Statistics of flash durations based on video records (2013-2017).

Flash Duration [ms]					
	2013	2014	2015	2016	2017
Minimum	85	99	32	46	37
Maximum	476	767	576	602	720
Mean	253.57	336	245.37	328	321.82
50% Probability	252	355	250	390	495
Standard Deviation	121.5	208	167.7	151	231

It has also been noted that 2015 received the lowest number of flashes as compared to other years and interestingly also accounts for the lowest flash duration of 32 ms, with lowest average flash duration and lowest 50% CPD, respective to all other years.

Although, the 50% probability based on the CPD of 2014 (355 ms) is 9% shorter as compared to 2016 (390 ms), which is a slight difference. Also, the same pattern can be seen between the year 2013 and 2015, with almost 2013 (252 ms) being on higher side with only 0.7% of the difference, with respect to 2015 (250 ms), which is making these years significantly having closer 50% CPD.

6.2 Inter-flash Time Duration (2013-2017)

Inter-flash time duration is defined as the time difference between two subsequent flashes. The subsequent flashes with shorter inter-flash time durations pose a severe threat to tall structures.

The data comprised of 44 inter-flash time intervals that proved to have the frequency distribution within the range of 80 s and 792 s.

Figure 6.3 displays the frequency distribution of inter-flash time durations for flashes received in the last five years (Table 6.1). The figure demonstrates that 68% of inter-flash time intervals are within 400 s and 32% of inter flash time intervals are within the range of 400 s to 640 s, which can be further elaborated as, the inter-flash time intervals within 400 s were 75% in 2013, 33.3% in 2014, 100% in 2015, 60% in 2016, and 80% in 2017. Also, the inter-flash time intervals beyond 400 s were 25% in 2013, 66.6% in 2014, 40% in 2016, and 20% in 2017.

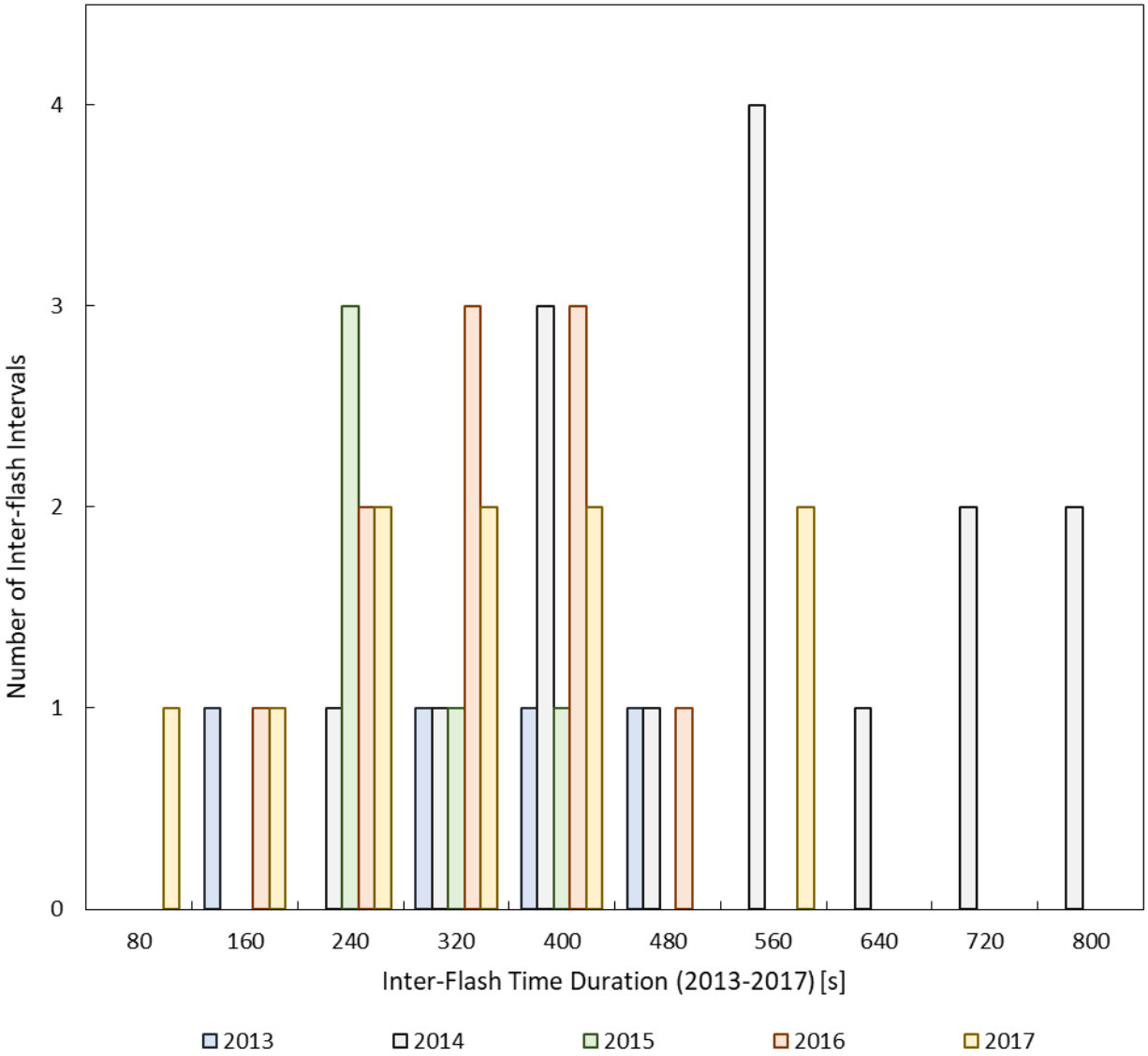

Figure 6.3 – Frequency distribution of inter-flash time duration (2013-2017).

Figure 6.4 presents the CPD of inter-flash time duration comprised by CN Tower flashes in each year, for comparison purpose. The figure and Table 6.3 reveal that 2014 had the highest inter-flash time of 792 s, and the largest average (502.5 s) and 50% CPD (540 s) in contrast to other years.

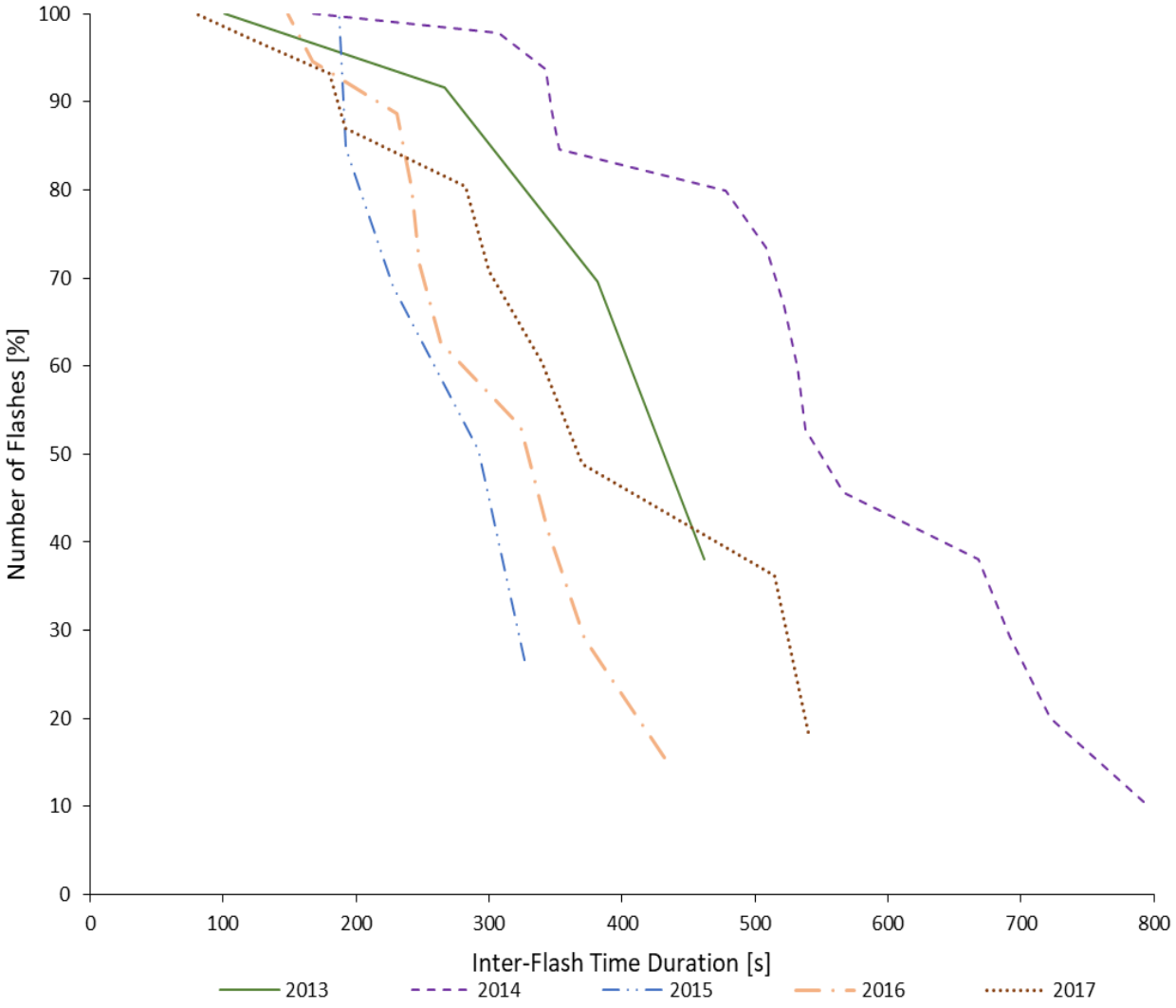

Figure 6.4 – Cumulative probability distribution of inter-flash time durations (2013-2017).

Table 6.3 Statistics of inter-flash time duration based on video records (2013-2017).

Inter-Flash Time [s]					
	2013	2014	2015	2016	2017
Minimum	101	168	187	149	80
Maximum	462	792	327	432	540
Mean	303	502.5	245.2	277.3	291.9
50% Probability	384	540	243	306	345
Standard Deviation	156.7	174.6	62	89.8	155

For comparison, it's also noted that the minimum inter-flash time duration of 2014 (168 s), 2015 (187 s) and 2016 (149 s) was above 150 s. Whereas, 2013 (101 s) and 2017 (80 s) had minimum inter-flash time duration within 100 s. The table also depicts that 2015 had lowest maximum inter-flash time, shortest overall average and lowest 50% CPD, as compared to other years.

6.3 Initial-Stage Current Duration (2013-2017)

In case of the grounded tall objects, upward negative discharge is initiated by upward positive leaders from the top of the tall object. The initial-stage current (ISC) is established, as the upward positive leaders bridge the gap between the object and the negative charge source in the cloud and the ISC usually lasts for some hundreds of milliseconds. The upward leader and the initial stage current constitute the initial stage of an upward flash [3]. The flashes which contain

long initial-stage current durations accounts for charge transfer for long time durations, which poses significant threat to the tall structures.

Table 6.4 Initial-stage current durations based on video records (2013-2017).

Initial-Stage Current Duration [ms]			
Year	Flash number	Date	Initial-Stage Current Duration [ms]
2013	1	July 8	85
	2	July 8	267
	3	July 8	158
	4	July 19	246
	5	July 19	228
	6	September 11	240
	7	September 11	182
2014	8	July 7	240
	9	July 7	219
	10	July 7	111
	11	September 1	161
	12	September 1	125
	13	September 5	240
	14	September 5	191
	15	September 5	591
	16	September 5	291
	17	September 5	442
	18	September 5	260
	19	September 5	620
	20	September 5	390
	21	September 5	210
	22	September 5	293
	23	September 5	335
	24	September 5	360
	25	September 5	99
2015	26	July 17	167
	27	July 17	225
	28	July 17	207
	29	September 8	132
	30	September 8	185
	31	September 12	198
	32	September 12	32

	33	September 12	218
2016	34	July 14	316
	35	July 14	350
	36	July 14	324
	37	July 14	310
	38	July 25	189
	39	July 25	207
	40	July 25	178
	41	September 7	178
	42	September 7	198
	43	September 7	142
	44	September 9	198
	45	September 9	242
	46	September 9	46
	47	September 9	298
2017	48	September 4	175
	49	September 4	160
	50	September 4	150
	51	September 4	210
	52	September 4	148
	53	September 4	513
	54	September 4	167
	55	September 4	293
	56	September 4	170
	57	September 4	289
	58	September 4	37

It's worth mentioning that flash characteristics of 58 optically recorded flashes clearly showed that all flashes contained initial-stage current, confirming that all flashes to CN Tower were upward initiated. Figure 6.5 presents the frequency distribution of initial-stage current durations for 58 flashes received in the last five years (Table 6.4). The figure shows that overwhelming majority (93%) of initial-stage current durations, are within 400 ms and 6.8% of initial-stage current durations are within the range of 400 ms and 700 ms, which can be categorized as, the initial-stage current duration within 400 ms accounts for: 100% in 2013, 83.3% in 2014, 100% in 2015, 100% in 2016, and 91% in 2017. The ISC duration within the range of 400 ms and 700 ms counts as 16.7% in 2014 and 9% in 2017.

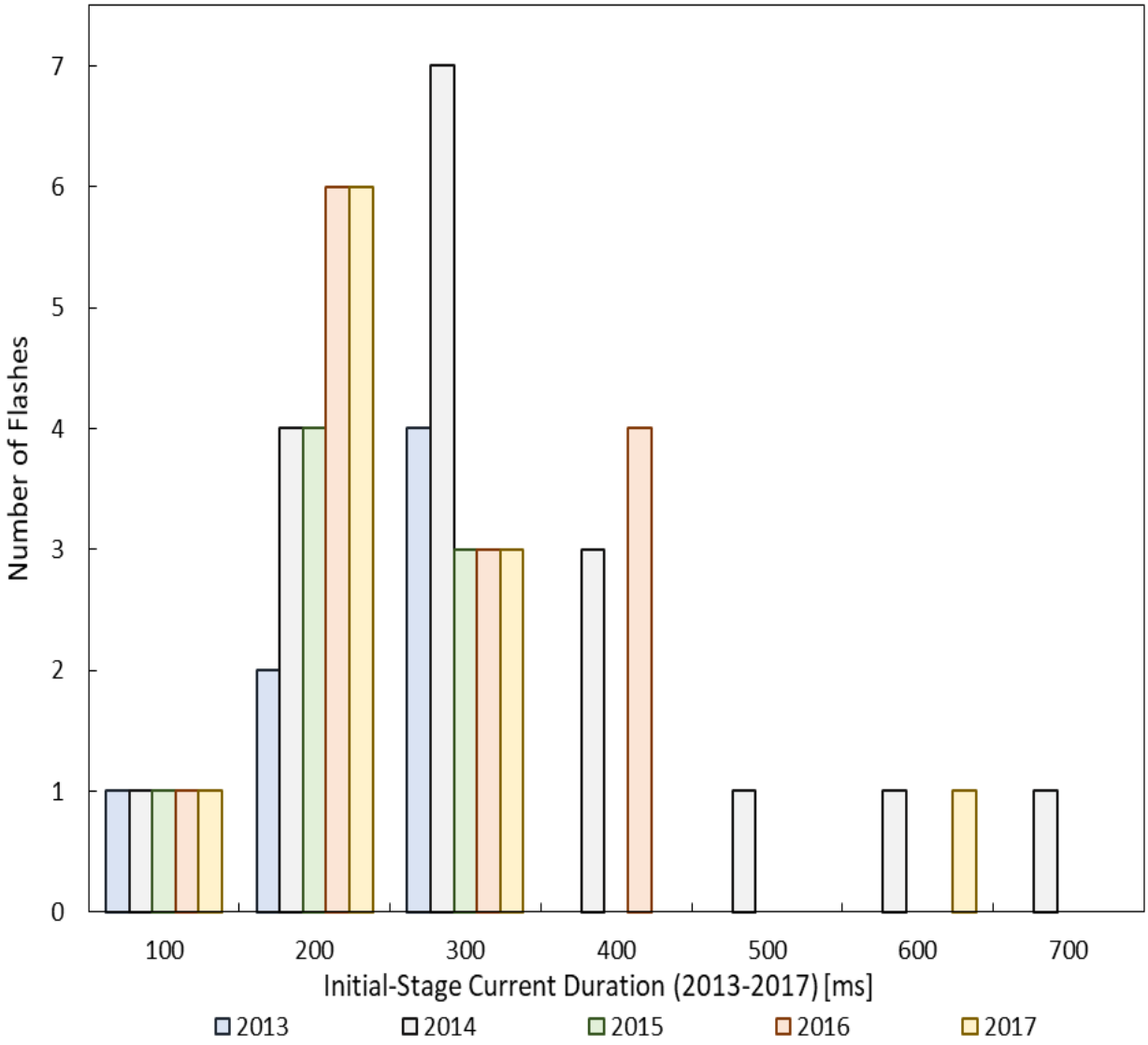

Figure 6.5 – Frequency distribution of initial-stage current durations (2013-2017).

Figure 6.6 presents the CPD of initial-stage current duration comprised by CN Tower flashes in each year, for comparison purpose. The figure and Table 6.5 clearly depict that year 2014 had minimum ISC duration of 99 ms, an average ISC duration of 298 ms and 50% CPD of 317 ms, which clearly overweighs the other years. Though, ISC duration of 2015 varied between 32 ms and 225 ms, with an overall average ISC duration of 170.5 ms, reflecting the shortest minimum, maximum and average as compared to other years.

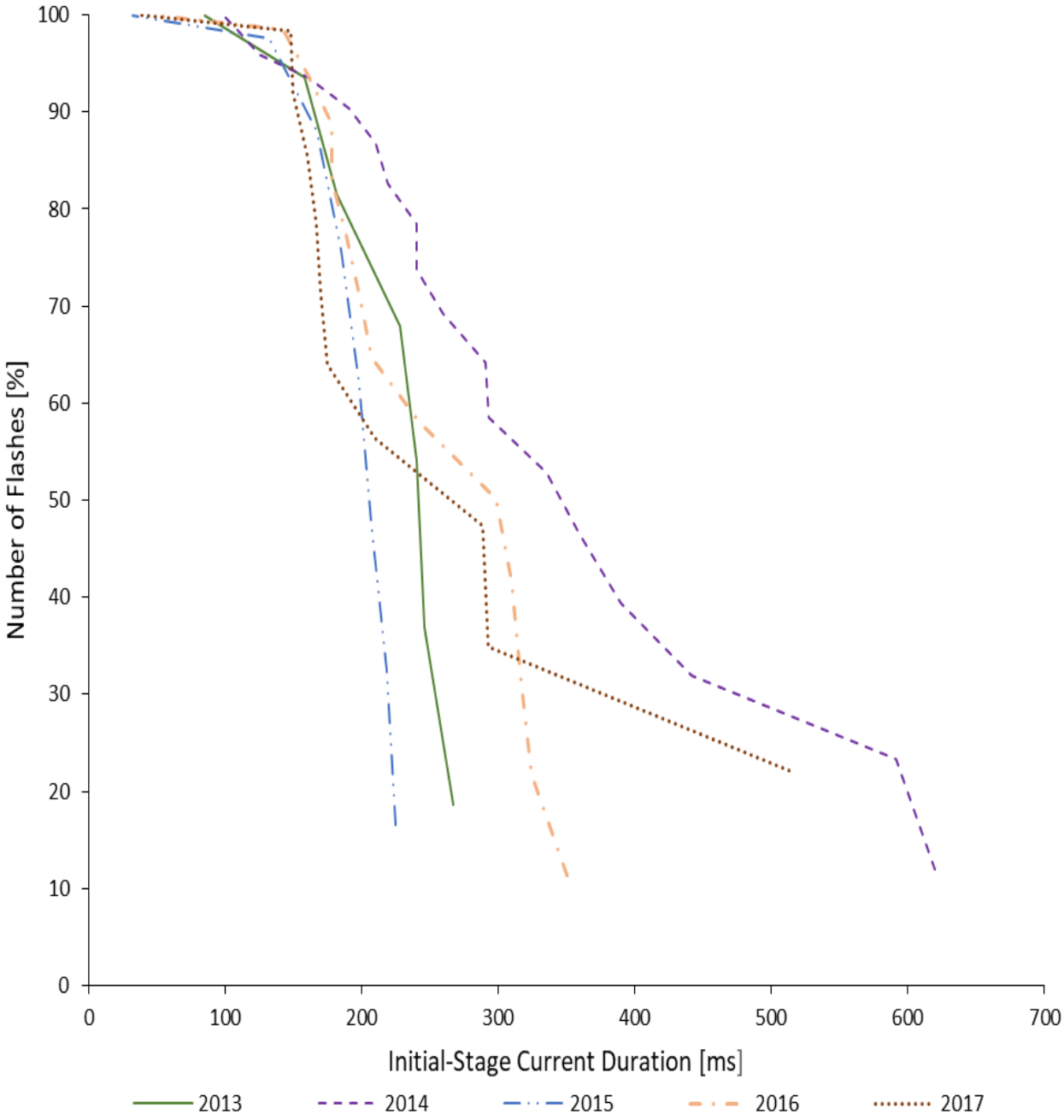

Figure 6.6 – Cumulative probability distribution of initial-stage current durations (2013-2017).

Table 6.5 Statistics of initial-stage current durations based on video records (2013-2017).

Initial-Stage Current Duration [ms]					
	2013	2014	2015	2016	2017
Minimum	85	99	32	46	37
Maximum	267	620	225	350	513
Mean	200.6	288	170.5	224	210
50% Probability	258	317	199	254	181
Standard Deviation	63.6	149	63.5	86.14	122

For comparison, it's worth mentioning that the maximum ISC duration of 2017 (513 ms) is 17% shorter as compared to the 2014 (620 ms) ISC duration, making it longest as compared to all other years. Also, maximum ISC duration of 2013 (267 ms) is 15.7% longer than 2015 (225 ms) maximum ISC duration.

Based on the cumulative probability distribution (Figure 6.6), the 50% CPD for the year 2015 (199 ms) is only 9% longer than 2017 (181 ms), with 2014 (317 ms) ISC duration leading all other years. It's worth mentioning that 50% CPD of ISC duration of 2013 (258 ms) and 2016 (254 ms) are close to each other.

6.4 Flash Multiplicity (2013-2017)

During the last five years, CN Tower was struck 58 times, which was simultaneously recorded by two imaging systems. Out of 58 flashes received, only 27 (46.5%) flashes contained a single or multiple return strokes. Flash multiplicity is defined as a number of return strokes per flash. More number of return strokes per flash can cause more damage, increasing the electromagnetic radiation in the area which causes interference in the electronic and communication systems. Table 6.6 demonstrates the detailed description of flash multiplicity and inter-stroke time duration for flashes received in the last five years.

Table 6.6 Flash multiplicity and inter-stroke time duration based on video records (2013-2017).

Flash Multiplicity and Inter-stroke Time [ms] (2013-2017)				
Year	Flash number	Date	Flash Multiplicity	Inter-Stroke Time Duration [ms]
2013	1	July 8	-	-
	2	July 8	1	-
	3	July 8	-	-
	4	July 19	1	-
	5	July 19	4	34
				58
				92
	6	September 11	-	-
	7	September 11	2	47
2014	8	July 7	-	-
	9	July 7	-	-
	10	July 7	-	-
	11	September 1	-	-
	12	September 1	-	-
	13	September 5	-	-
	14	September 5	-	-
	15	September 5	1	-
	16	September 5	1	-
	17	September 5	3	110
				25

	18	September 5	2	126
	19	September 5	2	64
	20	September 5	-	-
	21	September 5	-	-
	22	September 5	-	-
	23	September 5	1	-
	24	September 5	-	-
	25	September 5	-	-
2015	26	July 17	-	-
	27	July 17	-	-
	28	July 17	1	-
	29	September 8	-	-
	30	September 8	-	-
	31	September 12	5	29
				38
				56
				47
	32	September 12	-	-
	33	September 12	1	-
2016	34	July 14	1	-
	35	July 14	-	-
	36	July 14	2	114
	37	July 14	-	-
	38	July 25	1	-
	39	July 25	3	92
				85
	40	July 25	9	18
				84
				14
				72
				22
				12
				20
	41	September 7	1	-
	42	September 7	-	-
	43	September 7	-	-
	44	September 9	1	-
	45	September 9	1	-
	46	September 9	-	-
	47	September 9	2	86

2017	48	September 4	-	-
	49	September 4	-	-
	50	September 4	-	-
	51	September 4	-	-
	52	September 4	-	-
	53	September 4	1	-
	54	September 4	1	-
	55	September 4	4	86
				102
				58
	56	September 4	2	79
	57	September 4	2	49
	58	September 4	-	-

Figure 6.7 presents the frequency distribution of all 27 flashes containing return strokes (Table 6.6). It can be clearly depicted from the figure that 77.8% of flashes contained one to two return strokes, 14.8% of flashes contained three to four return strokes and 7.4% of flashes constituted 5 to 9 return strokes, which can be categorized as 2013 - 75% of flashes comprised one to two return strokes and 25% of flashes contained four return strokes, 2014 – 83.3% of flashes included one to two return strokes and 16.67% of flashes contained three to four return strokes, 2015 - 66.6% of flashes constituted one return stroke and 33.3% of flashes constituted five return strokes, 2016 - 77.7% of flashes comprised one to two return strokes and 22.2% of flashes contained three to nine return strokes, 2017 - 40% of flashes contained 1 to 2 return strokes and 20% of flashes contained four return strokes.

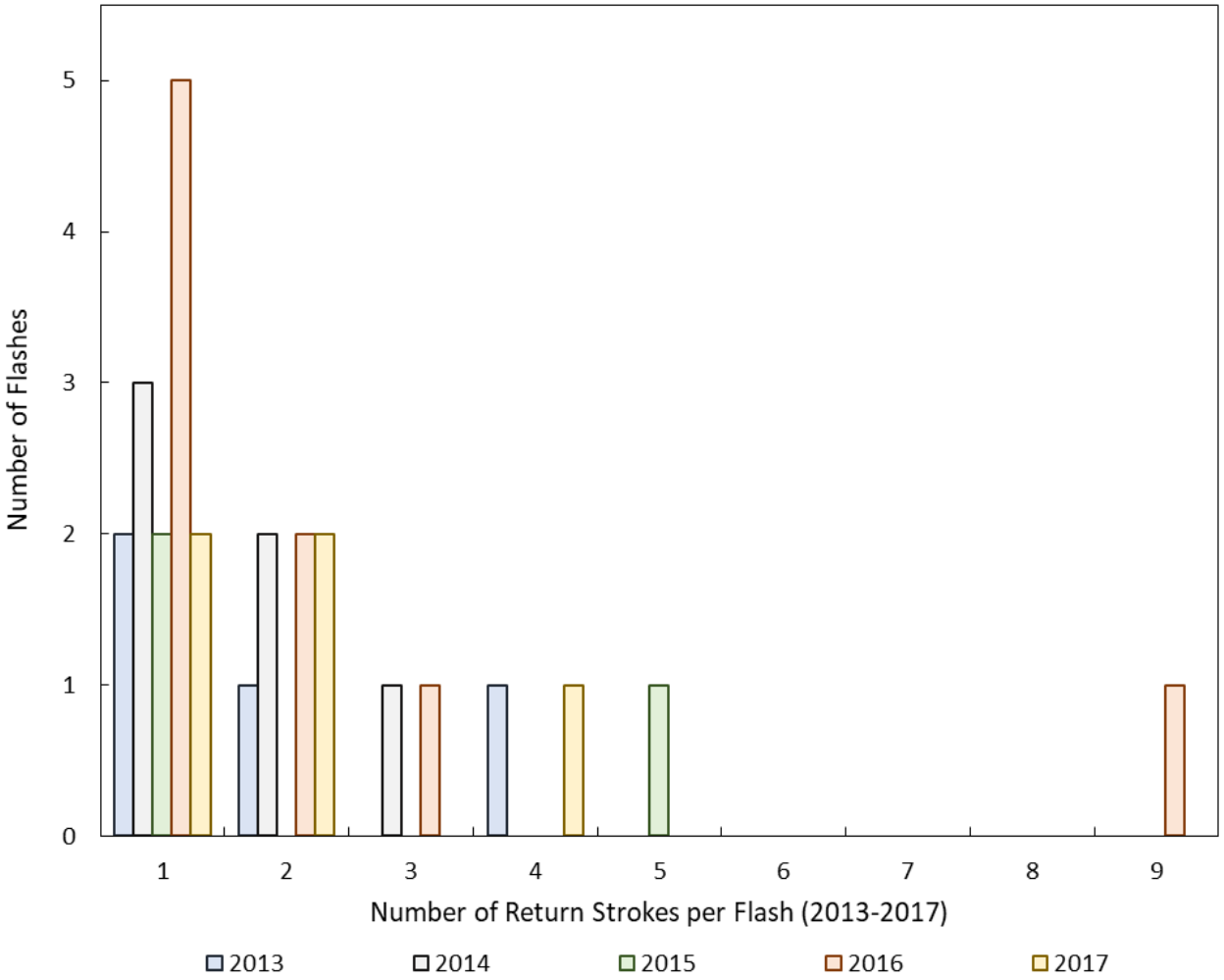

Figure 6.7 – Frequency distribution of flash multiplicity (2013- 2017).

Figure 6.8 illustrates the CPD of flash multiplicity comprised by CN Tower flashes in each year, for comparison purpose. The figure and Table 6.7 reveal that every year had at least one return stroke per flash. However, 2016 accounts for a maximum of nine return strokes, which is more in contrast with 2015, having only five return strokes as maximum, and 2013 and 2017 with a maximum of four return strokes each.

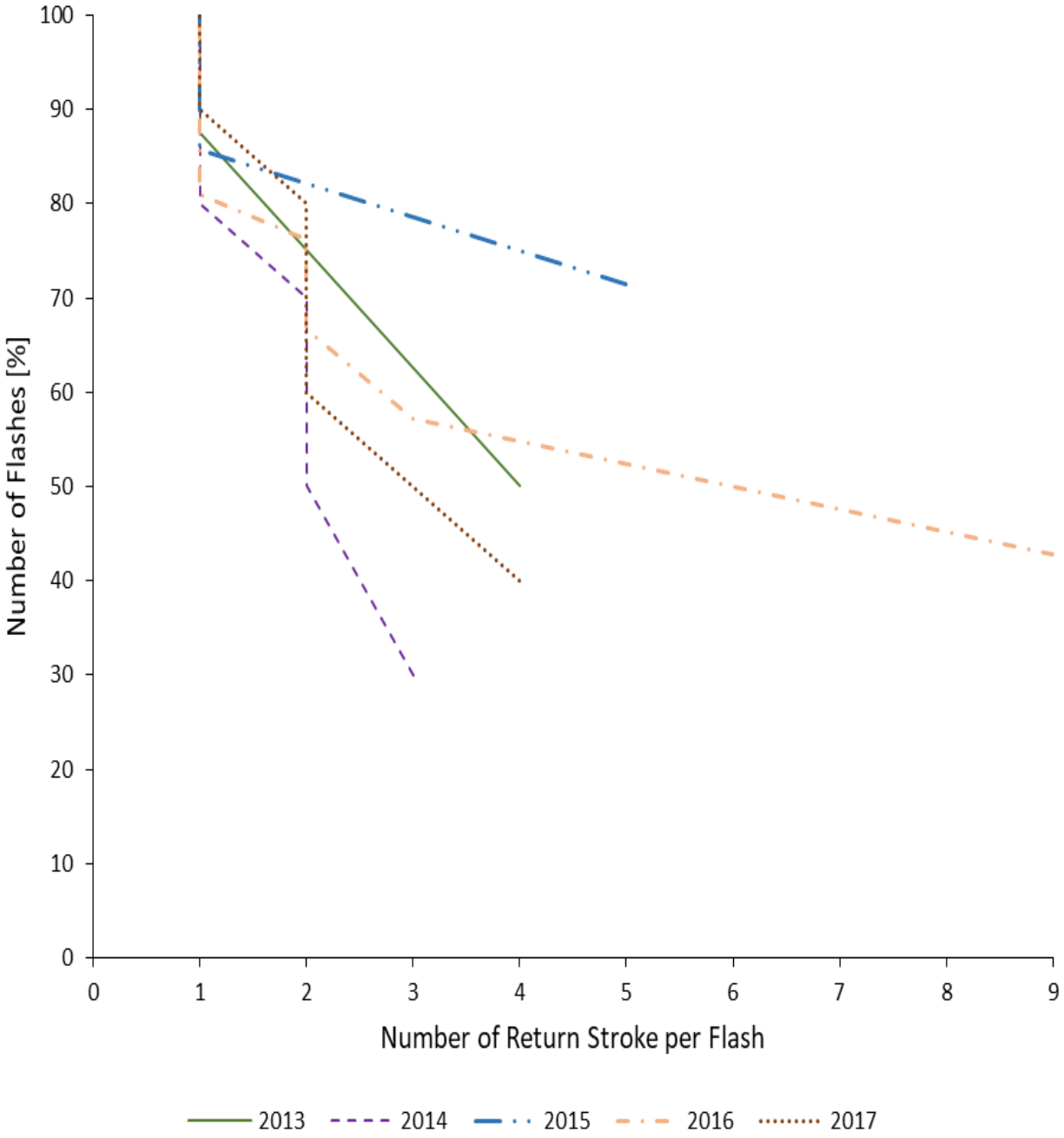

Figure 6.8 – Cumulative probability distribution of flash multiplicity (2013-2017).

Table 6.7 Statistics of flash multiplicity for 27 flashes based on video records (2013-2017).

Flash Multiplicity					
	2013	2014	2015	2016	2017
Minimum	1	1	1	1	1
Maximum	4	3	5	9	4
Mean	2	1.67	2.33	2.33	2
50% Probability	2	2	1	2	2
Standard Deviation	1.4	0.8	2.3	2.6	1.2

For comparison, it's worth mentioning that the year 2016 had an overall average multiplicity of 2.33, which is precisely similar to the average multiplicity of 2015. Whereas, the other three years (2013, 2014 and 2017) had 18.9% less average flash multiplicity.

It can also be noted from Figure 6.8 that 50% CPD of 2015 is shortest as it's 50% smaller than that of 2013, 2014, 2016 and 2017.

6.5 Inter-Stroke Time Duration (2013-2017)

The inter-stroke time (IST) duration is the time difference between the successive return strokes, comprised by multi-stroke flashes. The flashes with short time duration within successive return strokes poses more threat to tall structures. Figure 6.9 presents the frequency distribution of inter-stroke time durations for flashes received in the last five years (Table 6.6). The figure and Table 6.6 shows that data set of the last five years comprised 13 (22.4%) multi-stroke flashes, containing 28 inter-stroke intervals. Furthermore, it was observed that the inter-stroke duration

lied within the range of 12 ms and 126 ms, with an overall average of 62.51 ms. It's worth mentioning that 85% of IST duration lied within 100 ms and 14.2% of the total IST comprised duration ranging from 100 ms to 126 ms, which can be summarized as the inter-stroke time duration within 60 ms were 75% in 2013, 50% in 2014, 100% in 2015, 45% in 2016, and 40% in 2017. The inter-stroke time duration beyond 60 ms were 25% in 2013, 50% in 2014, 54.5% in 2016, and 60% in 2017.

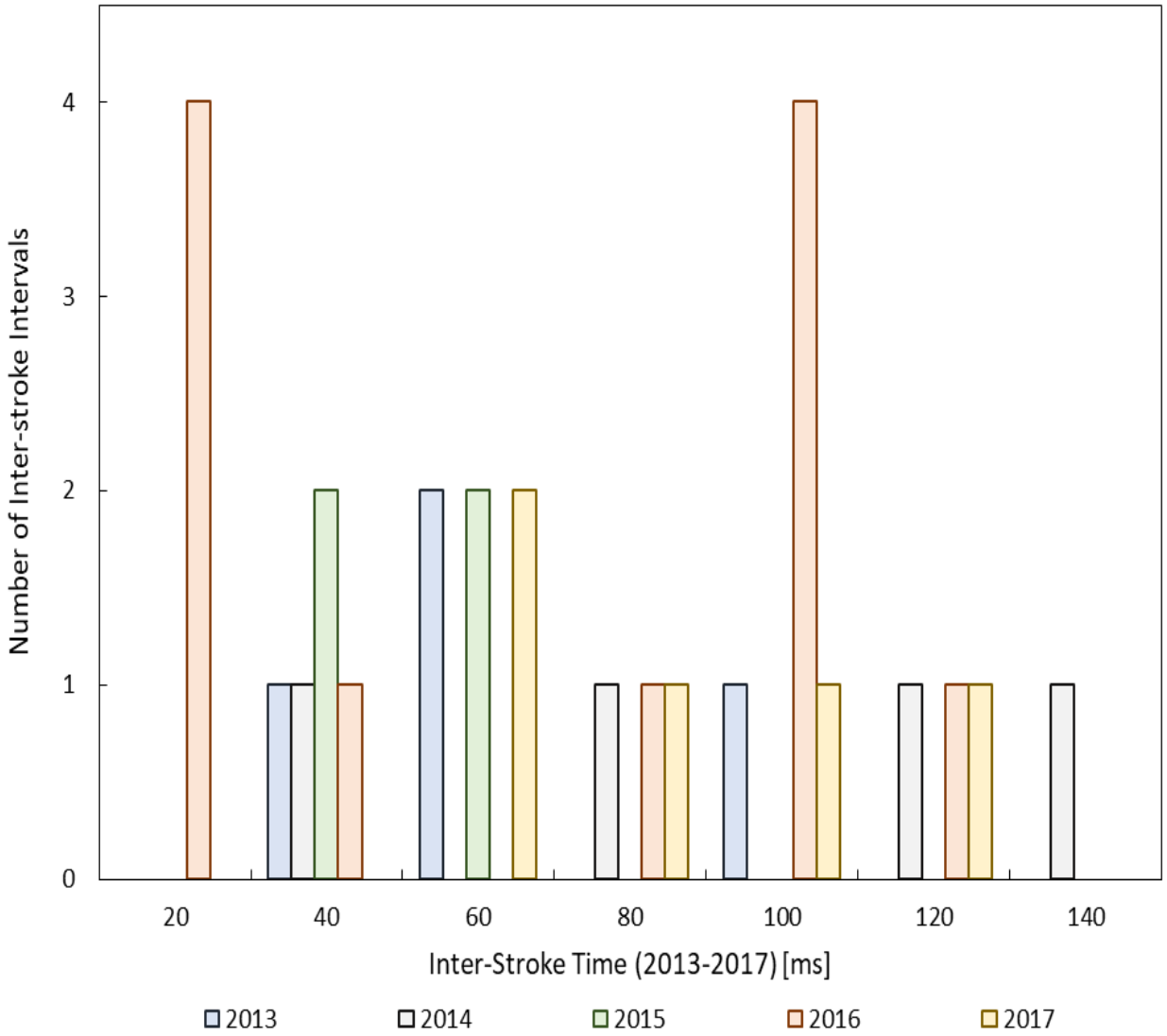

Figure 6.9 – Frequency distribution of inter-stroke time duration (2013-2017).

Figure 6.10 illustrates the cumulative probability of inter-stroke time duration comprised by CN Tower flashes in the last five years, for comparison purpose. The figure and Table 6.8 demonstrate that the minimum inter-stroke time duration of previous five years varied between 12 ms and 49 ms. However, the maximum inter-stroke time duration during the last five years ranged from 56 ms to 126 ms.

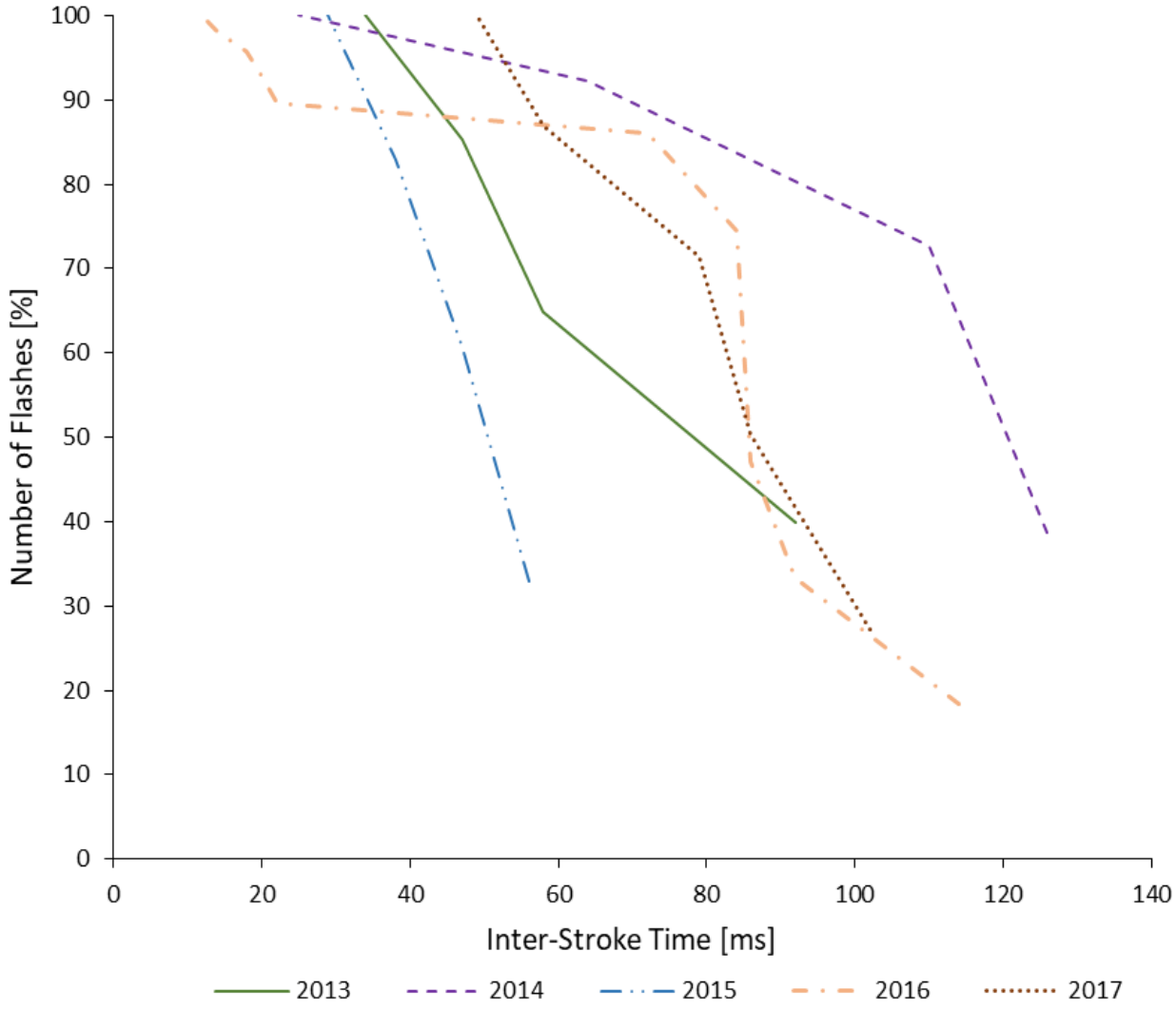

Figure 6.10 – Cumulative probability distribution of inter-stroke time (2013-2017).

Table 6.8 Statistics of inter-stroke time durations based on video records (2013-2017).

Inter-Stroke Time [ms]					
	2013	2014	2015	2016	2017
Minimum	34	25	29	12	49
Maximum	92	126	56	114	102
Mean	57.75	81.25	42.5	56.27	74.8
50% Probability	56	112	44	86	82
Standard Deviation	24.8	45.8	11.6	38.8	21.4

It's also noted that all years (2013-2017) had an inter-stroke time interval within 126 ms. For comparison, it's observed that the average inter-stroke time durations for flashes received in 2014 (81.25 ms) was leading and 7.9% longer as compared to the inter-stroke time average of 2017 (74.8 ms). Also, the inter-stroke time averages of 2013 (57.75 ms) and 2016 (56.27 ms) are almost close, with 2013 being 2.13% longer.

The cumulative probability distribution (Figure 6.10) demonstrates that a 50% CPD of inter-stroke time duration for 2014 (112 ms) is only among other years, which is above 100 ms. Whereas, 50% CPD of 2015 (44 ms) which is the lowest among all other years (below 50 ms).

6.6 Continuing Current Duration (2013-2017)

Continuing current is defined as the relatively low-level current of typically tens to hundreds of amperes that immediately follows a return stroke, in the same channel to ground, and usually lasts for tens to hundreds of milliseconds [3]. Table 6.9 demonstrates the detailed description of

the continuing current contained by flashes received in the last five years. The continuing currents with longer time durations pose severe threat to the tall structures, and electrical and communication systems as the flow of steady amount of current for continuous duration of the time cause heating effects that could melt or damage the resistive equipment's.

Table 6.9 Continuing current time durations based on video records (2013-2017).

Continuing Current Duration (2013-2017) [ms]			
Year	Flash number	Date	Continuing Current [ms]
2013	1	July 8	-
	2	July 8	-
	3	July 8	-
	4	July 19	12
	5	July 19	52
	6	September 11	-
	7	September 11	24
			14
2014	8	July 7	-
	9	July 7	-
	10	July 7	-
	11	September 1	-
	12	September 1	-
	13	September 5	-
	14	September 5	-
	15	September 5	156
	16	September 5	79
	17	September 5	68
			12
			45
	18	September 5	120
			72
	19	September 5	24
	20	September 5	-
	21	September 5	-
	22	September 5	-
	23	September 5	16
	24	September 5	-
	25	September 5	-
2015	26	July 17	-

	27	July 17	-
	28	July 17	62
	29	September 8	-
	30	September 8	-
	31	September 12	119
			87
	32	September 12	-
	33	September 12	-
2016	34	July 14	32
	35	July 14	-
	36	July 14	97
			48
	37	July 14	-
	38	July 25	-
	39	July 25	68
	40	July 25	-
	41	September 7	-
	42	September 7	-
	43	September 7	-
	44	September 9	-
	45	September 9	-
	46	September 9	-
	47	September 9	38
2017	48	September 4	-
	49	September 4	-
	50	September 4	-
	51	September 4	-
	52	September 4	-
	53	September 4	-
	54	September 4	62
	55	September 4	67
			114
	56	September 4	-
	57	September 4	33
	58	September 4	-

Table 6.9 revealed that continuing currents followed 25 out of 56 (45%) return strokes. Furthermore, 66.6% of flashes containing return strokes had return strokes followed by continuing currents, and 46% of multi-stroke flashes contained multiple strokes followed by continuing

currents. Figure 6.11 presents the frequency distribution of continuing current time durations for flashes received in the last five years (Table 6.9). The figure and Table 6.9 demonstrate that 76% of flashes contained continuing currents within 80 ms and 24% of flashes comprised continuing currents within the range of 80 ms and 160 ms, which can be further elaborated as, flashes with continuing current duration within 80 ms: 100% in 2013, 77.7% in 2014, 33.3% in 2015, 8% in 2016, and 75% in 2017. Also, flashes that contained the continuing current beyond 80 ms, can be categorized as: 22.2% in 2014, 66.6% in 2015, 20% in 2016, and 25% in 2017.

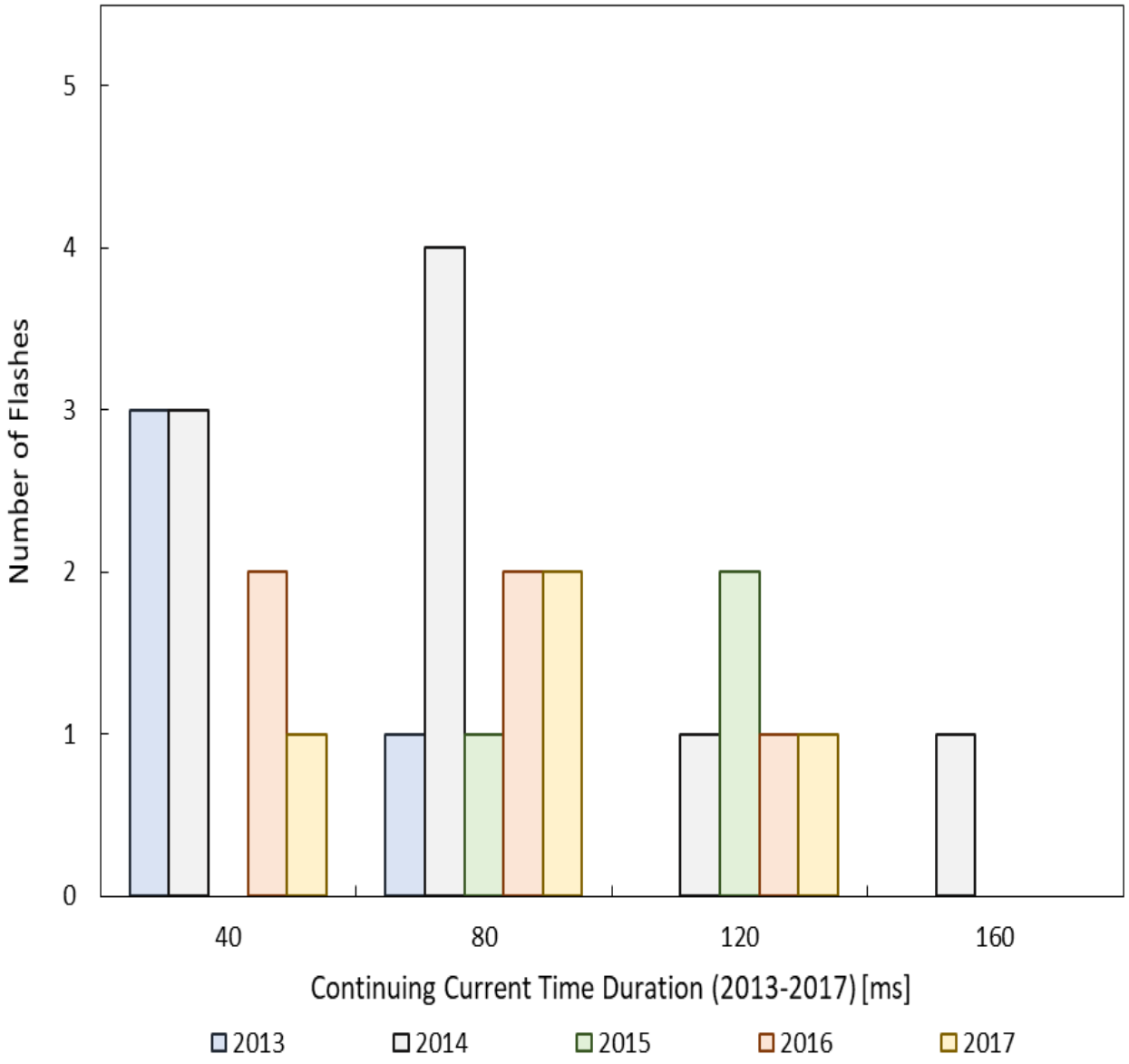

Figure 6.11 – Frequency distribution of continuing current time duration (2013-2017).

Figure 6.12 illustrates the CPD of continuing current time duration comprised by CN Tower flashes in the last five years, for comparison purpose. The figure and Table 6.10 reveal that 2013 and 2014 had minimum continuing current duration of 12 ms. Interestingly 2014 had the most extended continuing current duration of 156 ms, leading all other years, those had maximum lying within 97 ms and 119 ms.

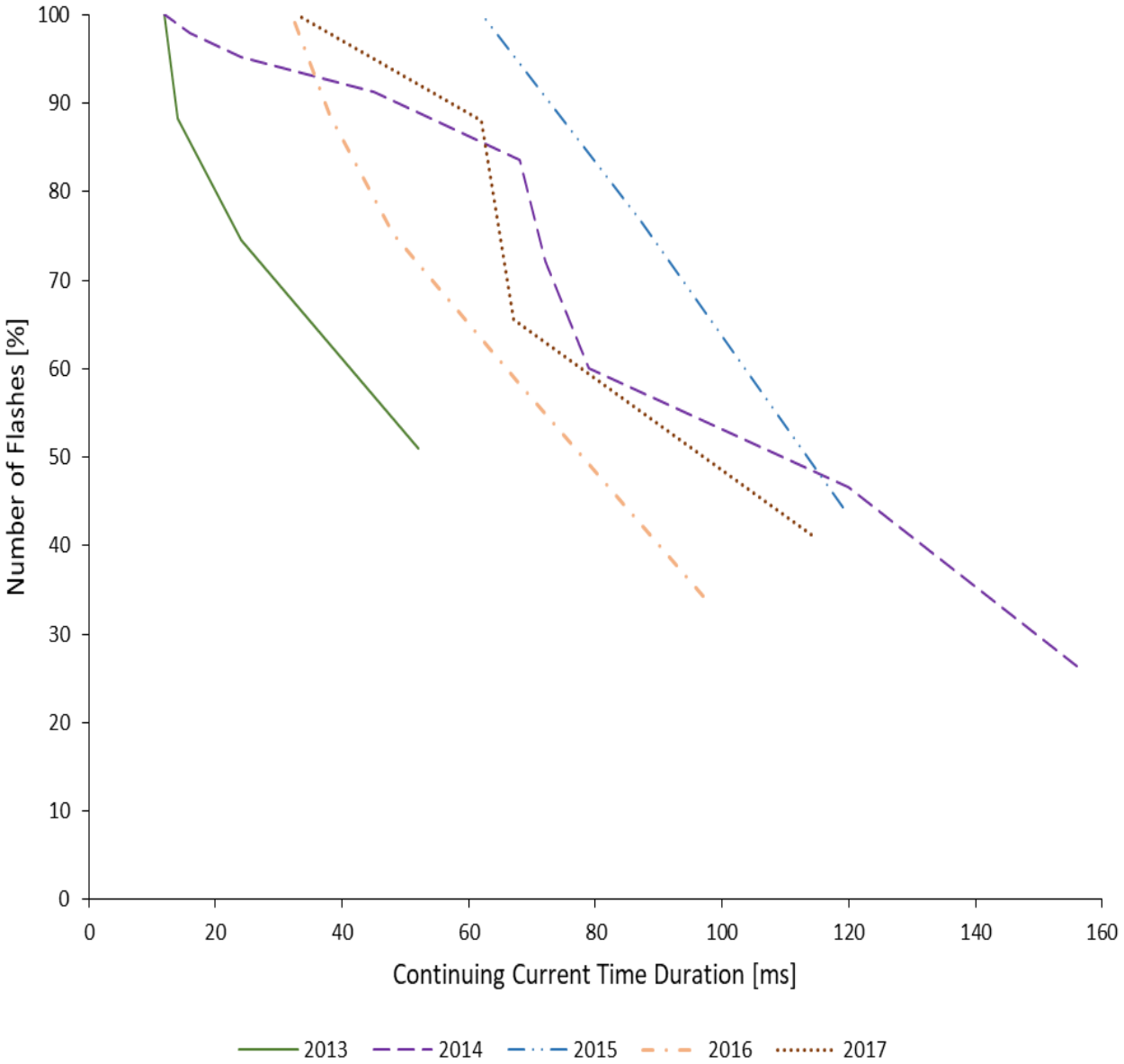

Figure 6.12 – Cumulative probability distribution of continuing current time duration (2013-2017).

Table 6.10 Statistics of continuing current time durations based on video records (2013-2017).

Continuing Current Time Duration [ms]					
	2013	2014	2015	2016	2017
Minimum	12	12	62	32	33
Maximum	52	156	119	97	114
Mean	25	65.8	89.3	56.6	69
50% Probability	22	76	89	58	66
Standard Deviation	18.43	48.5	28.6	26	33.5

The average continuing current duration of 2015 is 89.3 ms, due to a small number of flashes received in that year, comprising longest time duration of continuing currents, which is on average 39% longer as compared to other years.

It's worth mentioning that 2013 comprised lowest average continuing current duration of 25 ms, due to the short continuing current durations contained by all flashes received in that year (below 80 ms).

6.7 Comparison of CN Tower Major Storms

During the night of September 5, 2014, the CN Tower imaging systems recorded 13 flashes, with average flash duration of 399 ms. The storm started at 20:09:20 pm and lasted for 111.4 mins, and produced on an average a flash to tower every 556 s. It's worth mentioning that all 13 flashes comprised initial-stage current with an average duration of 332 ms. Also, 6 out of 13 flashes (46%) contained return strokes, with an average multiplicity of 1.67.

Similarly, during the night of September 4, 2017, there was another storm at the CN Tower, captured by two imaging systems. The storm started at 20:14:58 pm and lasted for 49.35 mins. The storm comprised 11 flashes, with an average flash duration of 321.8 ms, and produced on average a flash to tower every 291.9 s. It's worth mentioning that 5 out of 11 flashes (45%) contained return strokes, with an average multiplicity of 2. Also, all 11 flashes received during the storm contained initial-stage current with an average duration of 210 ms.

Based on both imaging system records, the statistical analyses of significant storms were conducted, and also the flash parameters namely flash duration, inter-flash time duration, initial-stage current duration, flash multiplicity, inter-stroke time duration, and continuing current duration are derived. The comparison of storms is conducted to obtain a better insight into the characteristics and to find various major differences between there flash parameters.

6.7.1 Flash Duration

Based on the analyses of 13 flashes recorded during 2014 storm and 11 flashes recorded during 2017 storm, by the two imaging systems, the flash time durations of flashes received during 2014 storm is found to vary between 99 ms and 767 ms. Whereas, the flash time durations of flashes received during 2017 storm is observed to vary between 37 ms and 720 ms.

Figure 6.13 presents the frequency distribution of flash time durations. The figure shows that the flash durations within 400 ms can be categorized as 69.2% in case of 2014 storm and 63.6% during 2017 storm. Furthermore, the flashes with the flash duration beyond 400 ms were 30.7% in 2014 and 36.3% in 2017.

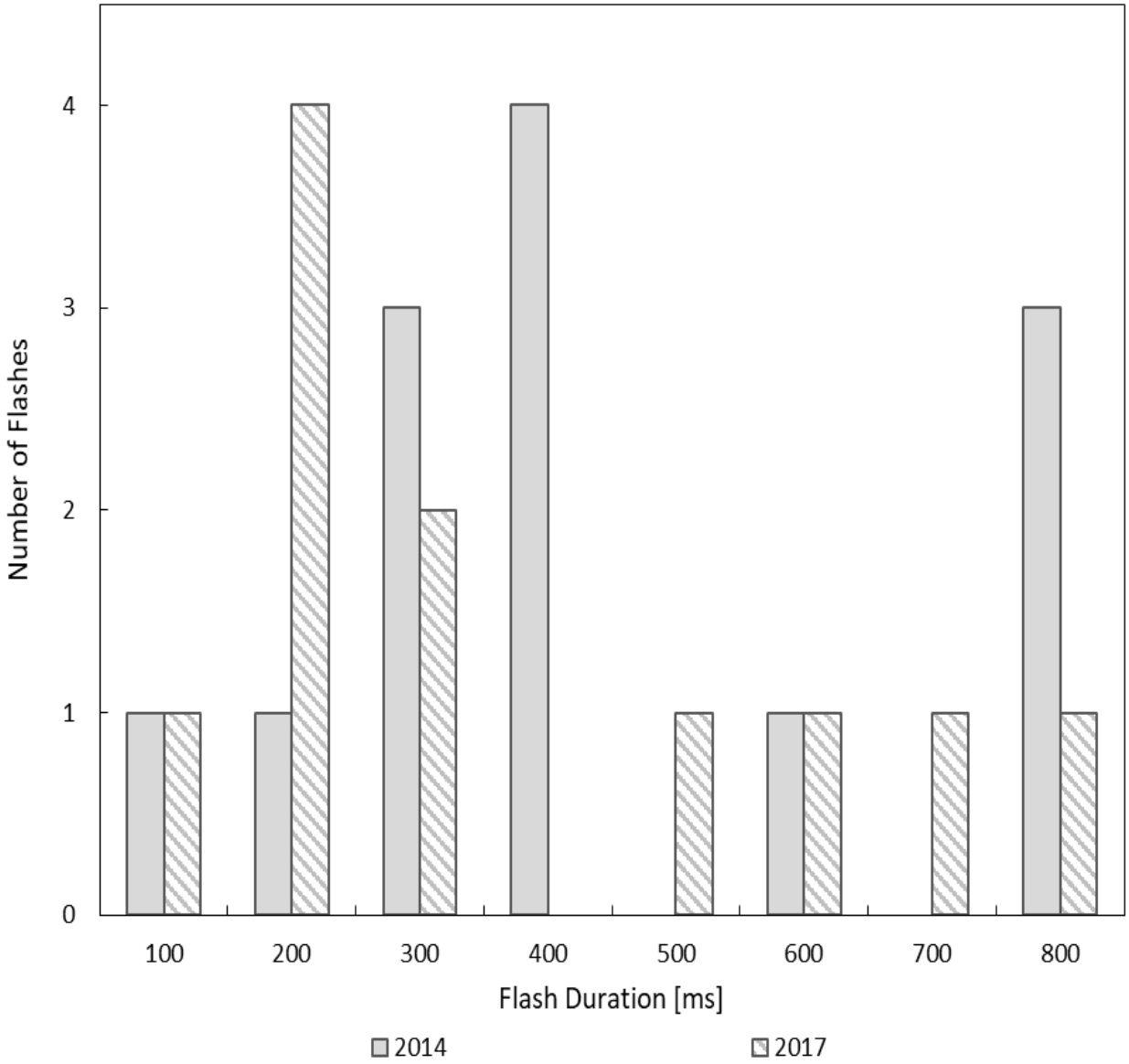

Figure 6.13 – Frequency distribution of the flash duration of flashes recorded during major storms (Sept. 5, 2014 and Sept. 4, 2017).

Table 6.11 reveals that the average flash duration of flashes received during 2014 storm is 20% longer as compared to the average flash duration of flashes received during 2017 storm. Also, Figure 6.14 presents that the 50% CPD of flash durations of storm 2017 is about 26% longer as compared to flash durations of 2014 storm.

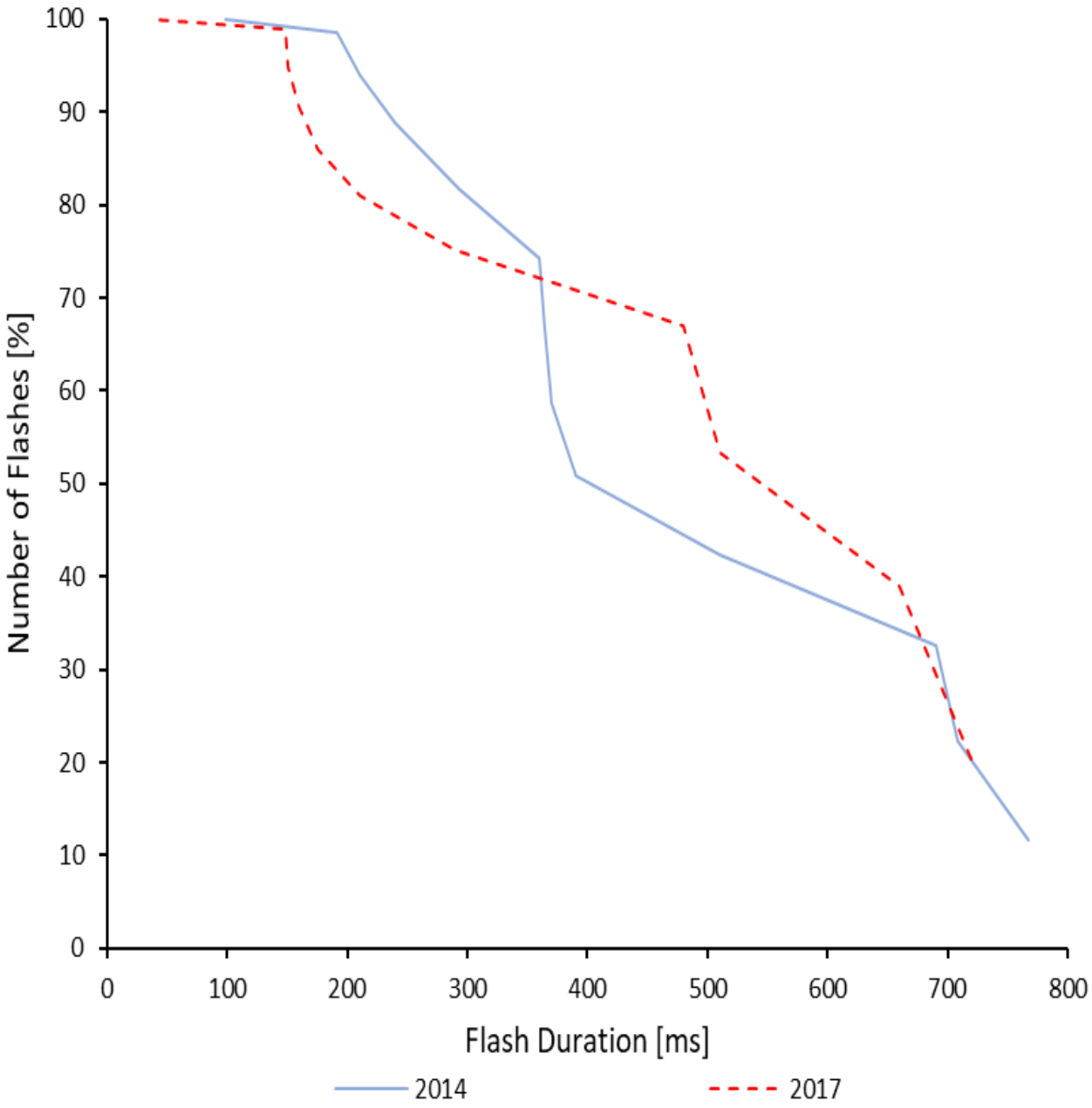

Figure 6.14 – Cumulative probability distribution of flash duration of flashes recorded during major storms (Sept. 5, 2014 and Sept. 4, 2017).

Table 6.11 Statistical summary of flash durations of flashes recorded during major storms (Sept. 5, 2014 and Sept. 4, 2017).

Flash Duration [ms]		
	2014 Storm	2017 Storm
Minimum	99	37
Maximum	767	720
Mean	399.4	321.8
50% Probability	367	497
Standard Deviation	211.6	231

It's worth mentioning that the 50% CPD of flash durations of 2017 (497 ms) storm is 26% greater than that of 2014 (367 ms) storm, flash durations (Table 6.11). The difference in the size of the two data sets and possibly the 5.6% more flashes contained by 2017 storm, with flash durations above 400 ms, may explain the discrepancies.

6.7.2 Inter-Flash Time Duration

Figure 6.15 shows the frequency distribution of inter-flash time duration of flashes captured during 2014 and 2017 storms. It's observed that the inter-flash time intervals of 2014 storm (16.67%) and 2017 storm (80%) are within 400 s. While, 83.3% (2014) and 20% (2017) of inter-flash time intervals are beyond 400 s.

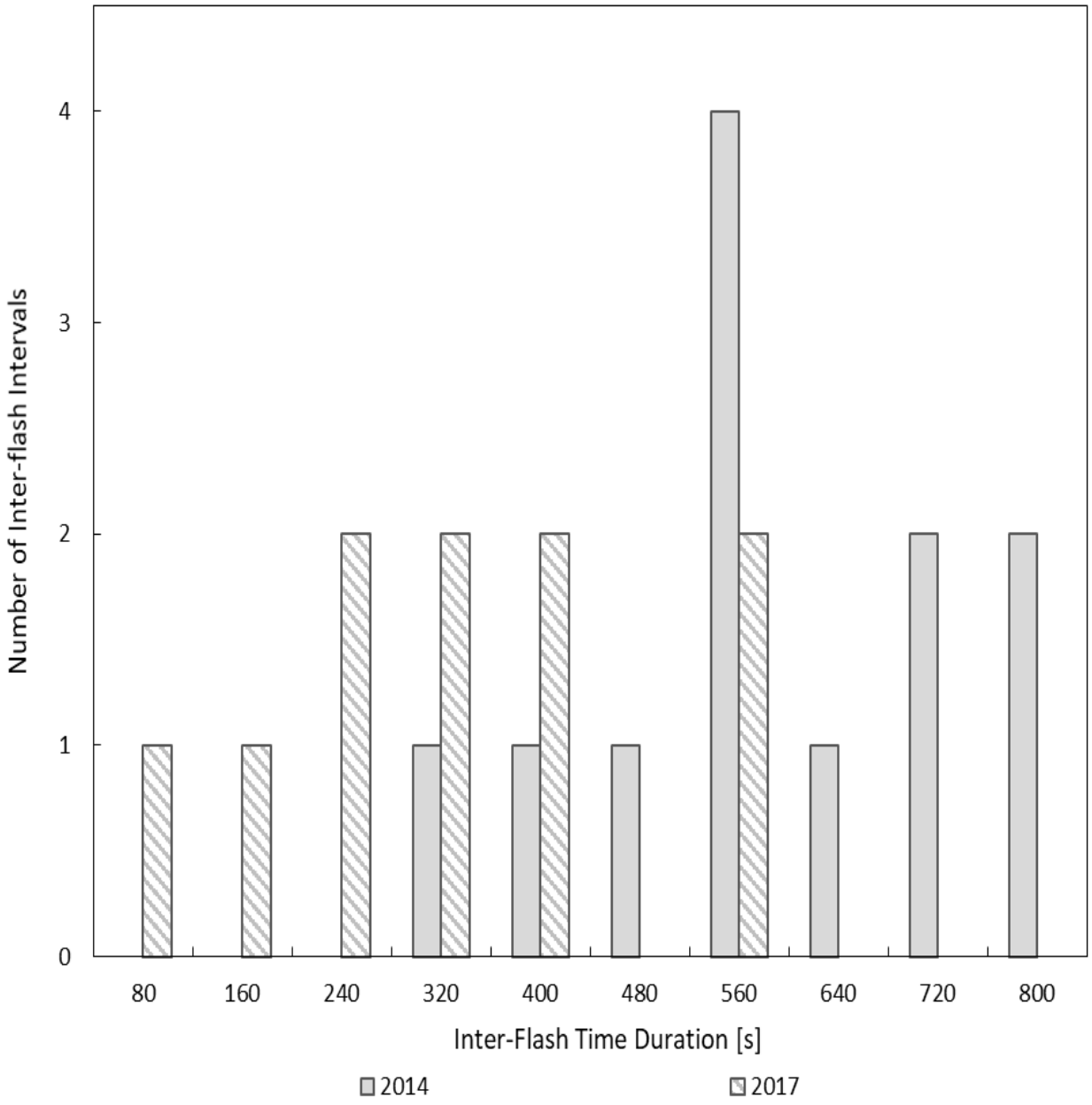

Figure 6.15 – Frequency distribution of inter-flash duration of flashes recorded during major storms (Sept. 5, 2014 and Sept. 4, 2017).

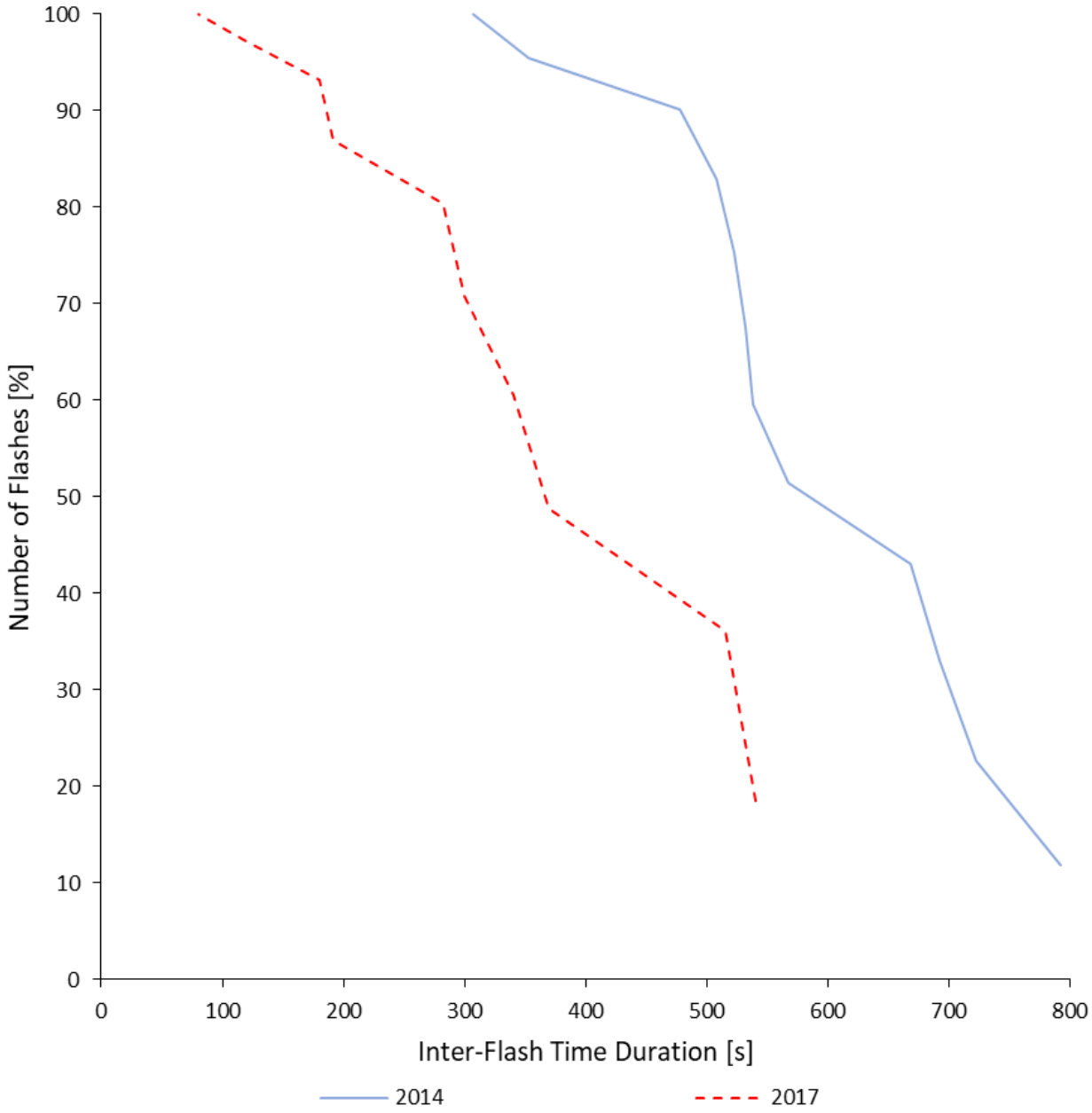

Figure 6.16 – Cumulative probability distribution of inter-flash time of flashes recorded during major storms (Sept. 5, 2014 and Sept. 4, 2017).

Table 6.12 Statistical summary of inter-flash durations of flashes recorded during major storms (Sept. 5, 2014 and Sept. 4, 2017).

Inter-Flash Time Duration [s]		
	2014 Storm	2017 Storm
Minimum	307	80
Maximum	792	540
Mean	556	291.9
50% Probability	550	348
Standard Deviation	143.9	155

Table 6.12 reveals that the inter-flash time durations for storm 2014 vary between 307 s and 792 s, on the other hand, the inter-flash time durations for 2017 storm varies between 80 s and 540 s.

For comparison, it's noted that the minimum inter-flash time duration of 2017 storm is 73% shorter than the minimum inter-flash time duration 2014 storm. However, the maximum inter-flash time duration of 2014 storm is 31.8% longer, as compared to 2017 storm. It's also concluded from the Table 6.12 that the average inter-flash time duration of 2017 storm is 47% smaller as compared to the average inter-flash time duration of 2014 storm. The discrepancies in the data are due to the nature of two storms.

It can be inferred from Figure 6.16 that 50% CPD of the inter-flash time duration of 2014 storm (550 s) is more as compared to the 2017 storm (348 s).

6.7.3 Initial-Stage Current Duration

During the 2014 and 2017 storms, the CN Tower optical recording systems captured 13 and 11 flashes respectively. Interestingly, all the flashes received during the storms contained initial-stage current. Figure 6.17 presents the frequency distribution of initial-stage current time durations, which made possible to conclude that the majority of 2014 (77%) and 2017 (90%) flashes have an initial-stage current duration within 400ms. Whereas, a small amount of flashes contained initial-stage current duration between 400 ms and 650 ms constituting 23% (2014) and 10% (2017).

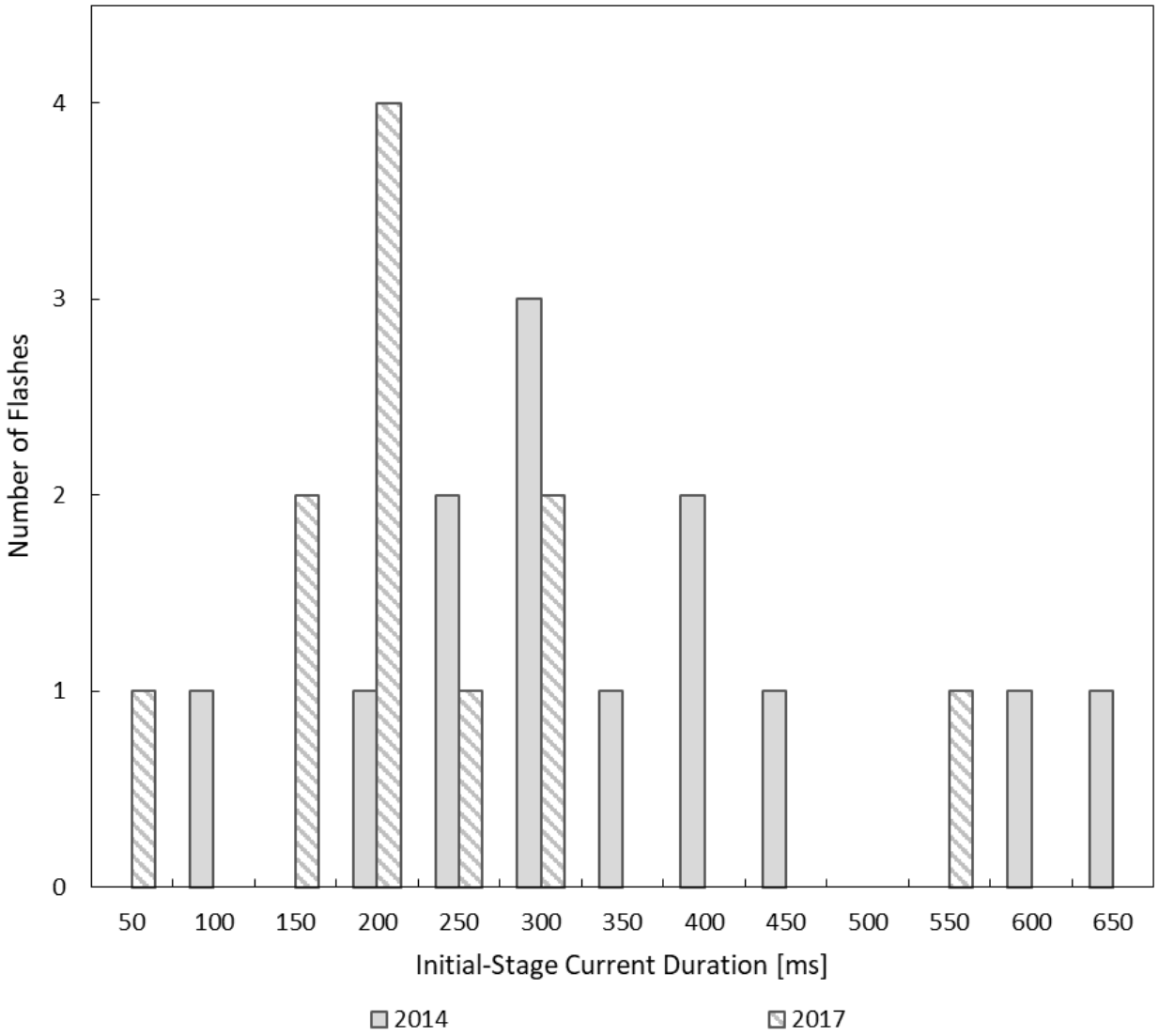

Figure 6.17 – Frequency distribution of initial-stage current duration of flashes recorded during major storms (Sept. 5, 2014 and Sept. 4, 2017).

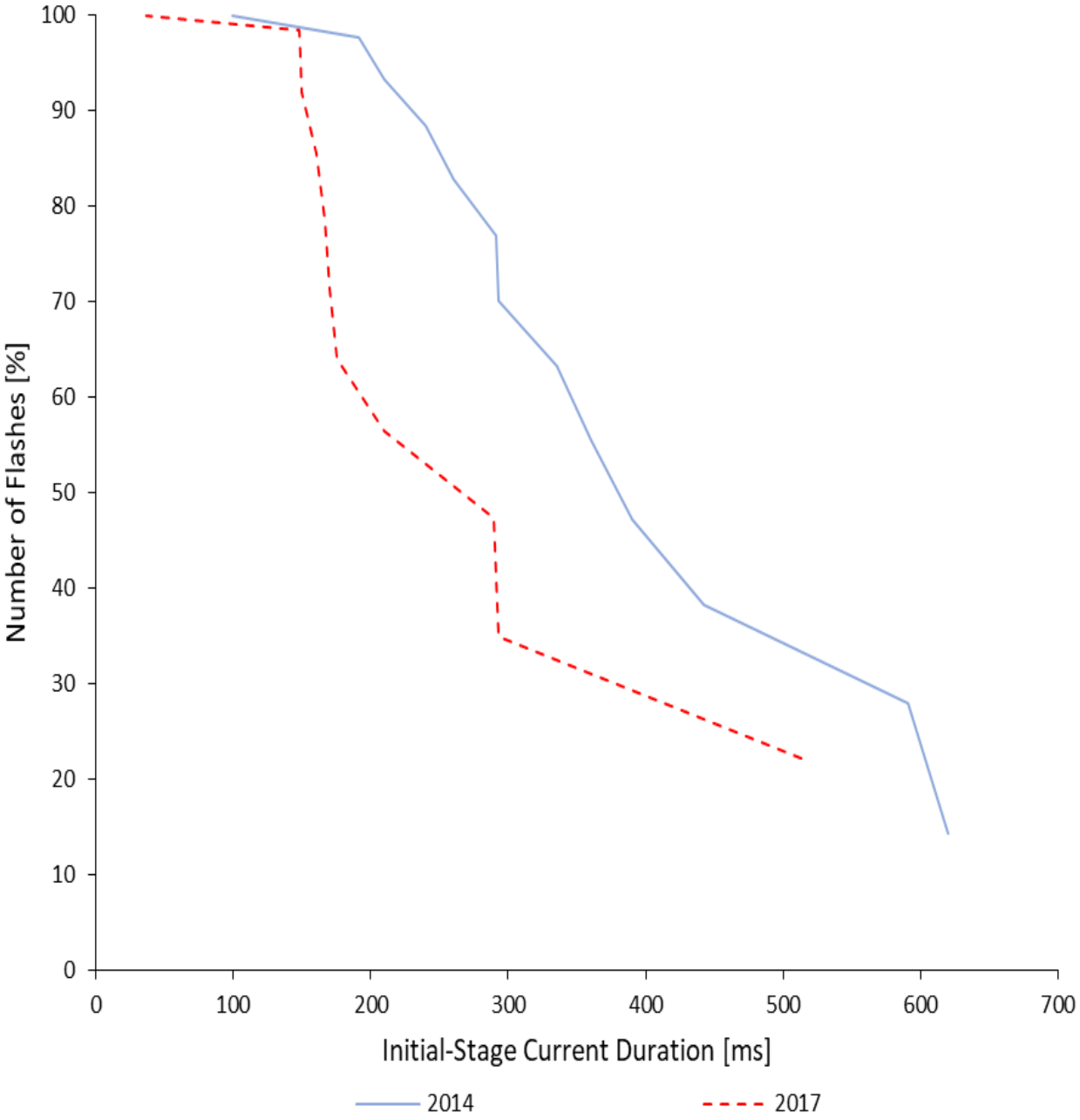

Figure 6.18 – Cumulative probability distribution of initial-stage current duration of flashes recorded during major storms (Sept. 5, 2014 and Sept. 4, 2017).

Table 6.13 Statistical summary of initial-stage current durations of flashes recorded during major storms (Sept. 5, 2014 and Sept. 4, 2017).

Initial-Stage Current Duration [ms]		
	2014 Storm	2017 Storm
Minimum	99	37
Maximum	620	513
Mean	332	210.2
50% Probability	360	188
Standard Deviation	150	122

Table 6.13 shows that minimum initial-stage current duration of 2014 (99 ms) is 62.6% longer than 2017 (37 ms), which is the markedly more substantial difference. Whereas, a maximum initial-stage current of 2014 (620 ms) is only 17% longer as compared to 2017 (513 ms).

For comparison, Table 6.13 and Figure 6.18 clearly states that storm of 2014 had more considerable average initial-stage current duration (332 ms) and 50% CPD (360 ms) as compared to the average initial-stage current duration (210 ms) and 50% CPD (188 ms) of 2017 storm.

6.7.4 Flash Multiplicity

Based on the datasets of 2014 and 2017 storms, 46% and 45% of flashes contained return strokes, respectively. Figure 6.19 illustrates the frequency distribution of flash multiplicity. The figure shows that 80% of flashes in both years had 1 or 2 return strokes. While only 16.6% of

flashes received during 2014 storm had three return strokes and 20% of flashes received during 2017 storm had four return strokes.

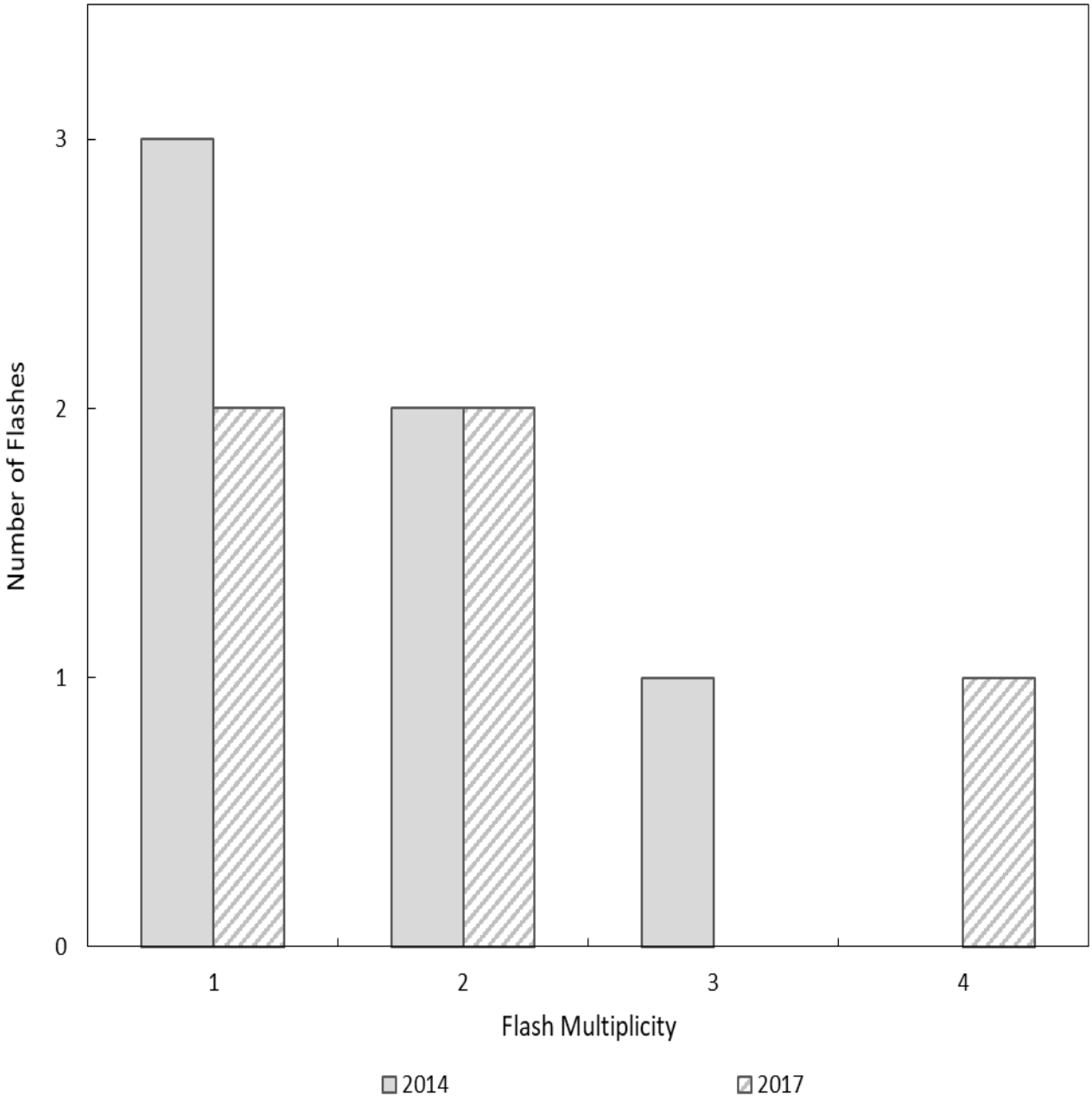

Figure 6.19 – Frequency distribution of flash multiplicity of flashes recorded during major storms (Sept. 5, 2014 and Sept. 4, 2017).

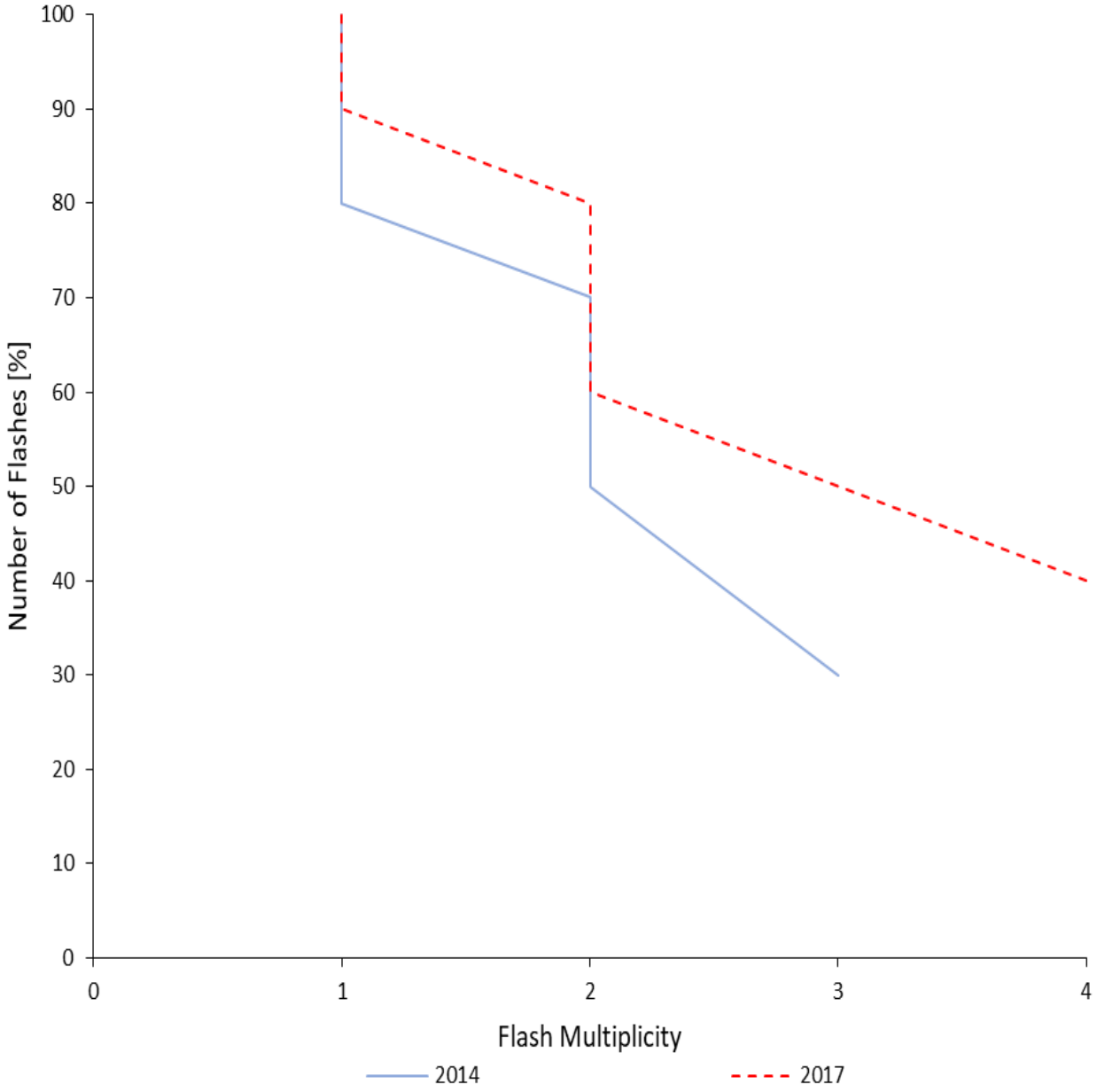

Figure 6.20 – Cumulative probability distribution of flash multiplicity of flashes recorded during major storms (Sept. 5, 2014 and Sept. 4, 2017).

Table 6.14 Statistical summary of flash multiplicity of flashes recorded during major storms (Sept. 5, 2014 and Sept. 4, 2017).

Flash Multiplicity		
	2014 Storm	2017 Storm
Minimum	1	1
Maximum	3	4
Mean	1.67	2
50% Probability	2	2
Standard Deviation	0.81	1.22

Table 6.14 clearly shows that storm of September 5, 2014, and storm of September 4, 2017, both had at least one return stroke. Whereas, 2017 had a maximum of 4 return strokes as compared to 2014 (3 return strokes), which has one less return stroke.

For the comparison purpose, it can be concluded from Table 6.14 and Figure 6.20, that both storms had similar average multiplicity with a modest difference. Also, 50% CPD of the two storms is identical.

6.7.5 Inter-Stroke Time Duration

Based on the data sets of the two storms, the storm of 2014 contains four inter-stroke time intervals, and the 2017 storm constitutes five inter-stroke time intervals. Figure 6.21 demonstrates the frequency distribution of inter-stroke time intervals. Furthermore, it's also concluded from the figure that 50% of 2014 inter-stroke time durations are within the range of 20 ms and 80 ms, and a similar percentage of flashes are within the range of 80 ms and 140 ms. Whereas, 2017 storm had 40% of inter-stroke intervals within 20 ms and 80 ms and 60% of flashes within 80 ms and

140 ms, meaning 10% a smaller number of inter-stroke time intervals within 20 ms and 80 ms and 10% more number of inter-stroke time intervals within 80 ms to 140 ms, as compared to the storm of 2014.

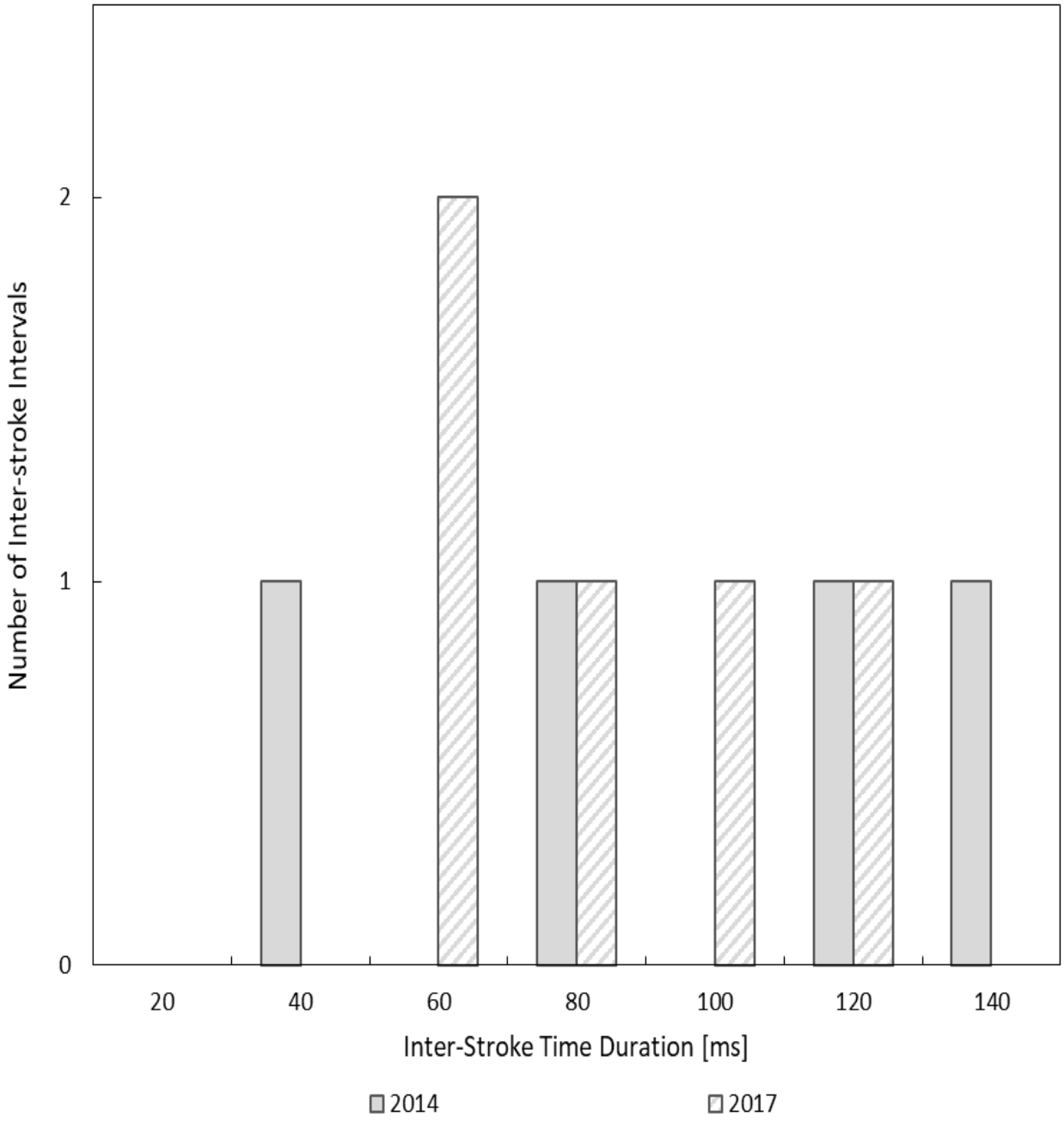

Figure 6.21 – Frequency distribution of inter-stroke time duration of flashes recorded during major storms (Sept. 5, 2014 and Sept. 4, 2017).

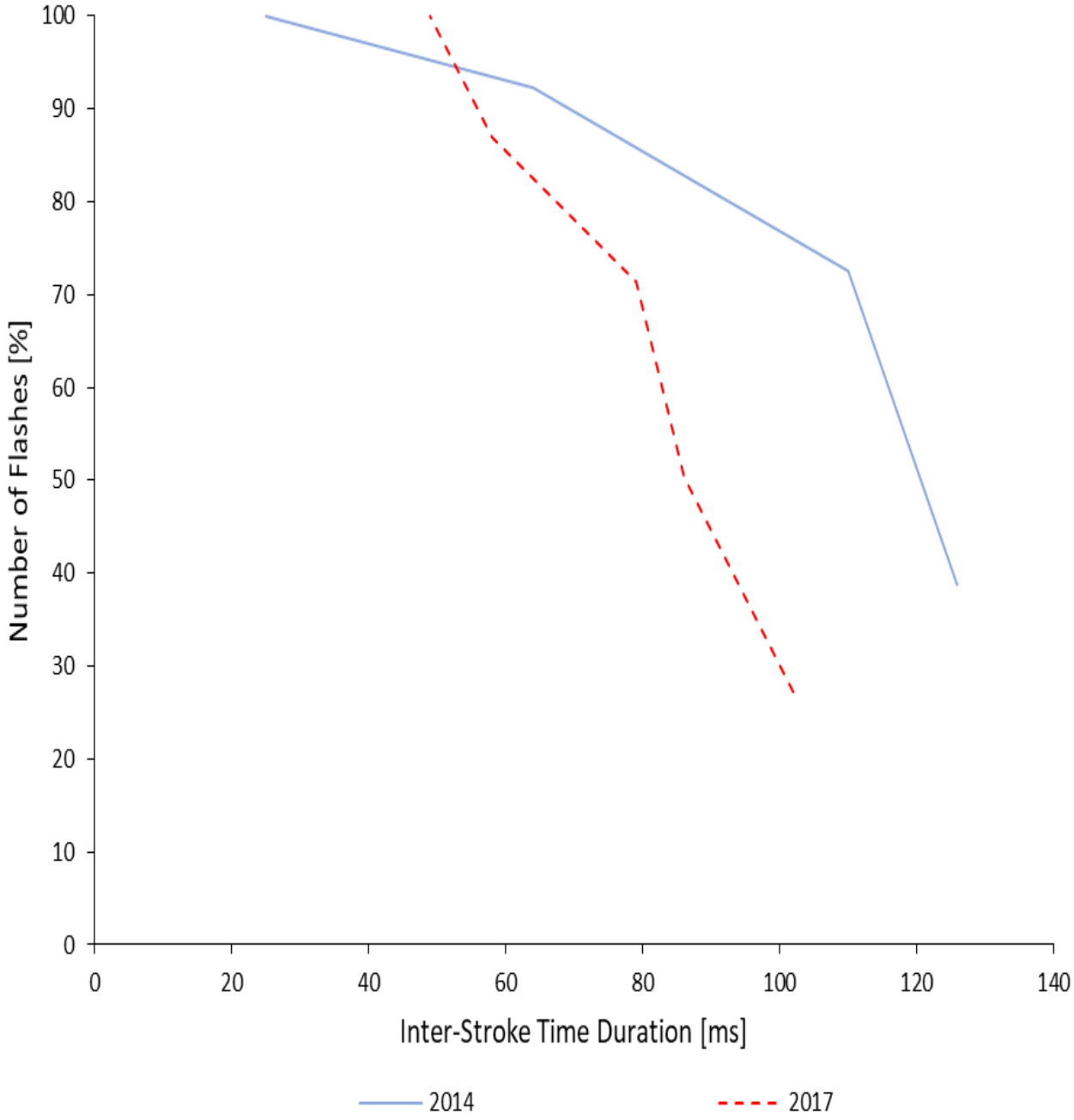

Figure 6.22 – Cumulative probability distribution of inter-stroke time duration of flashes recorded during major storms (Sept. 5, 2014 and Sept. 4, 2017).

Table 6.15 Statistical summary of inter-stroke time durations duration of flashes recorded during major storms (Sept. 5, 2014 and Sept. 4, 2017).

Inter-Stroke Time [ms]		
	2014 Storm	2017 Storm
Minimum	25	49
Maximum	126	102
Mean	81.25	74.8
50% Probability	112	83
Standard Deviation	45.8	21.4

Table 6.15 reveals that the inter-stroke time duration of 2014 storm is found to vary between 25 ms and 126 ms with an overall average of 81.25 ms. On the other hand, the inter-stroke time duration of 2017 storm is found to vary between 49 ms to 102 ms with an overall average inter-stroke time duration of 74.8 ms, which is 7.9% shorter than the average inter-stroke time duration of 2014 storm.

For the comparison, the Figure 6.22 shows that 2014 had greater 50% CPD as compared to 2017 storm.

6.7.6 Continuing Current Duration

Based on the data sets of the two storms it's observed that 2014 storm had six flashes (46%) containing continuing currents, while 2017 storm had three flashes (27%) containing continuing currents.

Figure 6.23 presents the frequency distribution of 2014 and 2017 storms. It's possible to infer from the figure that 77% of continuing current durations falls within 80 ms for 2014 and 2017 storms. Whereas, only about 23% of continuing current durations falls within the range of 80 ms to 160 ms for the two storms.

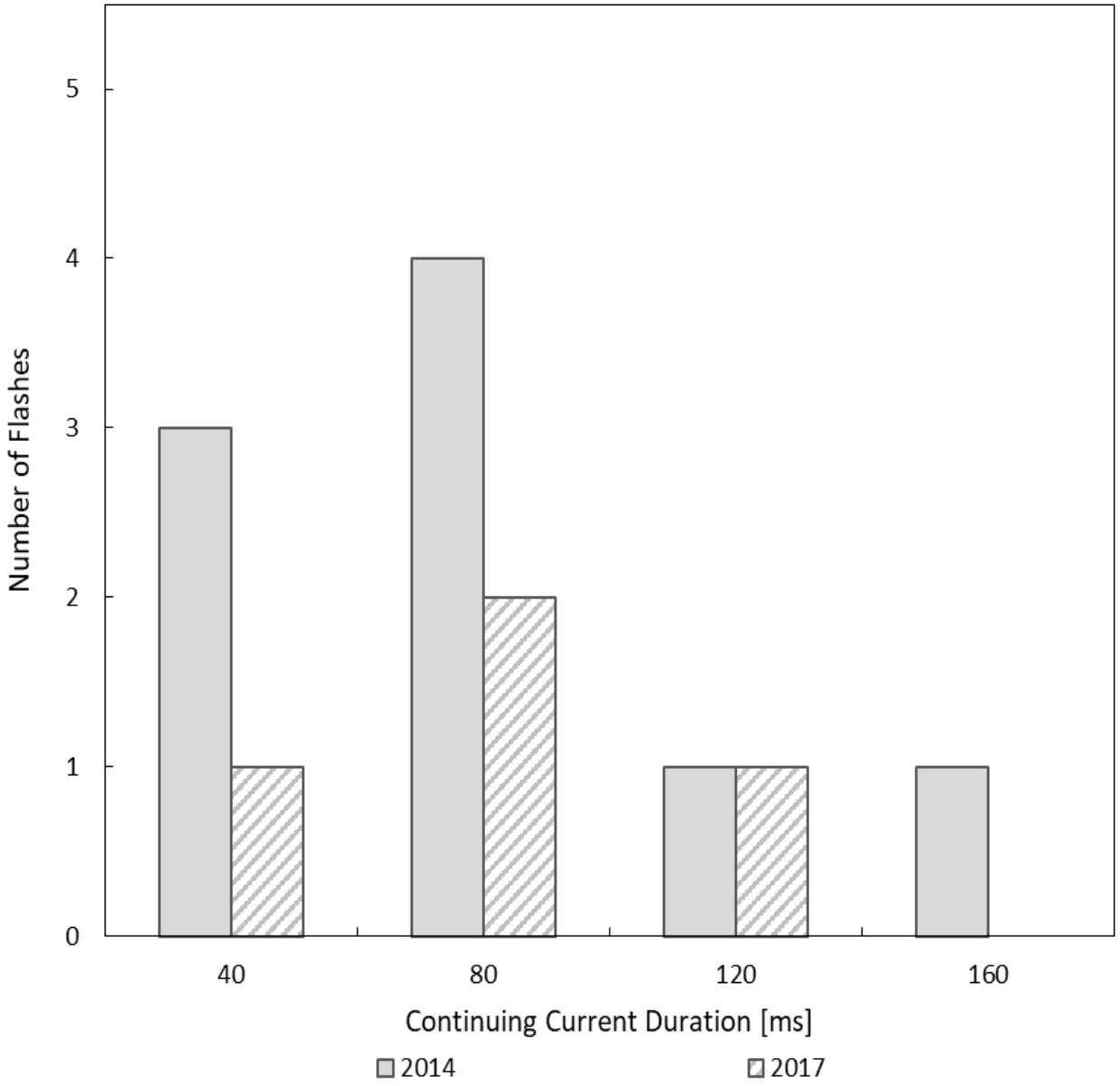

Figure 6.23 – Frequency distribution of continuing current duration of flashes recorded during major storms (Sept. 5, 2014 and Sept. 4, 2017).

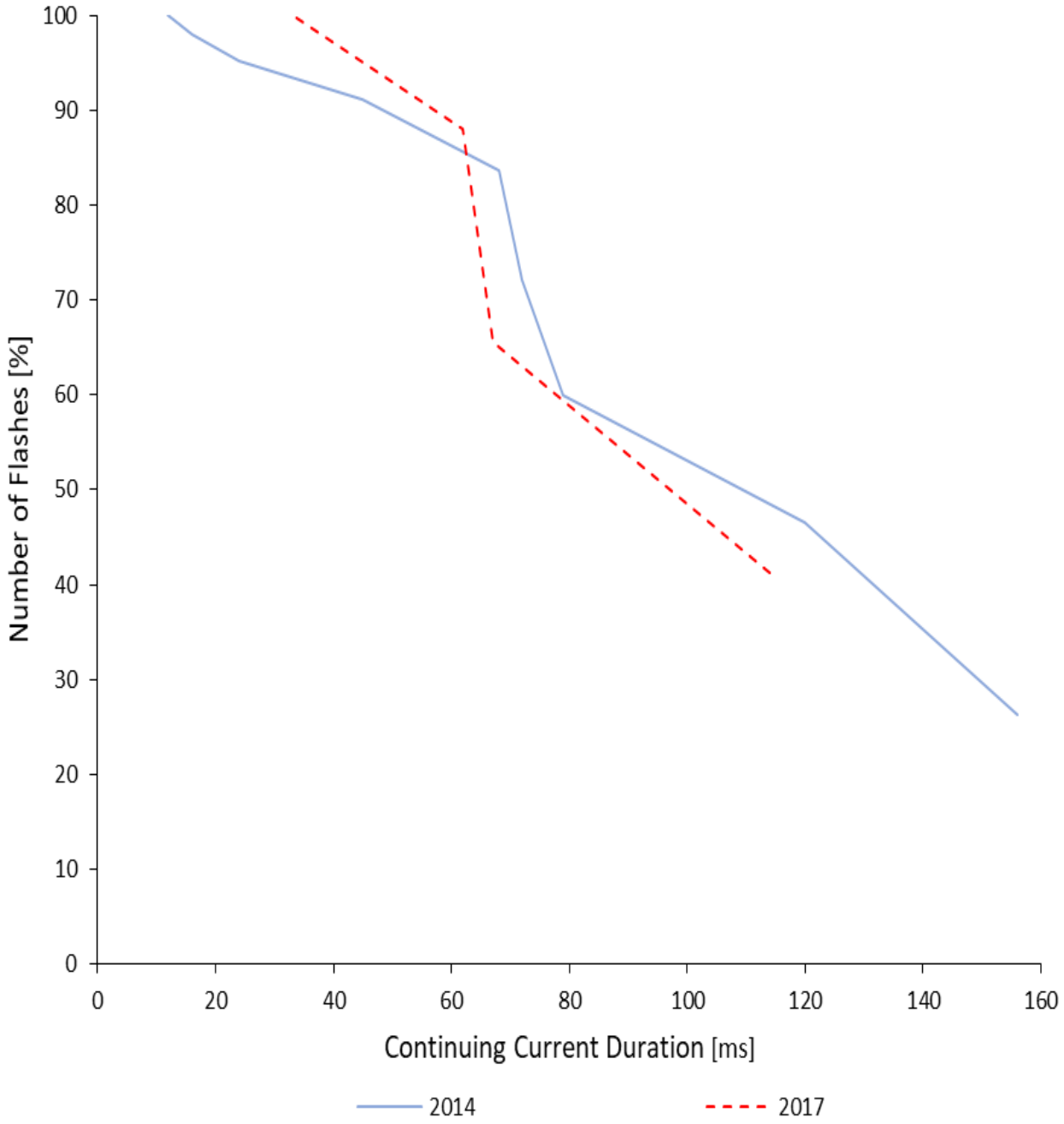

Figure 6.24 – Cumulative probability distribution of continuing current duration of flashes recorded during major storms (Sept. 5, 2014 and Sept. 4, 2017).

Table 6.16 Statistical summary of continuing current durations of flashes recorded during major storms (Sept. 5, 2014 and Sept. 4, 2017).

Continuing Current Time Duration [ms]		
	2014 Storm	2017 Storm
Minimum	12	33
Maximum	156	114
Mean	65.8	69
50% Probability	78	66
Standard Deviation	48	33.5

Table 6.16 clearly shows that continuing current time durations of 2014 storm is found to vary between 12 ms to 156 ms, with an overall average of 65.8 ms. Whereas, the continuing current time duration of 2017 storm is found to vary between 33 ms to 114 ms, with an overall average of 69 ms, which is almost the same to the average continuing current duration of the 2014 storm.

Figure 6.24 shows that the 50% CPD of 2014 storm is 15% longer as compared to that of the 2017 storm.

Chapter 7

Conclusions and Future Research

7.1 Conclusions

The principal objective of the work completed in this thesis focused on the statistical analysis of CN Tower lightning flash characteristics, based on the video records of Phantom v5.0 digital high-speed camera and Sony HDR PJ790VB digital continuously recording camera, which were acquired over the past five years (2013-2017). The existence and characteristics of lightning flash components, namely, the initial-stage current, return strokes, M-components and continuing currents were determined by examining video records (luminosity vs. time analysis).

It is worth mentioning that the characteristics of 58 optically recorded flashes clearly show that every recoded flash contained an initial-stage current, confirming that all flashes were upward initiated. Also, it has been inferred that the duration of the initial-stage current varied from 32 ms to 620 ms, with an overall average of 218.6 ms. Also, 27 out of the 58 flashes contained return strokes ranging from 1 to 9, with an average multiplicity of 2.16. It is important to mention that 56 return strokes were observed to hit the tower during the past five years. Furthermore, the flash time duration varied between 32 ms to 767 ms, with an overall average of 296.8 ms. Whereas, the inter-flash time duration ranged from 80 s to 792 s, with an overall average of 324 s. It is also important to say that the data set of the last five years only comprised 13 multi-stroke flashes, containing 28 inter-stroke intervals that varied between 12 ms to 126 ms, with an overall average

of 62.5 ms. Moreover, 25 out of the 56 return strokes were followed by continuing currents, with durations ranging from 12 ms to 156 ms, with an overall average duration of 61 ms.

The second objective of this thesis was to compare the statistical analyses of each year (2013-2017). Based on the analysis of the 58 video recorded flashes, it was observed that in 2014 got the highest number of flashes with extended flash durations of up to 767 ms, and the most substantial average flash duration as compared to all other years. However, 50% cumulative probability distribution (CPD) of 2017 overweighs that for 2014 and all other years because the flash duration of most of the flashes comprised by 2017 dataset is in the higher range (above 400 ms). Also, the 2014, we observed the highest inter-flash time duration of (792 s), with the largest overall average and 50% CPD in comparison with all other years. Furthermore, the initial-stage current in 2014 had the longest initial-stage current duration (620 ms), largest average (288 ms) and 50% CPD (317 ms), as compared with all other years. Moreover, the flash multiplicity of the 2016 data set accounts for the maximum of return strokes per flash, which clearly overweighs all other years. However, the average flash multiplicity of all years was almost identical (2).

The maximum inter-stroke time durations for all years varied between 102 ms and 126 ms, with 2014 leading all other years. It was also noted that the average (81.25 ms) and 50% CPD (112 ms) of the inter-stroke time duration of 2014 dataset was longest among all other years. The comparison of the statistical analyses of the continuing current time duration clearly showed that the 2014 dataset had the longest continuing current time duration (156 ms). Whereas, the 50% CPD of continuing current duration of 2015 was leading among all years.

Based on the analyses of video records for the last five years, it was noted that two significantly major storms were captured during the night of September 5, 2014, and September 4, 2017. During the storm of September 5, 2014, the CN Tower imaging systems recorded 13 flashes. The storm lasted for 111.4 mins, resulting in average a flash to the tower every 9 mins. Whereas, during the September 4, 2017 storm 11 flashes hit the tower and the storm continued for 49.35 mins, producing on an average a flash to tower every 4 mins and 48 s. However, interestingly during the storm of September 4, 2017, all eleven flashes were recorded by Sony continuously-recording camera, whereas the high-speed camera was only able to record four flashes out of storm's eleven flashes. The inter-flash times of the eleven flashes captured by the LSC were pivotal in time matching of the two data sets. The comparison between the lightning data recorded by

HSC and LSC illustrated that the economical LSC turns out to be an extremely valuable imaging system. As the continuously recording imaging system (LSC) confirmed the operation or the failure of the HSC. However, LSC does not have an adequate frame rate (60 fps) to capture every subtle detail of a flash, including M-components.

The comparison of the statistical analyses of these two significant storms was one of the objectives of this work, to further study the nature of the two major storms. The statistical analyses of flash durations of both storms clearly showed that 50% CPD in the 2017 storm was longer as compared to that 2014 storm, due to 6% more flashes from the 2017 storm having the flash duration above 400 ms. Similarly, the overall average of the inter-flash time duration of 2014 storm was longer as compared to the 2017 storm. Likewise, the 2014 storm had longer overall average initial-stage current duration as compared to 2017 storm. Furthermore, the 50% CPD of flash multiplicity of both storms were identical. Moreover, the overall average inter-stroke time duration of the 2014 storm was higher than that of the 2017 storm. Whereas, the 50% CPD of the continuing current duration of 2014 storm was higher than that of the 2017 storm.

To summarize, flashes with longer flash durations contains higher number of return strokes, with short inter-stroke time can pose severe threat to tall structures and electrical and communication systems especially when inter-stroke times are short. Study of various flash components is pivotal to study the nature of flashes to build a sophisticated protections system for tall structures.

7.2 Future Research and Recommendations

Simultaneous measurements and recordings of all relevant lightning parameters should continue. More equipment should be installed at closer distance from the CN Tower to better record the characteristics of CN Tower flashes and non-CN Tower flashes in the vicinity of the tower.

The digital high-speed imaging system currently in use to record CN Tower lightning flashes was updated in 2006 from Phantom v2.0 to Phantom v5.0, which made it possible to record lightning flashes to the tower at 1000 frames per second (fps), with higher recording length (1300

ms), which is more than double the record length of the previous high-speed imaging system, which was necessary for studying in more detail the flash characteristics of flashes. Although, the present high-speed imaging system can be utilized and a new high-speed camera with much higher frame rates must be acquired which would help in analyzing the speed of propagation of return strokes. Also, the required high-speed camera must have a built-in trigger, which would allow the camera to avoid getting triggered by false information outside its recording window. Moreover, the operation of the two high-speed cameras will make it possible to record the 3-dimensional trajectory of the flash.

The current continuously-recording low-speed camera has no time stamps, which could be made possible by the addition of a new continuously recording camera with time stamps. The simultaneous operation of the continuously recording camera has proved to be crucial and should be continued for recording CN Tower lightning flashes because the continuous recording of the camera enables to confirm the operation or failure of the high-speed cameras, which depends upon the external triggering device.

References

[1] Martin A. Uman, *"The Lightning Discharge"*, Florida: Academic Press, Inc., 1987.

[2] Martin A. Uman, *"All About Lightning"*, New York: Dover Publications, Inc., 1986.

[3] Vladimir A. Rakov, and Martin A. Uman, *"Lightning: physics and effects"*. Cambridge University Press, August 2003.

[4] Martin A. Uman, Lightning, Pittsburg PA: McGraw Hill, 1969.

[5] The Structure of Cold Clouds - University of Arizona http://www.atmo.arizona.edu/students/courselinks/spring15/atmo589/ATMO489. [accessed on July 17, 2018]

[6] Earle R. Williams, *"The Electrification of Thunderstorms"*, Scientific American, pp. 88-99, November 1988.

[7] G. Diendorfer, "Lightning initiated from tall structures—A review." In *Lightning Protection (XI SIPDA), 2011 International Symposium on*, pp. 298-303. IEEE, 2011.

[8] M. Megumu, Vladimir A. Rakov, Takatoshi Shindo, G. Diendorfer, M. Mair, F. Heidler, W. Zischank, M. A. Uman, R. Thottappillil, and D. Wang. "Initial stage in lightning initiated from tall objects and in rocket-triggered lightning." *Journal of Geophysical Research: Atmospheres* 110, no. D2 (2005).

[9] A.M. Hussein, M. Milewski, A. Abdelraziq, W. Janischewskyj, and F. Jabbar. "Visual characteristics of CN Tower lightning flashes." In *28th International Conference on Lightning Protection (ICLP), Kanazawa, Japan*, pp. 18-22, 2006.

[10] A.M. Hussein, S. Jan, V. Todorovski, M. Milewski, K. L. Cummins, and W. Janischewskyj. "Influence of the CN Tower on the lightning environment in its vicinity." In *Proceedings of the International Lightning Detection Conference (ILDC)*, pp. 1-19. 2010.

[11] W. Janischewskyj, A.M. Hussein, V. Shostak, I. Rusan, J-X. Li, and J-S. Chang. "Statistics of lightning strikes to the Toronto Canadian National Tower (1978-1995)." *IEEE Transactions on Power Delivery* 12, no. 3 (1997): 1210-1221.

[12] W. Janischewskyj, A.M. Hussein, M. Wiacek, and J. S. Chang. "Details of CN Tower flashes utilizing a digital high-speed camera." In *Proc. 24th International Conference on Lightning Protection*, pp. 101-106. 1998.

[13] A.M. Hussein, and M. Milewski. "CN tower lightning flash components." In *Lightning Protection (XI SIPDA), 2011 International Symposium on*, pp. 7-13. IEEE, 2011.

[14] A. M. Hussein, S. Kazazi, M. Anwar, M. Yusouf, and P. Liatos. "CN Tower lightning characteristics based on current-recorded flashes." In *Lightning Protection (ICLP), 2014 International Conference*, pp. 2028-2034. IEEE, 2014.

[15] A. Lafkovici, A.M. Hussein, W. Janischewskyj, and Kenneth L. Cummins. "Evaluation of the performance characteristics of the North American Lightning Detection Network based on tall-structure lightning." *IEEE Transactions on Electromagnetic Compatibility* 50, no. 3 (2008): 630-641.

[16] M. Milewski, "Lightning Return-Stroke Transmission Line Modelling Based on the Derivative of Heidler Function and CN Tower Data, "Ph.D. Thesis, Ryerson University, Toronto, Ontario, Canada, 2009.

[17] N. Mansour, "Lightning Environment in the Vicinity of the CN Tower During Major Storms, "MASc Thesis, Ryerson University, Toronto, Ontario, Canada, 2017.

[18] A. M. Hussein, M. Milewski, and W. Janischewskyj. "Characterization of CN tower lightning flash components." In *Proceedings of the International Conference on Ground & 4 Lightning Physics and Effects*, pp. 1-7. 2010.

[19] S. Kazazi, P. Liatos, and A.M. Hussein. "Simultaneous recording of cn tower lightning current and channel luminosity." In *Electrical and Computer Engineering (CCECE), 2014 IEEE 27th Canadian Conference on*, pp. 1-6. IEEE, 2014.

[20] Phantom Technical Specifications, “Phantom v5.0, “Vision Research Inc., Wayne, New Jersey, USA, 2000.

[21] A.M. Hussein, S. Kazazi, M. Anwar, M. Yusouf, and P. Liatos. "Characteristics of the most intense lightning storm ever recorded at the CN Tower." *Journal of Atmospheric and Solar-Terrestrial Physics* 154 (2017): 195-206.

[22] I. Sra, A.M. Hussein and P. Liatos, “CN Tower Lightning Flash Characteristics Based on High-Speed Imaging,” Proceedings, International Conference on Grounding and Lightning Physics & Effects, pp. 18-21, May 20-25, 2018, Pirenópolis, Brazil.

[23] A.M. Hussein, W. Janischewskyj, J-S. Chang, V. Shostak, W. A. Chisholm, P. Dzurevych, and Z-I. Kawasaki. "Simultaneous measurement of lightning parameters for strokes to the Toronto Canadian National Tower." *Journal of Geophysical Research: Atmospheres* 100, no. D5 (1995): 8853-8861.

[24] P. Liatos, and A.M. Hussein. "Characterization of 100-kHz noise in the lightning current derivative signals measured at the CN tower." *IEEE transactions on electromagnetic compatibility* 47, no. 4 (2005): 986-997.

[25] I. Sra, A.M. Hussein, “Luminosity Characteristics of the CN Tower Lightning Components,”*25th* International Lightning Detection Conference (ILDC) and 7th International Lightning Meteorology Conference (ILMC), pp. 1-12, March 12-15, 2018, Fort Lauderdale, Florida, USA.

Glossary

AGL	Above Ground Level
CC	Continuing Current
CG	Cloud-to-ground
CPD	Cumulative Probability Distribution
DL	Dart Leader
EMI	Electromagnetic Interference
HSC	High-Speed Camera
ISC	Initial-Stage Current
IST	Inter-stroke Time
LEMP	Lightning Generated Electromagnetic Pulse
LSC	Low-Speed Camera
RS	Return Stroke
SL	Stepped Leader